VOLUME 84 NO. HY6
NOVEMBER 1958

# JOURNAL of the

# Hydraulics Division

PROCEEDINGS OF THE
AMERICAN SOCIETY
OF CIVIL ENGINEERS

## MANUSCRIPTS

Journal of the

HYDRAULICS DIVISION

Proceedings of the American Society of Civil Engineers



CONTENTS

November, 1958

Papers

| | Number |
|---|---|
| Wave Forces on Submerged Structures by Ernest F. Brater, John S. McNown and Leslie D. Stair | 1833 |
| Snowmelt Runoff by J. Harold Zoller and Arno T. Lenz | 1834 |
| Discussion | 1856 |

Paper 1833 November, 1958 HY 6

Journal of the
HYDRAULICS DIVISION
Proceedings of the American Society of Civil Engineers

# WAVE FORCES ON SUBMERGED STRUCTURES

Ernest F. Brater,[1] M. ASCE, John S. McNown,[2] M. ASCE
and Leslie D. Stair[3]
(Proc. Paper 1833)

## SYNOPSIS

The magnitude and characteristics of forces resulting from oscillatory waves were determined for models of submerged barge-like structures. The wave profiles and the variation with time of the resulting horizontal and vertical forces were obtained for various wave heights, wave periods, and locations of the barge with respect to the water surface. The basic model was a right parallelepiped having the proportions of a typical barge. Modifications of this model were made to determine the effects of rounding the sides and of the inclusion of a slot in one end of the barge. Horizontal force measurements were also made for a flat plate having the same dimensions as the long vertical face of the barge. These studies provided design data needed for the application of analytical methods in the determination of forces on some types of submerged structures.

## INTRODUCTION

The design of off-shore structures such as oil drilling platforms and radar stations requires knowledge of the magnitude of the wave forces. Methods of calculating such forces have not been fully determined. Laboratory investigations have been made of wave forces on vertical piles, (1,2,3,4) horizontal struts(5,6) and on larger and more complicated structures.(7)

Note: Discussion open until April 1, 1959. To extend the closing date one month, a written request must be filed with the Executive Secretary, ASCE. Paper 1833 is part of the copyrighted Journal of the Hydraulics Division, Proceedings of the American Society of Civil Engineers, Vol. 84, No. HY 6, November, 1958.

1. Prof. of Hyd. Eng., Univ. of Mich., Ann Arbor, Mich.
2. Dean, School of Engineering and Architecture, Univ. of Kansas, Lawrence, Kans. (formerly Prof. of Eng. Mech., Univ. of Mich., Ann Arbor, Mich.)
3. Res. Engr., Boeing Airplane Corp., Seattle, Wash., (formerly Assoc. Res. Engr., Eng. Res. Inst., Ann Arbor, Mich.)

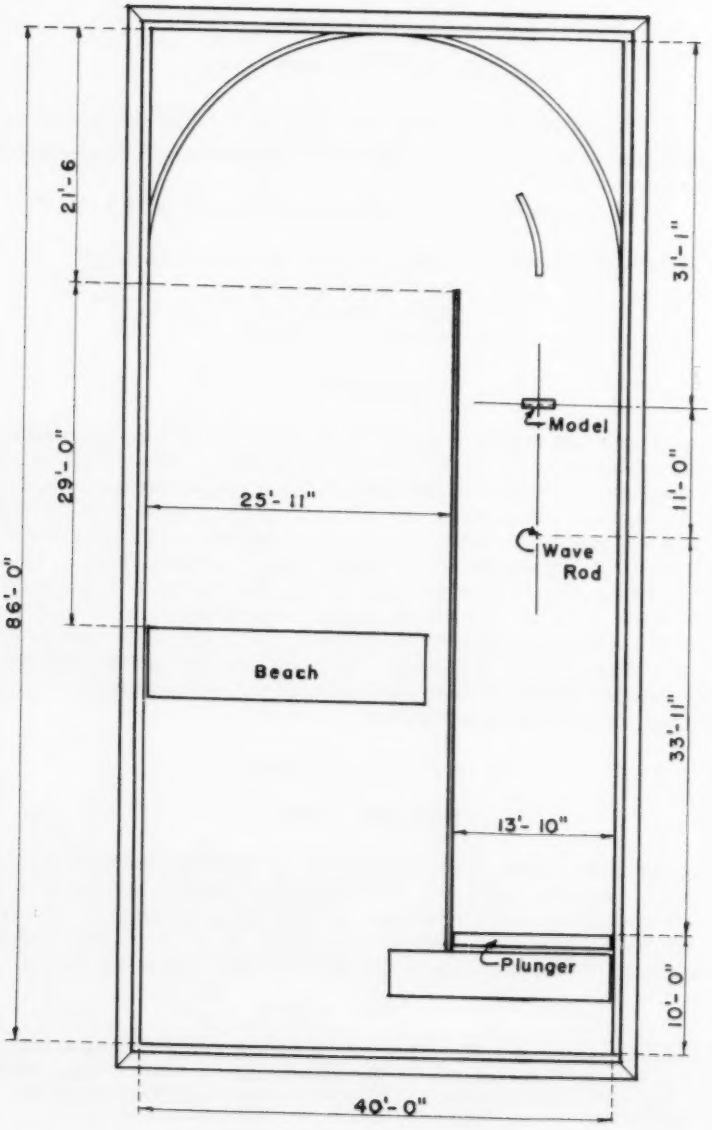


WAVE TANK

FIGURE 1

No laboratory investigations of forces on simple barge-like shapes have been reported.

The forces produced by oscillatory waves result from the orbital motion of the water. Acceptably accurate estimates can be made of orbital velocities and accelerations, and the associated pressure variations can be determined analytically. Also required for the computation of the drag and inertial forces are values of the coefficient of drag ($C_d$) and the coefficient of inertial resistance ($C_m$). The drag coefficients for various bodies have been determined experimentally for steady flow, but little is known about their magnitudes for unsteady flow. Values of $C_m$ have been determined theoretically as well as experimentally for certain shapes, but here again the applicability of such values to the conditions existing during wave motion has not been tested. These studies were planned to determine the necessary coefficients and a suitable method for estimating wave forces on structures placed in the sea.

## Testing Facilities

The experiments were conducted in the Lake Hydraulics Laboratory[8] of the University of Michigan. The wave tank used for these tests is 86 feet long and 40 feet wide and has walls 3' 10" high. The testing frame was located in a channel 13' 10" wide separated from the remainder of the tank by a temporary wall as shown in Fig. 1. Waves were created by a wave machine of the plunger type located at one end of the channel. The wave machine could be regulated to produce waves of various heights and periods. The model was centered in the channel approximately 45 feet from the plunger. After passing the model, the waves were reflected out of the channel into the larger portion of the tank where their energy was dissipated by means of an artifial beach (Fig. 1). Wave heights were measured by means of recording electric resistance gages.

The testing frame was mounted on two heavy I-beams supported on the walls of the wave channel. A photograph showing the method of supporting the model and some of the instrumentation is shown in Fig. 2. Details of the dynamometer frame are shown in Fig. 3. Two inverted U-shaped frames (U) served as the supporting structure for the models. A horizontal plate (P) was suspended from the U-frames by four slender aluminum rods (r) 4 feet long. The dynamometer plate was restrained from horizontal movement by 3 dynamometers designated in Fig. 3 as $h_a$, $h_b$, and N. The first two prevented the plate from moving in the direction of wave travel, and the third supplied horizontal restraint in the direction normal to wave motion. The models were suspended from the aluminum plate by two struts (s) streamlined in the direction of wave motion. The length of the struts was adjustable, so that the vertical position of the model could be varied.

Dynamometers $h_a$ and $h_b$ consisted of small aluminum cantilevers fastened to one of the I-beams, and connected to the dynamometer plate by means of small bars in such a manner as to be unaffected by vertical forces. Dynamometer N was fastened to a cross member as shown in Fig. 3. Electrical resistance gages were cemented on opposite sides of the cantilevers and connected to opposite arms of a Wheatstone bridge in a Brush strain amplifier. The dynamometers were calibrated by subjecting them to known horizontal forces and recording the corresponding change in resistance by means of an oscillograph. The relationship between the force on the dyna-

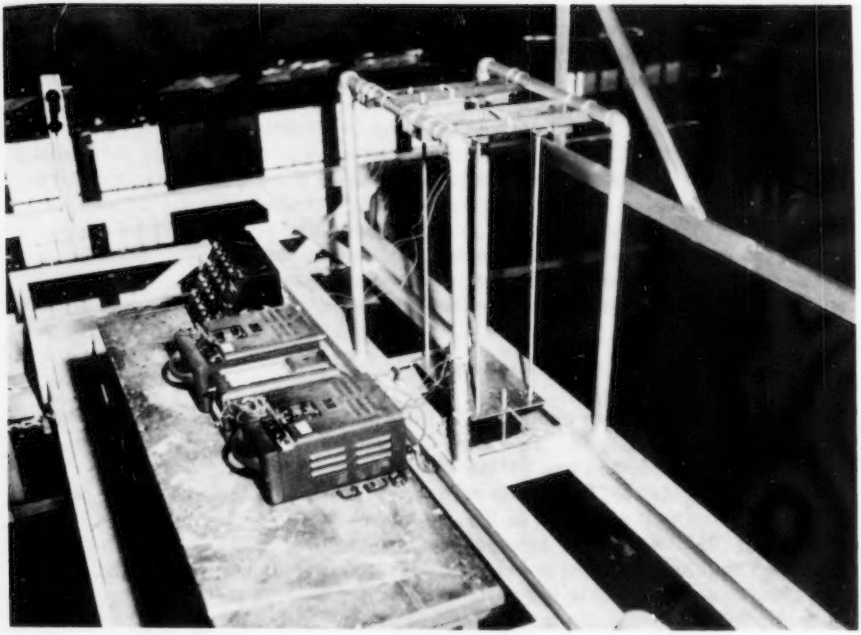

TESTING ARRANGEMENT
Fig. 2

mometers and the force on the model was determined by applying loads at various model positions and noting the resulting forces on the dynamometers.

Vertical forces were measured by means of two dynamometers, $v_a$ and $v_b$, which consited of slender horizontal beams through which the four supporting rods were connected to the testing frame as shown in Figs. 2 and 3. Strain gages were placed on top and bottom of the center of these beams. Vertical loads on the model produced bending moments in the beam and changes in the resistances of the strain gages which were recorded by means of an oscillograph. These dynamometers were so arranged that they were not affected by horizontal forces.

## Test Procedure

An extensive series of preliminary investigations was made before beginning the principal tests in order to determine the behavior of the waves in the testing area. One phase of the preliminary investigation was planned to determine the effect of the presence of the model on wave heights in the vicinity of the model. The placing of the model in the water caused variations in the wave height for some distance upstream. However, a point 11.0 feet upstream from the model was found to be free from this effect for all

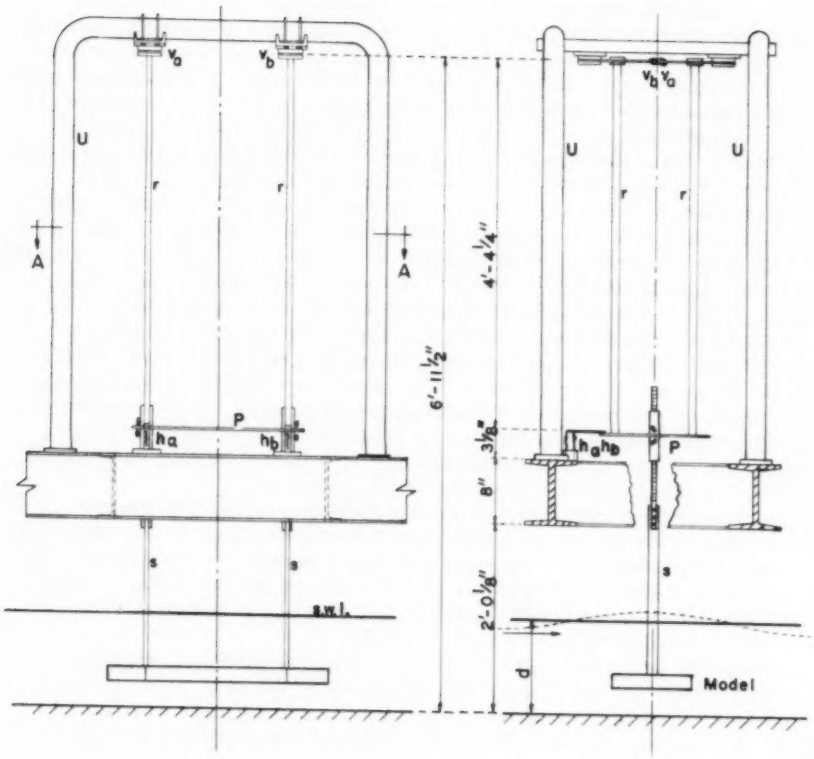


Front View

Side View

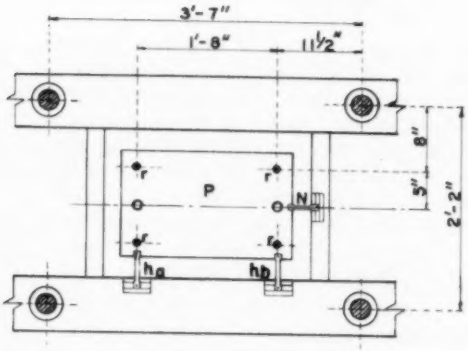


Section A-A

DYNAMOMETER FRAME

FIGURE 3

conditions, and was, therefore, selected as the wave gage location.

The variation in wave height in the direction perpendicular to the wave motion was also studied. For certain wave frequencies, standing transverse waves were developed which produced a variation in wave height from one side of the model to the other of as much as 40 per cent. For such conditions, a single measurement of wave height at the center of the model provided a value which differed as much as five per cent from the average effective wave height. This phenomenon was caused by the establishment of a resonant motion in the channel and tank, and no method was found to eliminate it. However, these standing transverse waves did not appear until approximately seventeen waves had passed the model following the beginning of a test. Also, the first 4 or 5 waves of a group changed in size and length as they progressed along the channel from the wave rod to the model. Both difficulties were avoided by using only those waves between the 5th and 17th in a series.

The dynamometers were calibrated by loading the model with known weights. The periodic loading resulting from wave motion was simulated by manual manipulation of the weights. The calibration coefficient for the sum of the two principal horizontal dynamometers differed by 2.5 per cent from the beginning until the end of the testing program. For the vertical dynamometers there was no measurable difference in the calibration coefficient from the beginning until the end of the testing program.

The wave rod was calibrated by raising and lowering the rod known amounts and noting the corresponding oscillograph reading. It was necessary to conduct the calibration in the wave tank itself because the calibration was affected by the chemical composition of the water or the grounding conditions. The calibration curve was nearly linear, and, although it remained virtually constant, a new calibration was made each day.

The desired water depth was maintained by adding water to compensate for evaporation. The water depth was measured at the front of the model. The concrete floor of the tank was relatively smooth but there were undulations as great as 1/4 inch in the region between the model and the wave machine.

Prior to starting a test run, the wave machine was adjusted to generate a wave of the desired height and period, and the model was placed at the desired elevation. During the first run simultaneous measurements were made of the wave height at a point 11 feet upstream from the model and of either the horizontal or the vertical forces. Such a test required three oscillograph channels because both the horizontal and vertical forces were obtained by adding the forces in two dynamometers. Upon completing such a run, one dynamometer was switched off and a record was obtained from a wave rod located at the side of and opposite the center of the model. The wave heights measured by this gage were distorted by the presence of the model and were used only to obtain a phase relationship between the wave and forces. In the early tests, records were also taken from dynamometer N to determine forces normal to the direction of wave motion. This was discontinued because these forces were found to be very small.

## The Experimental Program

The testing program was planned to determine horizontal and vertical forces on barges of several shapes for a variety of wave characteristics and

W = 2'-6" L' = 10" D = 1 7/8"

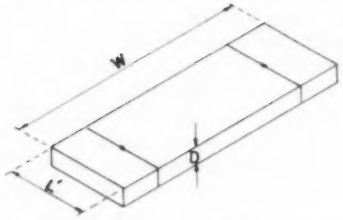


Rectangular Barge

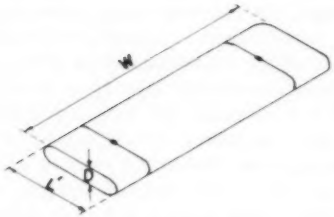


Rounded Barge

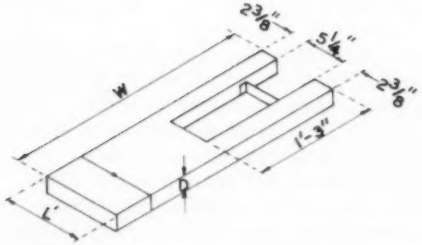


Slotted Rectangular Barge

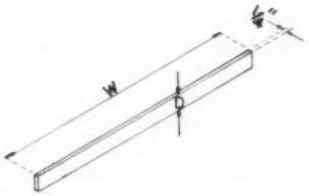


Flat Plate

## MODELS
FIGURE 4

for various barge locations. Representative results were sought throughout so as to establish trends rather than to provide complete results for all possible combinations of variables. The depth of water (d) was kept constant at one foot throughout the tests. This depth, as well as the model dimensions and the wave characteristics, were selected as being typical of representative prototype values reduced in a linear scale ration of 1 to 100.

The basic model was a rectangular parallelepiped 2' 6" long, 10 inches wide, and 1-7/8 inches high as shown in Fig. 4. Two modifications of the basic model were studied. One modification consisted of the inclusion of a slot in one end of the barge to simulate a typical drilling structure, and the second was the rounding of the upstream and downstream sides as shown in Fig. 4. Tests were also made on a flat plate having the same area as one side of the barge and a thickness of 1/4 inch. All tests were conducted with the top edges of the models horizontal and with the long side (2' 6" x 1-7/8") normal to the direction of wave motion.

For each barge position and wave period, waves of three sizes were projected against the model. The smallest wave height (H) in such a series was usually about 0.1 foot, the intermediate one approximately 0.2 foot and the largest greater than .25 foot. Three wave periods (T) were used in the tests on the basic model. These were approximately 1.4 seconds, 1.1 seconds, and 0.85 second, the corresponding wave lengths (L) being 7.1 feet, 5.2 feet, and 3.5 feet, respectively. Values of d/L thus varied from 0.14 to 0.29. Actual wave periods for individual tests differed slightly, the values given above being approximately the averages for the three groups of tests. For the period of 1.1 seconds, the model was tested at 10 locations varying from a position with the center of the barge 0.17 inches below the water surface to a location as near the bottom as possible without touching the bottom. For periods of 1.4 seconds and 0.9 second, all tests were conducted with the barge at mid-depth. The slotted and rounded barges were tested only for a wave having a period of 1.1 seconds.

## Oscillatory Wave Motion

Oscillatory waves are so called because the water particles oscillate in nearly closed orbits, there being substantially no forward motion of the fluid. In relatively deep water ($d/L > 0.5$), the orbits are circular at the water surface, becoming slightly elliptical and much smaller as the bottom is approached. In shallow water ($d/L < 0.5$), the particle orbits are elliptical throughout the depth. The analysis of the test data requires the use of theoretical relationships which define the form and orbital motion of the waves. Several rather complete summaries of wave theory are available.(9,10,11,12)

Equations for the shape of and motion in oscillatory waves were developed by Airy.(13) Although his derivation was based on the assumption that wave heights are small, his results are sufficiently accurate for many purposes even though used to describe waves with appreciable amplitudes. Stokes(14) developed equations which include the effect of wave height, but they are exceedingly cumbersome. The small refinement provided by them was not justified in the analysis of the test results. Consequently, the relationships utilized and presented in the following paragraphs are those credited to Airy.

The wave length (L), the distance from crest to crest of adjacent waves, is related to the other characteristics of a wave by the following expression:

$$L = \frac{gT^2}{2\pi} \tanh \frac{2\ d}{L} \qquad (1)$$

in which T is the wave period in seconds and d is the depth of water. The relationship between wave period, wave velocity (C), and wave length is

$$L = CT \qquad (2)$$

The approximate equation for the wave profile is

$$y = \frac{H}{2} \cos \frac{2\pi x}{L} \qquad (3)$$

in which x and y are the horizontal and vertical coordinates of the water surface and H is the wave height. Values of x are positive in the direction of

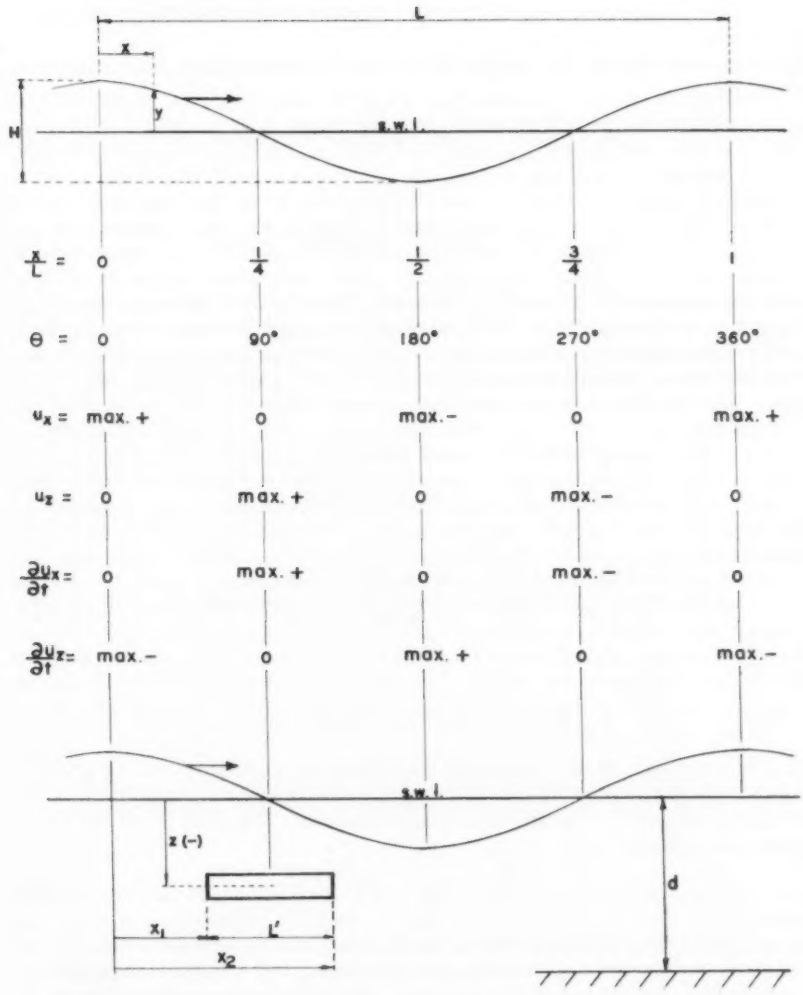


Characteristics of

OSCILLATORY WAVES

FIGURE 5

wave motion and y is measured positively upward from the still water level (s.w.l.) as illustrated in Fig. 5. The expression $2\pi x/L$ is the phase angle in radians which is designated as $\theta$. In degrees, $\theta$ varies from 0 at a crest to 360° at the preceding crest, as shown in Fig. 5. The phase angle can also be expressed in terms of time as $2\pi t/T$ where t varies from 0 to T during a wave cycle.

The equations for the horizontal and vertical components of the orbital velocity are

$$u_x = \frac{\pi H}{T} \frac{\cosh 2\pi(d + z)/L}{\sinh 2\pi d/L} \cos \theta \tag{4}$$

and

$$u_z = \frac{\pi H}{T} \frac{\sinh 2\pi(d + z)/L}{\sinh 2\pi d/L} \sin \theta \tag{5}$$

In these equations, z is the vertical distance from the still water surface to the point where the velocity is being determined, upward being taken as positive. The corresponding expression for horizontal and vertical accelerations can be determined by differentiating Eqs. (4) and (5) partially with respect to time. The resulting expressions are

$$\frac{\partial u_x}{\partial t} = \frac{2\pi^2 H}{T^2} \frac{\cosh 2\pi(d + z)/L}{\sinh 2\pi d/L} \sin \theta \tag{6}$$

and

$$\frac{\partial u_z}{\partial t} = \frac{-2\pi^2 H}{T^2} \frac{\sinh 2\pi(d + z)/L}{\sinh 2\pi d/L} \cos \theta \tag{7}$$

## Oscillatory Wave Forces

The forces produced on submerged structures by oscillatory waves are of two types: the drag force, resulting from the orbital velocity; and the inertial force, resulting from the orbital acceleration. The drag force can be expressed as follows,

$$F_d = C_d A \frac{\rho u^2}{2} \tag{8}$$

in which $C_d$ is a drag coefficient, $\rho$ is the density, A is the cross-sectional area of the structure in a plane normal to the force, and u is the component of the velocity in the direction of the force. The flow pattern referred to is that which would occur if flow were not disturbed by the presence of the model. Because of the nature of the velocity variation, the horizontal drag force varies from a maximum downstream value under the crest of a wave ($x/L = 0$) to a maximum upstream value under a trough ($x/L = 0.50$) as illustrated in Fig. 5.

For steady flow, the drag coefficient has been examined for many different shapes and has been found to be a function of the form and of the Reynolds

number.[15,16] However, it was not known whether such values could be used for the periodic unsteady flow produced by oscillatory waves. An additional complication arises for the case of large structures because of the variation of the motion within the dimensions of the body.

The inertial force is expressed by the equation,

$$F_i = C_m \rho V \frac{\partial u}{\partial t} \tag{9}$$

in which $C_m$ is the coefficient of inertial resistance, V is the displaced volume and $\partial u/\partial t$ is the component of the acceleration in the direction of the force for undisturbed flow. This type of force occurs for two reasons. The acceleration of the fluid is caused by a pressure gradient so that the pressure on the upstream face of the submerged structure is not the same as that on the downstream face. The resulting force can be shown to be equal to the product of the acceleration and the mass of the displaced volume. Also, because of the presence of the body, the accelerations in the flow around the body are increased, thus requiring an additional force. This force divided by the acceleration of the ambient flow is called the virtual mass, and is conveniently expressed by its ratio to the mass of the fluid displaced by the body. Thus, $C_m$ is the sum of a term, approximately unity, for the pressure gradient force, and the coefficient of virtual mass.

The variation of the horizontal acceleration, Eq. (6), is such that the horizontal inertial force varies from a maximum downstream value at $x/L = 1/4$ to a maximum upstream value at $x/L = 3/4$ as illustrated in Fig. 5.

Values of the virtual mass coefficient have been determined theoretically and experimentally for bodies of various shapes. For irrotational flow without separation, values are available for elliptical cylinders and ellipsoids[17] and for infinitely long bodies of rectangular cross-section[18] as shown in Fig. 6. The corresponding values obtained experimentally,[19,20] by oscillations at high frequency and small amplitude, correspond fairly well with the theoretical values. Values of $C_m$ obtained in this manner may not be applicable to flows in which separation plays a predominant role. In fact, the development of a wake has been found to cause marked changes in both $C_d$ and $C_m$.[9] Variations in flow over the length of large bodies cause further uncertainties. Consequently, the applicability of theoretical results to flows produced by oscillatory waves must be tested experimentally.

The total force is the sum of the two forces given by Eqs. (8) and (9).

$$F = C_d A \frac{\rho u^2}{2} + C_m \rho V \frac{\partial u}{\partial t} \tag{10}$$

Because the two forces are 90° out of phase, the maximum combined downstream force may occur at any value of x from $x/L = 0$ to $x/L = 1/4$, depending on the relative magnitude of the components. The magnitude and location of the maximum force for the case of cylindrical piles has been discussed by Morison and others.[2,3]

For large structures, it is convenient to express the horizontal inertial force in terms of the pressures exerted on the body. If the rectangular outline shown in Fig. 5 is assumed to contain only the undisturbed fluid, and if convective accelerations are neglected, then an application of the equations of motion to this volume of fluid in the x-direction yields the following expression

$$(p_1 - p_2) A_x = \rho V \frac{\partial u_x}{\partial t} \tag{11}$$

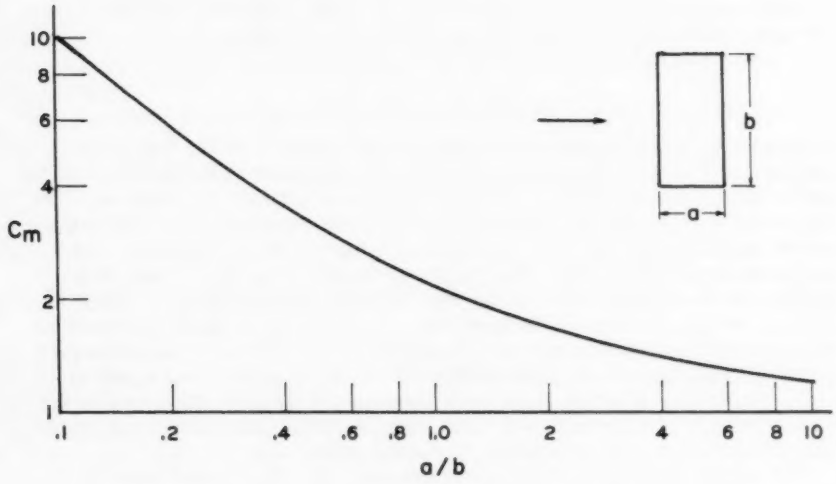


$C_m$ FOR TWO DIMENSIONAL FLOW PAST RECTANGULAR BODIES

Fig. 6

in which $p_1$ and $p_2$ are the pressures on the two sides of the volume of fluid, $A_x$ is the cross-sectional area of the volume taken normal to the force, and $\partial u_x/\partial t$ is the average horizontal acceleration of the fluid. Substitution in Eq. (9) results in the following expression for the inertial force

$$F_i = C_m (p_1 - p_2) A_x \tag{12}$$

From the equation of motion written for the vertical direction, the following relationship can be obtained,

$$\frac{\partial p}{\partial z} = -w + \rho \frac{\partial u_z}{\partial t} \tag{13}$$

in which w is the unit weight of the fluid.

The substitution of the value of $\partial u_z/\partial t$ from Eq. (7) and integration yields

$$p = -wz + \rho \frac{\pi LH}{T^2} \frac{\cosh 2\pi(d + z)/L}{\sinh 2\pi d/L} \cos \theta + C \tag{14}$$

The constant C can be evaluated because of the fact that p = 0 for points on the water surface, i.e., for z = y. The expression for the pressure then becomes

$$p = w(-z+y)+\rho \frac{\pi LH}{T^2} \frac{\cosh 2\pi(d+z)/L - \cosh 2\pi(d+y)/L}{\sinh 2\pi d/L} \cos\theta \quad (15)$$

The value of $(p_1 - p_2)$ to be used in Eq. (12) is found by inserting in Eq. (15) appropriate values of x and y for the two sides of a submerged body.

For the particular case of a rectangular barge centered at the quarter point of a wave, substitution in Eq. (15) yields

$$(p_1-p_2) = wH \cos \frac{2\pi x_1}{L}\left[K - 2 \sinh^2\left(\frac{\pi H \cos 2\pi x_1/L}{2L}\right)\right] \quad (16)$$

in which K is defined as follows,

$$K = \frac{\cosh 2\pi(d + z)/L}{\cosh 2\pi d/L} \quad (17)$$

and $x_1$ is the value of x at the upstream side of the model as shown in Fig. 5. Eq. (16) indicates that the pressure difference on the two sides of the body results from the difference in the water surface elevation, $\triangle H$, ($\triangle H = H \cos 2\pi x_1/L$) modified by the term in the brackets which corrects for vertical accelerations.

The difference in the pressures occurring under a crest and a trough can also be obtained from Eq. (16) by letting $x_1 = 0$ and $z = -d$. Then

$$\frac{(p_c - p_t)}{wH} = K - 2 \sinh^2 \frac{\pi H}{2L} \quad (18)$$

in which $p_c$ is the pressure under a crest and $p_t$ the pressure under an adjacent trough. Folsom[21,22] measured values of the ratio shown on the left side of Eq. (18) as part of a study of a pressure wave gage and compared them with K. He found that the measured values of the ratio were between 10 and 20 per cent less than K. The correction provided by the additional term in the right side of Eq. (18) improves somewhat the correspondence between theory and the results of Folsom's experiments.

## Wave Forces on a Flat Plate

The results of the tests for horizontal forces on the flat plate are presented in Table 1. The wave heights (column 4), measured forces (columns 5 and 7), and location of model at the time of maximum force (columns 6 and 8) were determined by averaging values from three or four successive waves. Heights of individual waves were taken as the average height of a crest above adjacent troughs. Separation of the upstream force from the downstream value was based on the assumption that position of the oscillograph pen corresponding to zero force did not shift during a test. Although this change was small, it may have caused minor inconsistencies in individual values.

The wave lengths shown in column 3 were computed by means of Eq. (1). The measurement of wave lengths was not part of the routine testing program. Nevertheless, a number of wave lengths were measured and the observed values corresponded with the computed values within 5 per cent.

TABLE I

RESULTS OF TESTS ON A FLAT PLATE

| 1 | 2 | 3 | 4 | 5 | 6 | 7 | 8 | 9 | 10 | 11 | 12 |
|---|---|---|---|---|---|---|---|---|---|---|---|
| | | | | Measured Values | | | | Computed Values | | | |
| | | | | Downstream Forces | | Upstream Forces | | | | | |
| z/d | T Sec | L Feet | H Feet | Max. Force Pounds | x/L | Max. Force Pounds | x/L | x/L | $F_i$ Pounds | $F_d$ Pounds | Max. Force Pounds |
| -0.5 | 1.15 | 5.52 | 0.206 | 0.50 | 0.16 | 0.43 | 0.69 | 0.13 | 0.30 | 0.14 | 0.44 |
| -0.5 | 1.11 | 5.26 | 0.069 | 0.13 | 0.21 | 0.13 | 0.72 | 0.25 | 0.16 | 0 | 0.16 |
| -0.5 | 1.12 | 5.32 | 0.314 | 0.83 | 0.05 | 0.87 | 0.63 | 0.08 | 0.32 | 0.51 | 0.83 |
| -0.5 | .872 | 3.66 | 0.086 | 0.21 | 0.23 | 0.19 | 0.74 | 0.25 | 0.19 | 0 | 0.19 |
| -0.5 | .875 | 3.68 | 0.280 | 0.63 | 0.15 | 0.59 | 0.69 | 0.16 | 0.51 | 0.11 | 0.62 |
| -0.5 | .884 | 3.74 | 0.288 | 0.72 | 0.13 | 0.74 | 0.68 | 0.15 | 0.51 | 0.14 | 0.65 |
| -0.5 | 1.41 | 7.19 | 0.049 | 0.06 | 0.24 | 0.06 | 0.72 | 0.25 | 0.09 | 0 | 0.09 |
| -0.5 | 1.36 | 6.86 | 0.250 | 0.58 | 0.09 | 0.63 | 0.65 | 0.08 | 0.21 | 0.39 | 0.60 |
| -0.5 | 1.42 | 7.24 | 0.144 | 0.34 | 0.11 | 0.34 | 0.67 | 0.14 | 0.19 | 0.07 | 0.26 |
| -0.25 | .871 | 3.65 | 0.082 | 0.28 | 0.20 | 0.23 | 0.71 | 0.25 | 0.25 | 0 | 0.25 |
| -0.75 | 1.16 | 5.59 | 0.289 | 0.92 | 0.10 | 0.82 | 0.58 | 0.09 | 0.30 | 0.32 | 0.62 |
| -0.75 | .875 | 3.68 | 0.296 | 0.65 | 0.15 | 0.75 | 0.64 | 0.25 | 0.51 | 0 | 0.51 |
| -0.75 | 1.38 | 6.98 | 0.245 | 0.75 | 0.09 | 0.67 | 0.59 | 0.08 | 0.21 | 0.32 | 0.53 |

In the analysis of the wave forces on a flat plate, both the drag force and the inertial force were found to be significant. The total horizontal force is determined from Eq. (10) by using the horizontal components of the velocities and accelerations. Values of F were computed by inserting into Eq. (10) the quantities which apply to this case. Values of $C_d$ and $C_m$ were selected to give the best correspondence with the measured phase angles and magnitudes of the maximum forces. A value of 3.5 was found for $C_d$ and the value of $C_mV$ was found to be 1.75 times the volume of the circumscribing cylinder, which is 1.75 times the theoretical value(20) for an infinitely long thin flat plate. Because these values are large, an effect of the unsteadiness of the flow on the shape of the wake is indicated. Values of $u_x$ and $\partial u_x/\partial t$ were computed from Eqs. (4) and (6), respectively.

For any particular value of wave height and wave period and for a particular model location, F is a function only of the phase angle and Eq. (10) can be expressed as follows:

$$F = C_d' \cos^2\theta + C_m' \sin\theta \tag{19}$$

in which

$$C_d' = C_d A \frac{\rho \pi^2 H^2}{2T^2} \left[\frac{\cosh 2\pi(d+z)/L}{\sinh 2\pi d/L}\right]^2 \tag{20}$$

and

$$C_m' = C_m \rho V \frac{2\pi^2 H}{T^2} \left[\frac{\cosh 2\pi(d+z)/L}{\sinh 2\pi d/L}\right] \tag{21}$$

The phase angle corresponding to the maximum force is obtained by setting $dF/d\theta = 0$, with the result shown in Eq. (22).

$$\sin\theta_{max} = \frac{C_m'}{2C_d'} \tag{22}$$

Computed values of $\theta_{max}$ expressed in terms of x/L are shown in column 9 of Table 1 and the corresponding values of $F_d$, $F_i$, and F are shown in columns 10, 11, and 12, respectively. Computed phase angles and forces are presented together with measured values in Table 1. These values are also compared graphically in Fig. 7, in which computed values are plotted against both upstream and downstream measured values. Although there is considerable scatter in the data for the phase angle (Fig. 7a), the trends indicate good correspondence between measured and computed values. The correspondence between measured and computed forces, shown in Fig. 7b, is good for z/d = -0.25 and -0.50. For z/d = -0.75 the measured values exceed the computed values by about 30 per cent.

## Horizontal Forces on Barge Models

Results of tests for barge models are presented in Tables 2 and 3. In Table 2 are shown results of a number of tests for which the data were analyzed in considerable detail. The values of wave height, maximum force, and phase angle at the time of the maximum force were determined by

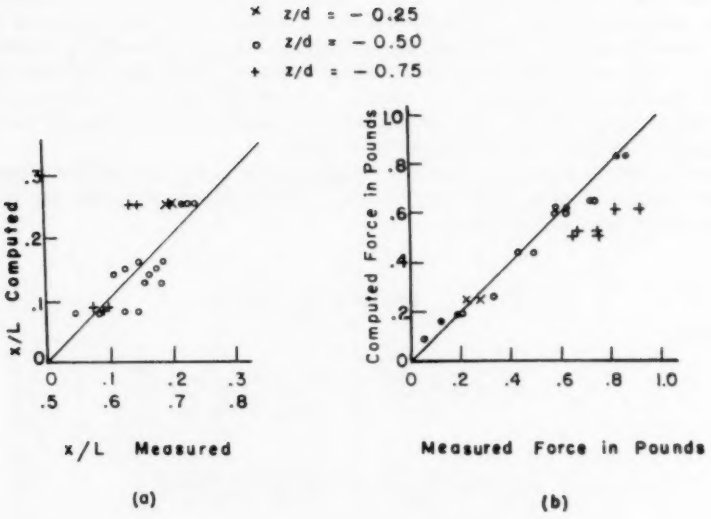


FLAT PLATE DATA

Fig. 7

averaging the results for three or four successive waves. The downstream forces were separated from the upstream values and are shown separately in Columns 8 and 11. The upstream forces were, on the average, 6.6 per cent smaller than the downstream forces. These values are subject to the same instrumental limitations as are those for the flat plate.

The difference in water surface elevation on the two sides of the barge, $\Delta H$, at the time of the occurrence of the maximum force were scaled from the oscillograph charts. The values are shown for the maximum downstream forces in column 9 and for the maximum upstream forces in column 12.

In Table 3 are shown the results of a number of tests which illustrate the effect on the force of the position of the barge in the vertical. These tests were conducted on the rectangular model for three different wave heights with the wave period held constant at approximately 1.1 seconds. The location of the center of the barge (-z) was varied from 0.08 feet to 0.92 feet below the water surface. In the latter position, the barge was very close to, but not touching, the bottom. Three different wave heights were used as shown

TABLE 2

HORIZONTAL FORCES ON BARGE MODELS

| 1 | 2 | 3 | 4 | 5 | 6 | 7 | 8 | 9 | 10 | 11 | 12 | 13 | 14 |
|---|---|---|---|---|---|---|---|---|---|---|---|---|---|
| | | | | | | Downstream Force | | | Upstream Force | | | | |
| Type of Model | z/d | T Sec | L Ft | H Ft | H/L | x/L | Av. Max. Force Pounds | ΔH Feet | x/L | Av. Max. Force Pounds | ΔH Feet | $C_m$ | ΔH Computed Feet |
| Rectangular | -0.25 | 1.09 | 5.12 | 0.206 | .0402 | 0.13 | 3.07 | 0.097 | 0.77 | 2.68 | 0.094 | 1.59 | 0.101 |
| " | -0.50 | 1.09 | 5.12 | 0.202 | .0395 | 0.25 | 2.24 | 0.092 | 0.79 | 2.11 | 0.094 | 1.49 | 0.095 |
| " | -0.75 | 1.08 | 5.06 | 0.209 | .0412 | 0.26 | 2.10 | 0.094 | 0.77 | 2.04 | 0.091 | 1.50 | 0.103 |
| " | -0.92 | 1.09 | 5.12 | 0.207 | .0404 | 0.23 | 2.30 | 0.098 | 0.73 | 2.23 | 0.091 | 1.70 | 0.102 |
| " | -0.25 | 1.11 | 5.26 | 0.272 | .0517 | 0.12 | 3.45 | 0.116 | 0.77 | 3.28 | 0.123 | 1.39 | 0.129 |
| " | -0.50 | 1.10 | 5.19 | 0.269 | .0519 | 0.23 | 2.69 | 0.119 | 0.77 | 2.32 | 0.119 | 1.31 | 0.129 |
| " | -0.75 | 1.11 | 5.26 | 0.272 | .0518 | 0.23 | 2.44 | 0.137 | 0.76 | 2.37 | 0.109 | 1.34 | 0.129 |
| " | -0.92 | 1.12 | 5.32 | 0.278 | .0522 | 0.21 | 2.85 | 0.126 | 0.77 | 2.64 | 0.113 | 1.59 | 0.130 |
| " | -0.25 | 1.11 | 5.26 | 0.064 | .0124 | 0.23 | 1.02 | 0.031 | 0.80 | 0.85 | 0.030 | 1.76 | 0.030 |
| " | -0.50 | 1.11 | 5.26 | 0.073 | .0139 | 0.23 | 0.85 | 0.035 | 0.76 | 0.82 | 0.032 | 1.52 | 0.035 |
| " | -0.75 | 1.11 | 5.26 | 0.073 | .0139 | 0.26 | 0.82 | 0.036 | 0.78 | 0.68 | 0.034 | 1.67 | 0.035 |
| " | -0.92 | 1.10 | 5.19 | 0.074 | .0143 | 0.25 | 0.84 | 0.037 | 0.77 | 0.84 | 0.035 | 1.72 | 0.036 |
| " | -0.50 | .862 | 3.58 | 0.061 | .0170 | 0.23 | 0.72 | 0.040 | 0.77 | 0.77 | 0.043 | 1.52 | 0.041 |
| " | -0.50 | .873 | 3.66 | 0.210 | .0575 | 0.18 | 2.45 | 0.135 | 0.72 | 2.35 | 0.110 | 1.52 | 0.137 |
| " | -0.50 | 1.41 | 7.17 | 0.113 | .0158 | 0.21 | 1.20 | 0.045 | 0.75 | 1.01 | 0.040 | 1.59 | 0.040 |
| " | -0.50 | 1.41 | 7.17 | 0.212 | .0296 | 0.15 | 2.26 | 0.078 | 0.76 | 1.96 | 0.063 | 1.46 | 0.076 |
| Rounded | -0.25 | 1.11 | 5.26 | 0.224 | .0426 | 0.16 | 2.99 | | 0.81 | 2.82 | | 1.53 | 0.102 |
| " | -0.75 | 1.11 | 5.26 | 0.247 | .0470 | 0.23 | 2.14 | | 0.76 | 1.97 | | 1.35 | 0.112 |
| " | -0.75 | 1.11 | 5.26 | 0.121 | .0230 | 0.25 | 1.14 | | 0.74 | 1.12 | | 1.45 | 0.055 |
| " | -0.75 | 1.11 | 5.26 | 0.295 | .0560 | 0.22 | 2.40 | | 0.74 | 2.29 | | 1.27 | 0.134 |
| Slotted | -0.75 | 1.11 | 5.26 | 0.168 | .0319 | 0.28 | 1.42 | 0.065 | 0.78 | 1.52 | 0.075 | 1.74 | 0.080 |
| " | -0.75 | 1.12 | 5.32 | 0.316 | .0593 | 0.15 | 2.49 | 0.177 | 0.77 | 2.47 | 0.116 | 1.62 | 0.149 |

TABLE 3

HORIZONTAL FORCES ON RECTANGULAR BARGE

For T = 1.1 Seconds

| z | Average Maximum Force in Pounds | | |
|---|---|---|---|
| | H = .27 ft. | H = .21 ft. | H = .071 ft. |
| -.08 | 2.99 | 2.85 | 1.07 |
| -.17 | 3.54 | 3.21 | 1.22 |
| -.25 | 3.31 | 2.87 | .94 |
| -.33 | 3.08 | 2.54 | .89 |
| -.42 | 2.71 | 2.25 | .86 |
| -.50 | 2.45 | 2.17 | .83 |
| -.58 | 2.48 | 2.05 | .75 |
| -.67 | 2.41 | 2.03 | .73 |
| -.75 | 2.40 | 2.09 | .75 |
| -.83 | 2.43 | 2.10 | .79 |
| -.92 | 2.80 | 2.25 | .73 |

in Table 3. Individual wave heights varied by less than five per cent from the average values for each group. The forces shown in Table 3 are the average of the upstream and downstream forces. From the results shown in Table 2, it can be estimated that the downstream forces were about 3 per cent larger than the average values shown.

The maximum horizontal forces were created when the quarter points of a wave ($x/L = 1/4$ or $3/4$) were approximately at the center of the barge as shown in Table 2, columns 7 and 10. Hence, the resistance caused by the velocity was negligible, and the maximum horizontal force was of the inertial type expressed by Eq. (9) or (12). Computed values of $\triangle H$ are shown in Table 2, column 14, together with the measured values for the rectangular and slotted barges (columns 9 and 12). The average of the computed values is 2 per cent higher than the average of the measured values for the downstream forces and 11 per cent higher than the measured upstream values.

Values of $C_m$ were computed for each test from Eqs. (12), (16), and (17) and are shown in column 13. The value of $x_1$ is $(L/4 - L'/2)$ in which L' is the width of the barge. For the case of the rounded barge an average width of 0.800 feet was used instead of the maximum width of 0.833 feet. The method of determining the values of $C_m$ is illustrated by the following computation for the test recorded at the top of Table 2. The value of K, from Eq. (17), is 0.784, and $\triangle H = 0.101$ (from column 14). The value of $(p_1 - p_2)$, from Eq. (16) is 4.94 psf. Finally, $C_m$ is found from Eq. (12).

$$C_m = \frac{F_1}{(p_1 - p_2)\, A_x} = \frac{3.07}{4.94 \times 0.39} = 1.59$$

For the slotted barge the displaced mass is used as a reference. In the computation of $C_m$, the forces on the inner faces of the slots ($p_1'$ and $p_2'$) must be considered. The expression for the force is as follows:

$$F = C_m \left[(p_1 - p_2)\, A_x - (p_1' - p_2')\, A_x'\right] \qquad (23)$$

in which $A_x'$ is the area of the inner faces of the slots.

The test data are summarized graphically in Fig. 8. The coefficient of inertial resistance for the rectangular barge is plotted against the ratio of wave height to wave length for three values of z/d with T constant at 1.1 seconds in Fig. 8a. The values of $C_m$ decrease significantly as the waves become steeper. The curves indicate the approximate trends.

In Fig. 8b, values of $C_m$ for the rectangular barge are plotted against the relative wave height for three wave periods, the barge position (z/d) being -0.50. In Fig. 8c, $C_m$ is plotted against relative wave height for three different barge shapes, for constant values of both z/d and T.

The wave force is plotted against z for three different wave heights in Fig. 9. These are the data from Table 3 with all force values increased by three per cent to transform them from average to downstream forces in accordance with the results presented in Table 2. The theoretical curves for the three wave heights were determined by means of Eqs. (12) and (16). The several constant values of $C_m$ used in determining these curves were selected to give a good average fit.

The tabulated data and the graphs indicate a general conformity between theory and test results. However, forces produced by the largest waves were less than would be expected from the results for the smaller ones. This is illustrated in Fig. 8 by the decrease in $C_m$ with increasing wave steepness and also in Fig. 9 in which the value of $C_m$, which produces the best fit for the largest waves, is much less than that for smaller waves. Some deviation from the theoretical curves is also indicated in Fig. 9 for tests with the model very near the bottom or very near the water surface.

The forces on the rounded barge were approximately 14 per cent less than those on the rectangular barge. The reasons for the lower force on the rounded barge can be explained with reference to Eq. (9), which shows the force to be proportional to the product of $C_m$ and the displaced mass. Four per cent of the reduction is the result of the smaller displaced mass of the rounded barge. The remaining reduction in force was caused by the increased streamlining with the resulting lower values of $C_m$, as illustrated in Fig. 8c.

Although the displaced mass of the slotted barge is 26 per cent less than that of the rectangular barge, the horizontal forces were only approximately 19 per cent less. Thus, the reduction in mass is partially offset by the additional disturbance attributable to the odd configuration of the slotted barge and the resulting increase in $C_m$ illustrated in Fig. 8c.

Values of $C_m$ for the rectangular model varied from 1.31 to 1.76. The value obtained from theoretical considerations of two-dimensional flow for this shape is 1.33 as shown in Fig. 6. Differences are expected because of

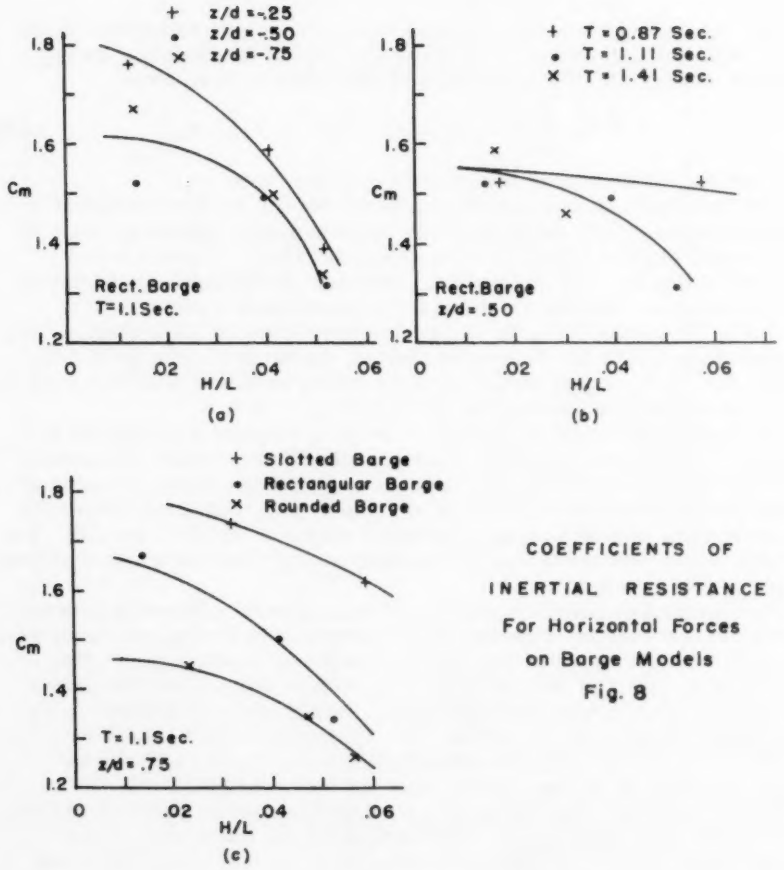


COEFFICIENTS OF INERTIAL RESISTANCE For Horizontal Forces on Barge Models Fig. 8

effects of periodic wake formation and because the effective dimension of the barge is an appreciable fraction of the wave length.

## Vertical Forces on Barge Models

Test results for the determination of vertical forces are shown in Table 4. In this case, the dynamometers were not sensitive enough to warrant the separation of upward forces from downward forces. However, the records do indicate that upward and downward forces were nearly equal for inter-

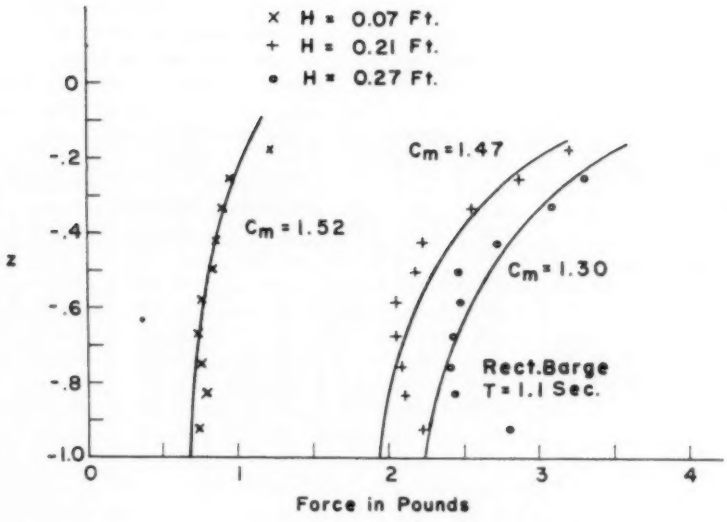


HORIZONTAL FORCES

on Barge Models

Fig. 9

mediate values of z, and that the upward force was greater than the downward force if the barge was located near the water surface or near the bottom. The values of vertical forces, shown in Table 4, are the averages of the upward and downward forces. The location of the barge with respect to a wave crest at the time of occurrence of the maximum force is shown for a number of tests on each of the barges in columns 6 and 7. Wave lengths, shown in column 4, were computed from Eq. (1).

The maximum downward vertical forces on the barge occurred if the crest was directly above the center of the barge ($x/L = 0$) as shown in column 6 of Table 4. The maximum upward force occurred in most cases if the trough was nearly over the center of the barge ($x/L = 1/2$), as shown in column 7. Thus, the vertical forces are also primarily inertial. Vertical forces can be analyzed by means of Eqs. (7) and (9).

Values of $C_m$, obtained from Eqs. (7) and (9) and enumerated in Table 4, can be compared with the classical values obtained from theory shown in Fig. 6.[18] Although theoretical results for rectangular bodies are available only if the length is infinite (two dimensional flow), experiments which have been conducted [19,20] indicate that the end effects for the lengths used are reductions in the virtual mass coefficient of five to ten per cent. For the proportions of the barge used in these tests, the theoretical value for two dimensional flow is 6.1, which is nearly the same as the average of the observed values. The average observed value for the rounded barge (referred

TABLE 4

VERTICAL FORCES ON BARGE MODELS

| 1 | 2 | 3 | 4 | 5 | 6 | 7 | 8 | 9 |
|---|---|---|---|---|---|---|---|---|
| Type of Model | z | T Sec | L Feet | H Feet | x/L Downward Force | x/L Upward Force | Av. Max. Force Pounds | $C_m$ |
| Rectangular | -0.25 | 1.09 | 5.12 | 0.215 | -0.10 | 0.26 | 7.31 | 4.8 |
| " | -0.50 | 1.09 | 5.12 | 0.198 | 0 | 0.42 | 4.54 | 5.2 |
| " | -0.75 | 1.09 | 5.12 | 0.198 | 0 | 0.50 | 2.15 | 5.2 |
| " | -0.92 | 1.08 | 5.06 | 0.196 | 0 | 0.49 | 1.33 | 10.0 |
| " | -0.50 | 1.13 | 5.39 | 0.306 | -0.01 | 0.27 | 5.63 | 4.4 |
| " | -0.50 | .834 | 3.39 | 0.252 | -0.01 | 0.39 | 6.48 | 4.2 |
| " | -0.50 | .832 | 3.38 | 0.066 | -0.03 | 0.46 | 2.06 | 5.1 |
| " | -0.50 | 1.40 | 7.11 | 0.210 | 0 | 0.41 | 3.45 | 5.7 |
| " | -0.50 | 1.48 | 7.60 | 0.110 | 0 | 0.45 | 1.89 | 6.6 |
| " | -0.17 | 1.1 | 5.2 | 0.207 | | | 5.85 | 3.4 |
| " | -0.33 | 1.1 | 5.2 | 0.187 | | | 6.67 | 5.9 |
| " | -0.42 | 1.1 | 5.2 | 0.193 | | | 5.69 | 5.8 |
| " | -0.58 | 1.1 | 5.2 | 0.199 | | | 3.96 | 5.5 |
| " | -0.67 | 1.1 | 5.2 | 0.194 | | | 3.14 | 5.8 |
| " | -0.83 | 1.1 | 5.2 | 0.205 | | | 1.72 | 5.9 |
| Rounded | -0.25 | 1.11 | 5.26 | 0.229 | 0 | 0.28 | 7.43 | 4.9 |
| " | -0.58 | 1.11 | 5.26 | 0.230 | 0 | 0.37 | 3.72 | 4.8 |
| " | -0.75 | 1.12 | 5.32 | 0.228 | 0 | 0.42 | 2.38 | 5.4 |
| " | -0.75 | 1.11 | 5.26 | 0.147 | 0 | 0.53 | 1.80 | 6.2 |
| " | -0.42 | 1.1 | 5.2 | 0.230 | | | 6.00 | 7.2 |
| " | -0.25 | 1.1 | 5.2 | 0.135 | | | 5.96 | 6.6 |
| " | -0.42 | 1.1 | 5.2 | 0.141 | | | 5.26 | 7.6 |
| " | -0.58 | 1.1 | 5.2 | 0.148 | | | 2.60 | 5.1 |
| " | -0.67 | 1.1 | 5.2 | 0.147 | | | 2.22 | 5.6 |
| Slotted | -0.58 | 1.11 | 5.26 | 0.152 | 0 | 0.45 | 1.50 | 3.8 |
| " | -0.58 | 1.11 | 5.26 | 0.321 | 0 | 0.32 | 2.40 | 2.9 |
| " | -0.75 | 1.10 | 5.19 | 0.322 | -0.03 | 0.34 | 1.49 | 3.1 |
| " | -0.25 | 1.1 | 5.2 | 0.145 | | | 3.51 | 4.7 |
| " | -0.42 | 1.1 | 5.2 | 0.151 | | | 2.29 | 4.0 |
| " | -0.25 | 1.1 | 5.2 | 0.289 | | | 6.25 | 4.1 |
| " | -0.42 | 1.1 | 5.2 | 0.316 | | | 4.11 | 3.5 |
| " | -0.75 | 1.1 | 5.2 | 0.317 | | | 2.02 | 4.2 |

to the somewhat smaller displaced mass of this shape) was 5.9, which is not significantly different from that of the rectangular barge. In comparison, for an elliptical section with the same proportions, an extreme in rounding, a theoretical value of 6.33 is obtained for two dimensional flow. Finally, an average value of $C_m$ of 3.8 was obtained from the tests on the slotted barge using its displaced mass as a reference. Although no theoretical value can be obtained for this shape, the weighted average of the theoretical values for two dimensional flow, for the unslotted portion (6.1), and for the legs (2.5), is 4.9. In view of geometrical differences and possible effects of separation, the theoretical and observed values of $C_m$ correspond surprisingly well.

The data are also shown graphically in Fig. 10. The forces on the rectangular and rounded models were plotted for various values of z in Fig. 10a. The group for the rectangular barge for a wave period of 1.1 seconds comprises the values shown in Table 4 for which the wave heights were approximately 0.20 feet. The group for the rounded barge is made up of the values from Table 4 having wave heights of approximately 0.23 feet. For this group, the forces were reduced by the ratio 0.20/0.23 before plotting, because, for a small range in wave height, the forces vary linearly with the wave height in accordance with the theory. The curves shown in Fig. 10a were determined from Eq. (7) and (9), using a $C_m$ of 5.5. This value was selected to give the best fit for this group of data. In Fig. 10b are shown groups of points for the rounded and slotted models. These values are the ones shown in Table 4 for wave heights of approximately 0.15 feet. The curves in Fig. 10b were determined from Eqs. (7) and (9) using the values of $C_m$ shown.

Good agreement was found between analytical and test values of the vertical forces on the three models used in this study. Values of $C_m$ correspond quite well with the theoretical values for two dimensional flow except for the cases in which the models were very near the surface or the bottom. In these cases, there was some indication that the upward forces were larger than the downward ones so that the values reported here (which are the average of the upward and downward forces) should be increased somewhat for design purposes. Further studies are required to determine the exact nature of the forces in these locations.

## SUMMARY

Forces exerted on submerged bodies by waves can be reliably predicted as a combination of the inertial and drag forces if the appropriate coefficients can be determined. The tests on the models of barge-like structures showed that the inertial forces were predominant so that only the coefficient of inertial resistance was needed to predict the maximum force. For the horizontal forces, the measured coefficient was approximately 1.5 compared to 1.33 as estimated from theory for flow without separation. For the vertical forces, the measured and estimated values of the coefficient were approximately six for the unslotted barge. Some systematic variation in the coefficient was found with relative wave height and with the vertical position of the model. Measured values for the slotted and rounded barges were also in good correspondence with theoretical values. Because the forces were primarily inertial, the rounding of the edges of the barge did not cause large changes in the forces.

The maximum horizontal forces on a vertical plate placed normal to the

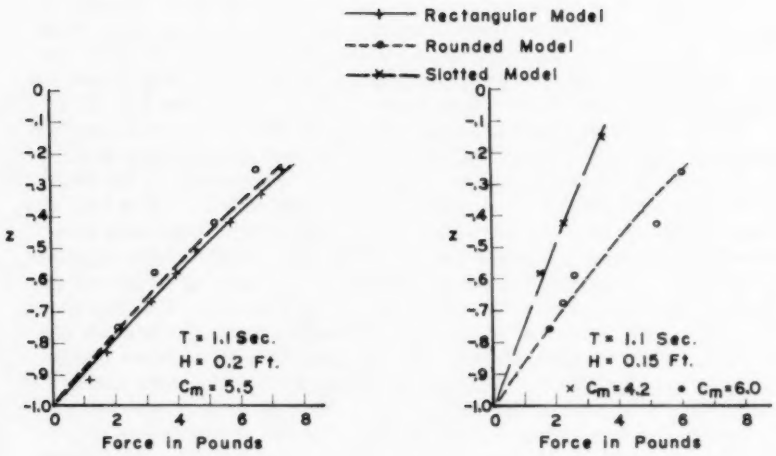


VERTICAL FORCES

on Barge Models

Fig. 10

direction of wave propagation were predictable if a drag coefficient of 3.5 and a virtual mass equal to 1.75 times that of the circumscribing cylinder were used. Both of these values are large because the growth of the wake in unsteady flow increases the drag coefficient and because the presence of any wake increases the virtual mass. The phases of the wave which produced the maximum forces corresponded satisfactorily with the predicted values.

## ACKNOWLEDGMENT

Funds for this research were provided by the Horace H. Rackham School of Graduate Studies of the University of Michigan, the Shipbuilding Division of the Bethlehem Steel Company, and the Shell Oil Company. The writers wish to express appreciation to the technical personnel of the latter organizations, particularly Mr. J. E. Steele, of the Bethlehem Steel Company, and Mr. L. E. Borgman, of the Shell Oil Company, for helping to plan the research program. Appreciation is also due to Mr. Nobuhiro Yotsukura, a graduate student, who painstakingly processed most of the test data.

## REFERENCES


1. "The Force Exerted by Surface Waves on Piles," Morison, J. R., M. P. O'Brien, J. W. Johnson, and S. A. Schaaf, Petroleum Trans., Amer. Inst. Mining Engrs., v. 189, 1950, pp. 149-154.

2. "The Design of Piling," Morison, J. R., Proc. 1st Conf. on Coastal Eng., 1951, pp. 254-258.

3. "Experimental Studies of Forces on Piles," Morison, J. R., J. W. Johnson, and M. P. O'Brien, Proc. 4th Conf. on Coastal Eng., 1954, pp. 340-370.

4. "Re-analysis of Existing Wave Force Data on Model Piles," Crooke, R.C., Tech. Memo. No. 71, Beach Erosion Board, U. S. Army Engineers, 1955.

5. "The Forces on Cylinders and Plates in an Oscillating Fluid," Keulegan, G. H., and L. H. Carpenter, NBS Rep. 4821, Sept. 1956.

6. "Drag in Unsteady Flow," McNown, J. S., Int. Congr. of Appl. Mech., Brussels, 1956.

7. "Model Study of an Off-shore Drilling Structure," Brater, E. F., and L. C. Maugh, Tech. Rep. No. 6, Univ. of Mich. Lake Hydr. Lab., 1953 (unpublished).

8. This laboratory is a facility of the Engineering Research Institute and the Department of Civil Engineering.

9. "A Summary of the Theory of Oscillatory Waves," O'Brien, M. P. and M. A. Mason, U. S. Beach Erosion Board Tech. Rep. No. 2, 1941.

10. "Elements of Wave Theory," Wiegel, R. L. and J. W. Johnson, Proc. 1st Conf. on Coastal Eng., 1951.

11. "Wave Motion," Keulegan, G. H., Chap. XI, Engineering Hydraulics, Edit. by Rouse, Wiley, 1950.

12. "Surface Waves and Offshore Structures," Ried, R. O. and C. L. Bretschneider, Tech. Rep., Texas A. and M. Res. Found., 1953.

13. "On Tides and Waves," Airy, G. B., Encyclopaedia Metropolitana, v. 5, London, 1845.

14. "On the Theory of Oscillatory Waves," Stokes, G. G., Trans. Cambridge Philosophical Society, v. VIII, 1847.

15. Basic Mechanics of Fluids, Rouse, Hunter and J. W. Howe, John Wiley and Sons, Inc., 1953, p. 183.

16. Fluid Mechanics, Streeter, V. L., McGraw-Hill Book Co., 1951, p. 314.

17. Hydrodynamics, 6th Ed., Lamb, H., Cambridge University Press, 1932.

18. "Sur la Resistance des Fluides," Riabouchinski, D., Int. Congr. of Math., Strasbourg, 1920, pp. 568-585.

19. "Virtual Masses of Rectangular Plates and Parallelepipeds in Water," Yu, Yee-Tak, Jour. of Applied Physics, v. 16, 1945, p. 724.

20. "Virtual Mass and Acceleration in Fluids," Stelson, T. E. and F. T. Mavis, Proc. ASCE, v. 81, Separate No. 670.

21. "Sub-Surface Pressures Due to Oscillatory Waves," Folsom, R. G., Trans. Amer. Geoph. Union, Dec. 1947, pp. 875-881.

22. "Measurement of Ocean Waves," Folsom, R. G., Trans. Amer. Geoph. Union, Oct. 1949, pp. 691-699.

Paper 1834 November, 1958 HY 6

Journal of the
HYDRAULICS DIVISION
Proceedings of the American Society of Civil Engineers

# SNOWMELT RUNOFF

J. Harold Zoller,[1] M. ASCE and Arno T. Lenz,[2] M. ASCE
(Proc. Paper 1834)

## SYNOPSIS

The primary factors relating to the melting of snow were evaluated for the snowmelt periods of 1938 through 1952 for the Big Eau Pleine River basin in Wisconsin. Convection and condensation melt potentials were computed from equations developed by previous investigators. A nomograph was devised for computing radiation snowmelt potential from insolation, as related to sun position determined by date, modified by cloud cover and albedo. The assumption was made that the runoff for any day would be a function of the summation of melt potentials for that day. A snowmelt unit hydrograph was developed and relative daily hydrographs were computed for each day. These relative hydrographs were then combined by a trial and error procedure to reproduce the recorded snowmelt hydrograph for each year. From this process the daily runoff values which contributed to the total hydrograph were computed. These daily runoff values were compared with the total melt potentials for the same days, and the correlation noted was expressed by an equation.

## INTRODUCTION

Spring runoff caused by the melting of the winter's accumulation of snow often provides an opportunity for the annual storage of a major part of the regional water resources. Reservoirs may be drawn down to produce water power during the high demand winter months with certain knowledge that melting of the existing snowpack will replenish the reservoir supply in the spring.

Note: Discussion open until April 1, 1959. To extend the closing date one month, a written request must be filed with the Executive Secretary, ASCE. Paper 1834 is part of the copyrighted Journal of the Hydraulics Division, Proceedings of the American Society of Civil Engineers, Vol. 84, No. HY 6, November, 1958.

1. Prof. of Civ. Eng., Univ. of New Hampshire, Durham, N. H.
2. Prof. of Civ. Eng., Univ. of Wisconsin, Madison, Wisc.

Research has revealed techniques by means of which the quantity of water which will become available in the snowmelt runoff of any basin may be estimated with considerable accuracy if certain minimum data are acquired.

The pattern of key research in the past has been to concentrate in small control areas the instrumentation necessary to measure every conceivable quantity suspected of being an agent in the melt phenomenon. This approach has yielded, and is continuing to yield, information of a most vital nature. However, to be of any practical value, this information must also be applicable to large basins where average instrumentation exists for the recording of pertinent data. If such applicability can be universally demonstrated, then the ultimate goal of the researchers will be attained.

Most of the concentrated research in the field of snowmelt has been confined to the mountainous areas of western United States, where much of the annual precipitation occurs in the form of snow. Here, snow may accumulate to great depths in the winter months and its melting season may extend from March to July or even later at the higher elevations. In these areas melting is almost always confined to the daylight hours and occurs chiefly as a result of insolation, air temperature and air turbulence produced by wind and topography.

In contrast, the snowpack in central Wisconsin is seldom over two feet in thickness at the time of initial melting and is commonly nearer one foot in thickness. It lies largely in open fields on gently rolling topography. Its melting season which also begins in March, never extends beyond April and has a continuous duration of from four to twenty days. During periods of high melt potential, melting may occur throughout the night as well as during the daylight hours, and the melting achieved by condensation of moisture on the cold snow surface may also be a major factor. Thus the problem of forecasting the rate of runoff from melting snow may be recognized as more difficult in many ways under the conditions imposed by Wisconsin's climate than would be the case for many regions farther west.

## Melt Potential Theory

The primary factors relating to the melting of snow are: Temperature of the air, temperature of the soil, wind velocity and air turbulence, humidity, rainfall and cloud cover. These factors are measurable, within certain limits, and from their recorded values the potential melting capacities attributable to convection, condensation, radiation, conduction and rainfall may be deduced. In addition, certain basic characteristics such as elevation, aspect, topography, cover, latitude and soil conditions are influential in the final melting capacity of a given melt potential.

A study was made of the melt potential—runoff characteristics of the Big Eau Pleine River Basin of Central Wisconsin. In this study the assumption was made that runoff in the snowmelt season was a direct function of the heat exchange relations between the snowpack and its environment. Accordingly, the total melt potential was determined for every six-hour interval in the snowmelt periods of the years 1938 to 1952. This total melt potential for any interval was considered to be the algebraic sum of the radiation melt potential, the convection melt potential and the condensation melt potential for that interval. It was further assumed that the runoff which occurred for any day would occur in a distribution indicated by the variation in melt potential

for that day. For example, if the total melt potential on a given day for the six-hour interval beginning at 9 a.m. were 1.5 inches and the total melt potential for the interval beginning at 3 p.m. were 0.5 inches, all other melt potentials for the day being negative, then it was assumed that the runoff hydrograph for that day's melt was a combination of the 9 a.m. and the 3 p.m. hydrographs in the ratio of 3 to 1 respectively. This procedure involved the determination of a snowmelt unit hydrograph and the determination of average daily discharges due to periods of melting beginning at different hours in the day. Negative melt potential summations were ignored because their effect is minimized by the low conductivity of the snowpack and because the time duration of negative melt potentials was short. Finally, it was reasoned that, if the theory and assumptions listed above were correct, a correlation would be found between the daily melt potential and the daily runoff for the various years being investigated.

### Convection Melt Potential

The convection melt potential is the quantity of water in inches which theoretically would be melted from snow of 100 per cent quality in a given time interval by the convective transfer of heat. The factors which are of importance in determining convective heat transfer are air temperature and turbulence, as indicated by wind velocity. Because preliminary studies with intervals of time equal to one day proved ineffective, the unit of time finally selected for investigation was six hours. Air temperatures and wind velocities were recorded at the Wausau CAA airport at 12:30 a.m., 6:30 a.m., 12:30 p.m. and 6:30 p.m. for the period of study. The 9 a.m. to 3 p.m. six-hour period is generally the most important snowmelt period of the day and the 12:30 p.m. temperature and wind velocity data may be considered fairly representative of that period. Thus, the four quarter-day periods were selected to begin at 3 a.m., 9 a.m., 3 p.m., and 9 p.m. It was assumed in all cases that the wind velocity and temperature readings were average values for the six-hour periods in which they occurred.

Although the Wausau CAA Airport is located completely outside the upper Big Eau Pleine Basin, approximately 30 miles east of the center of the basin, the Wausau data are considered applicable. Temperatures at Wausau and Medford, 20 miles northwest of the center of the basin, exhibit a very good correlation for the snowmelt period.

The convection melt potential was determined from Wilson's (1941) equation:

$$M = KV(T-32^{\circ})$$

"where M is the depth of water in inches melted from snow in six hours, V is the wind velocity in mph, T is the dry-bulb temperature in degrees F and K is a constant involving the latent heat of ice, exposure of instruments, air density, conversion of units, and certain considerations involved in the theory of turbulence." A value of K = 0.002 was used. This value of K corresponds closely to Light's (1941) value of K = 0.00176 as computed for the physical conditions imposed by the Big Eau Pleine Basin. The convection melt potential data for the snowmelt period of the year 1943 are tabulated in Table I.

### Condensation Melt Potential

The condensation melt potential may be defined as the amount of water in inches liberated from snow, plus condensate, as condensation occurs on the

TABLE I
CONVECTION AND CONDENSATION MELT POTENTIALS - 1943

| Date | Period* | Dry Bulb Temperature in °F | Dew Point in °F | Wind Velocity in mph | Convection Melt Potential in Inches | Condensation Melt Potential in Inches |
|---|---|---|---|---|---|---|
| March | | | | | | |
| 23 | 1 | 18 | 15 | 2 | -.06 | -.02 |
| | 2 | 39 | 26 | 20 | .28 | -.10 |
| | 3 | 39 | 29 | 16 | .22 | -.04 |
| | 4 | 33 | 29 | 8 | .02 | -.02 |
| 24 | 1 | 33 | 30 | 10 | .02 | -.02 |
| | 2 | 46 | 32 | 6 | .16 | 0 |
| | 3 | 43 | 32 | 8 | .18 | 0 |
| | 4 | 34 | 32 | 2 | 0 | 0 |
| 25 | 1 | 30 | 30 | 8 | -.04 | -.01 |
| | 2 | 40 | 36 | 14 | .22 | .05 |
| | 3 | 43 | 37 | 14 | .30 | .06 |
| | 4 | 39 | 38 | 10 | .14 | .05 |
| 26 | 1 | 34 | 24 | 20 | .08 | -.12 |
| | 2 | 36 | 19 | 20 | .18 | -.18 |
| | 3 | 34 | 17 | 18 | .08 | -.18 |
| | 4 | 25 | 15 | 16 | -.22 | -.16 |
| 27 | 1 | 16 | 11 | 6 | -.20 | -.07 |
| | 2 | 26 | 13 | 12 | -.14 | -.13 |
| | 3 | 28 | 13 | 8 | -.06 | -.09 |
| | 4 | 23 | 14 | 6 | -.10 | -.07 |
| 28 | 1 | 19 | 16 | 12 | -.32 | -.12 |
| | 2 | 29 | 25 | 12 | -.08 | -.07 |
| | 3 | 30 | 23 | 14 | -.06 | -.09 |
| | 4 | 29 | 25 | 15 | -.10 | -.07 |
| 29 | 1 | 28 | 24 | 14 | -.12 | -.09 |
| | 2 | 38 | 29 | 18 | .22 | -.05 |
| | 3 | 45 | 37 | 7 | .18 | .03 |
| | 4 | 43 | 39 | 16 | .36 | .10 |
| 30 | 1 | 46 | 44 | 6 | .16 | .07 |
| | 2 | 61 | 47 | 12 | .70 | .19 |
| | 3 | 61 | 49 | 10 | .58 | .18 |
| | 4 | 53 | 46 | 14 | .58 | .20 |
| 31 | 1 | 49 | 45 | 2 | .06 | .03 |
| | 2 | 47 | 37 | 22 | .66 | .09 |
| | 3 | 45 | 35 | 12 | .30 | .03 |
| | 4 | 38 | 26 | 12 | .14 | -.06 |
| April | | | | | | |
| 1 | 1 | 33 | 30 | 6 | .02 | -.01 |
| | 2 | 33 | 31 | 7 | .02 | -.01 |
| | 3 | 36 | 22 | 10 | .08 | -.07 |
| | 4 | 28 | 19 | 12 | -.10 | -.11 |
| 2 | 1 | 23 | 19 | 14 | -.26 | -.14 |
| | 2 | 31 | 16 | 18 | -.04 | -.18 |
| | 3 | 30 | 14 | 10 | -.04 | -.11 |
| | 4 | 22 | 10 | 2 | -.04 | -.02 |
| 3 | 1 | 18 | 14 | 4 | -.12 | -.05 |
| | 2 | 35 | 18 | 16 | .10 | -.15 |
| | 3 | 37 | 25 | 18 | .18 | -.10 |
| | 4 | 36 | 23 | 12 | .10 | -.08 |
| 4 | 1 | 32 | 26 | 8 | 0 | -.04 |
| | 2 | 49 | 36 | 28 | .98 | .09 |
| | 3 | 48 | 26 | 28 | .90 | -.14 |
| | 4 | 39 | 24 | 20 | .28 | -.12 |

* Periods 1 to 4 at 3 a.m., 9 a.m., 3 p.m., and 9 p.m. respectively.

surface of the snow. The factors which determine the condensation melt potential are the dew point and the wind velocity, as related by Wilson's (1941) equation:

$$M = a\ V\ (e-6.11)$$

where M is the depth of water melted plus condensate per six hours in inches, a is a constant involving the latent heat of ice, exposure of instruments and conversion units, and is equal to 0.0032 for basins with elevations less than 3000 feet, V is wind velocity in miles per hour, e is the vapor pressure of the air in millibars, and 6.11 is the saturation vapor pressure in millibars at 32° F. Records of dew point and wind velocity at Wausau were again considered applicable to the Big Eau Pleine Basin. The condensation melt potential data for the snowmelt period of 1943 are tabulated in Table I.

## Radiation Melt Potential

Adequate data for the direct determination of incident solar radiation for the Big Eau Pleine Basin were not available. Thus it became necessary to reconstruct the insolation characteristics from the six-hourly cloud cover data, recorded at the Wausau CAA Airport. Since records of both cloud cover and incident solar radiation were available for Madison, Wisconsin, a correlation between these factors was established for use with the Wausau data.

Cloud cover is an estimated quantity, reported in tenths by a ground observer. A cloud cover of zero represents a cloudless sky, 10 represents a complete overcast and intermediate values represent intermediate conditions. It must be emphasized however, that although two days may be reported correctly as having 10-tenths cloud cover, the insolation reaching the earth for those two days may be vastly different since cloud canopies differ in their capacity to filter out solar radiation. A further indication of the inaccuracy involved in the use of cloud cover data in determining incident radiant solar energy is illustrated by several periods in which the noon cloud cover reported was 10-tenths and the duration of sunshine reported for the hours preceding and following the noon cloud cover observation were each 60 minutes. In other words, although the sky was completely overcast, the clouds were of such a nature that the sunshine was visibly able to penetrate them continuously. Obviously, the insolation corresponding to 10-tenths cloud cover on such a day will not correlate properly with the insolation corresponding to 10-tenths cloud cover on a day when heavy clouds are extant.

The Madison insolation records for several 15-day periods were checked for the 19-year period 1931-1949 inclusive, and the highest insolation value for each daylight hour within each interval was determined. From these values were determined the maximum composite insolations which are equal to the daily insolation in langleys which would have occurred at Madison if the highest insolation values for each hour within a given period had all occurred on the same day. These values were plotted against time to give the Maximum Composite curve shown on Fig. 1. This curve represents the daily insolation summation which is approximately the highest insolation that could possibly occur at Madison for each day represented. The average insolation experienced in Madison is seen from Fig. 1 to be a function of this maximum composite insolation.

The latitude correction to adapt the Madison data to the Big Eau Pleine Basin is 0.97. This correction was considered insignificant in comparison

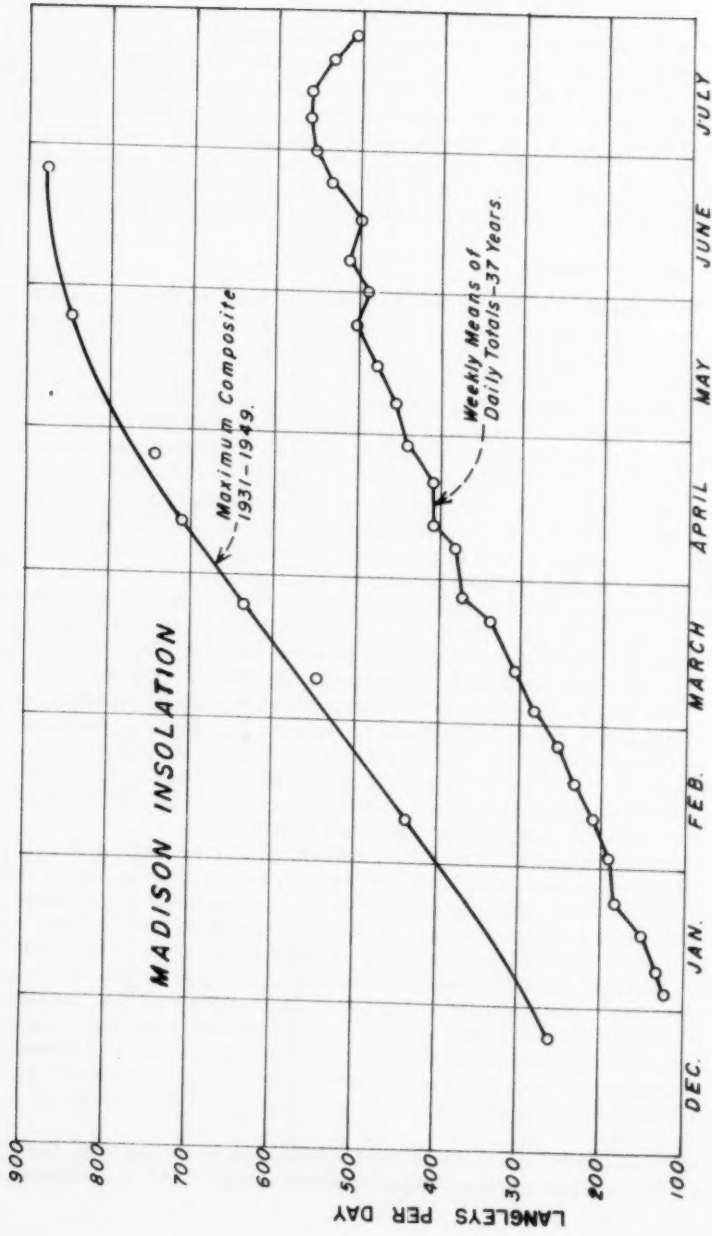
MADISON INSOLATION
Maximum Composite 1931-1949.
Weekly Means of Daily Totals-37 Years.
LANGLEYS PER DAY
900
800
700
600
500
400
300
200
100
DEC.
JAN.
FEB.
MARCH
APRIL
MAY
JUNE
JULY

FIG. 1

with uncertainties involved in other assumptions and was not used. Its neglect results in a constant error for which compensation may be made in the selection of the proper albedo value.

Insolation values from Madison were converted to percentages of the maximum composite insolation by dividing the insolation value recorded by the maximum composite insolation for that day as determined from Fig. 1. These data were then plotted against various combinations of cloud cover data. It was found that a significant correlation existed between the per cent of maximum composite insolation per half day and the sum of either the 6:30 a.m. and 12:30 p.m. cloud cover values or the 12:30 p.m. and the 6:30 p.m. cloud cover values, expressed in tenths. Table II summarizes the results of this correlation study. It is significant to note that errors resulting from approximating the insolation from cloud cover data are later minimized materially by corrections for albedo and back radiation. It is also emphasized that the greatest accuracy of insolation determination occurs during periods of minimum cloud cover, or during periods when maximum melting from insolation would occur.

Thus, from the cloud cover data at Wausau for any day the per cent of the maximum composite insolation for that day may be determined from Table II. For example, on March 30, 1943, the 6:30 a.m., 12:30 p.m. and 6:30 p.m. cloud covers were 0.4, 0.5 and 0.8, respectively. The sum of the 6:30 a.m. and the 12:30 p.m. cloud cover values is 0.9 and the sum of the 12:30 p.m. and

TABLE II

INSOLATION-CLOUD COVER RELATIONS

| Summation of 6:30a & 12:30p, or 12:30p & 6:30p Cloud Cover-Tenths | Percent of Maximum Composite Insolation per half day | Summation of 6:30a & 12:30p or 12:30p & 6:30p Cloud Cover-Tenths | Percent of Maximum Composite Insolation per half day |
|---|---|---|---|
| 0 | 44 | 10 | 34 |
| 1 | 43 | 11 | 33 |
| 2 | 43 | 12 | 31 |
| 3 | 42 | 13 | 29 |
| 4 | 41 | 14 | 27 |
| 5 | 41 | 15 | 25 |
| 6 | 40 | 16 | 23 |
| 7 | 38 | 17 | 21 |
| 8 | 37 | 18 | 19 |
| 9 | 36 | 19 | 17 |
| 10 | 34 | 20 | 15 |

the 6:30 p.m. cloud cover values is 1.3. From Table II the morning insolation was 36 per cent of maximum for the half day and the afternoon insolation was 29 per cent of maximum, so the daily total was 65 per cent of the maximum composite insolation for that day. From Fig. 1 the maximum composite insolation (March 30) was 658 langleys. Thus, the computed insolation for March 30, 1943 was 428 langleys.

The radiation components effective in producing snowmelt potential may be considered to follow the pattern shown in Fig. 2. The shortwave incident radiation (428 langleys on March 30) consists of the direct and diffuse solar radiation. The net longwave emissive radiation consists of back-radiation from snow, partially balanced by incident diffuse longwave sky radiation. This net longwave radiation has been shown to be emissive (Fig. 2b) and essentially constant at 0.10 langleys per minute. During hours of darkness when there is no insolation the energy loss has been termed non-concurrent radiation. During daylight hours this emissive (concurrent) radiation must be deducted from the incident radiation to obtain the net radiation. It is evident that the duration and amount of the concurrent and non-concurrent radiations are functions of the total daily insolation. Thus, the insolation effective in producing melt for any day is the computed insolation for that day minus the concurrent back radiation.

A variable amount of the incident solar radiation is reflected from the snow surface and is thus unavailable for melting. The percentage reflected, called albedo, to be used in reducing the effective insolation is a function of the density, structure, moisture content, depth and purity of the snowpack. Because sufficient records were not available to permit a proper evaluation of albedo variation, a constant albedo value of 60 per cent was assumed for the entire snowmelt period. For an albedo of 60 per cent, the computed insolation for March 30, 1943, of 428 langleys would become 171 langleys.

The net concurrent radiation is a function of the envelope of effective radiation and has been determined from the authors' emperical equation:

$$r = 38.5 + 0.0633\ p = 49 \text{ langleys}$$

in which: r is the net concurrent radiation in langleys per day and p is the net insolation as reduced for albedo in langleys per day. Subtracting the net concurrent radiation of 49 langleys would leave 122 langleys, which would be sufficient to produce $122 \div (80 \times 2.54) = 0.60$ inches of melt. During the same day, the net non-concurrent radiation was $(60 \times 24 \times .1) - 49 = 95$ langleys, which is the amount of heat liberated in freezing 0.47 inches of water at $32^\circ$ F.

The insolation nomograph of Fig. 3 provides an easy means of solving for the radiation melt potential. To solve for the melt potential using Fig. 3 it is necessary to know the date, the per cent of total insolation and the albedo. A straight edge is placed on the nomograph from the date to the per cent of total insolation and the intersection with the net insolation line is noted. A horizontal line through this net insolation will determine the melt for various albedo values and the amount of water frozen by non-concurrent radiation. Utilizing the data of March 30, 1943, a straight edge placed from March 30 to 65 per cent indicates a net insolation of 428 langleys per day. A horizontal line through this net insolation value intersects the 60 per cent albedo line at a melt of 0.60 inches per day and indicates that 0.47 inches of water would be frozen by non-concurrent emissive longwave radiation. The radiation melt potential calculations for the snowmelt period of the year 1943 are tabulated in Table III.

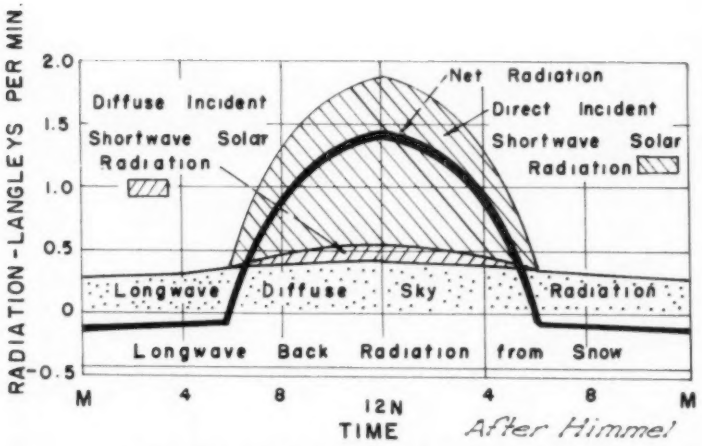


(a) RELATIVE RADIATION COMPONENTS

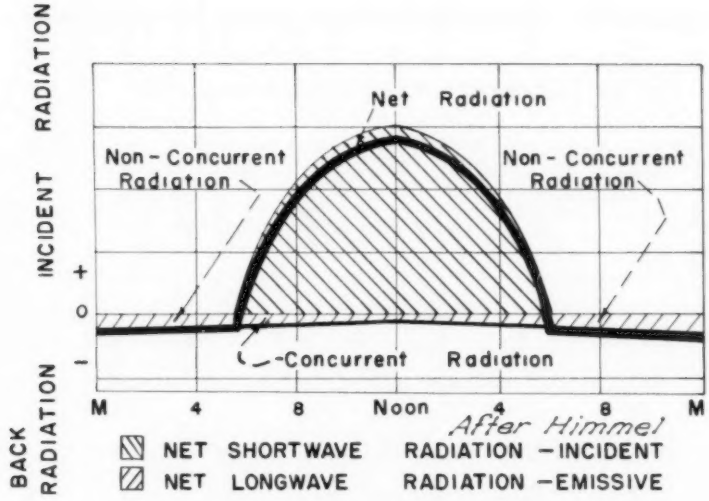


(b) NET RADIATION COMPONENTS

FIG. 2

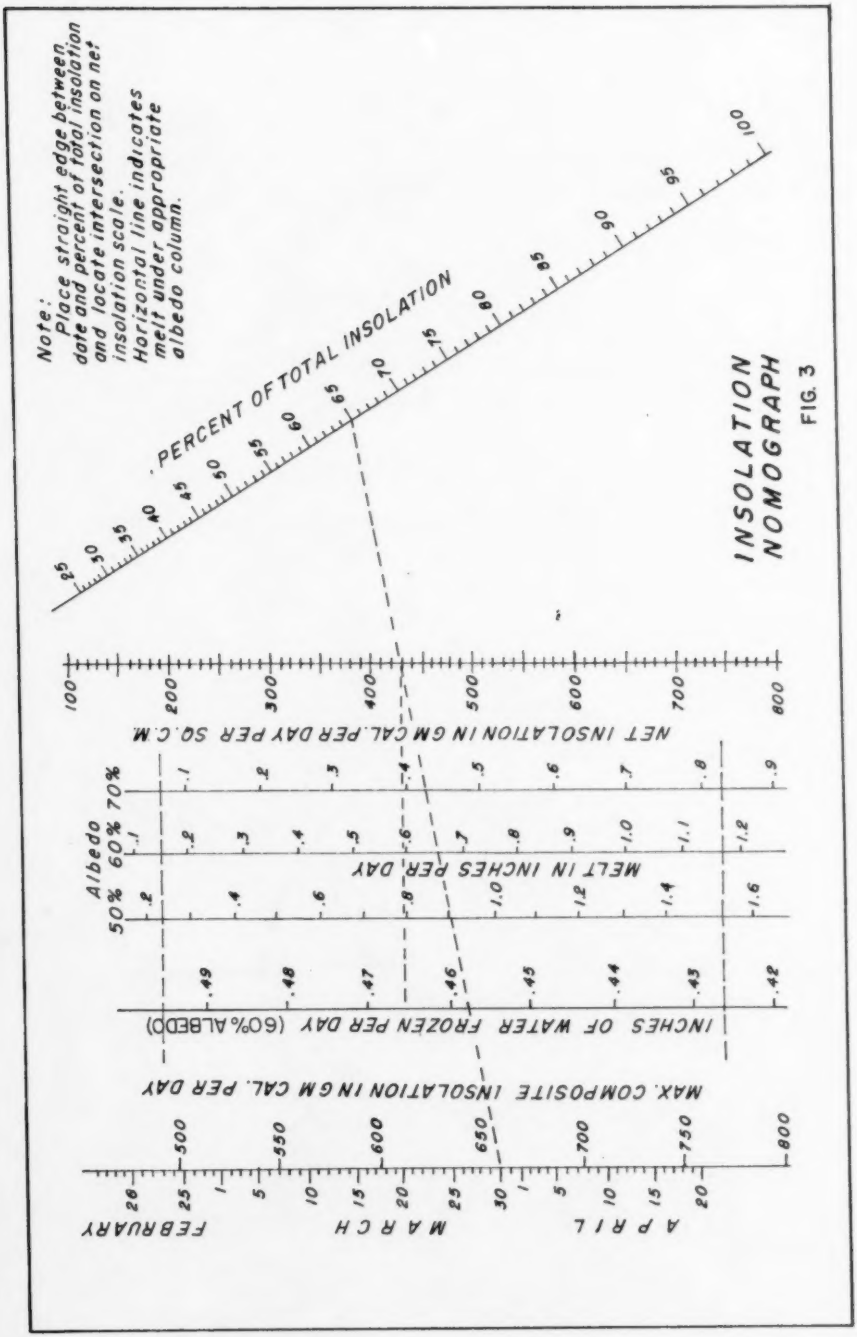
Note:
Place straight edge between date and percent of total insolation and locate intersection on net insolation scale.
Horizontal line indicates melt under appropriate albedo column.
PERCENT OF TOTAL INSOLATION
INSOLATION NOMOGRAPH
NET INSOLATION IN GM CAL. PER DAY PER SQ. C.M
Albedo 50% 60% 70%
MELT IN INCHES PER DAY
INCHES OF WATER FROZEN PER DAY (60% ALBEDO)
MAX. COMPOSITE INSOLATION IN GM CAL. PER DAY
FEBRUARY
MARCH
APRIL
FIG. 3

TABLE III

RADIATION MELT POTENTIAL - 1943

| Date | 6:30a + 12:30p Period Cloud Cover in Tenths | Percent of Maximum Insolation | 12:30p + 6:30p Period Cloud Cover in Tenths | Percent of Maximum Insolation | Daily Percent of Maximum Insolation | Daily Insolation in Langleys | Radiation Melt Potential in Inches per day |
|---|---|---|---|---|---|---|---|
| March | | | | | | | |
| 23 | 13 | 29 | 12 | 31 | 60 | 377 | .50 |
| 24 | 8 | 37 | 9 | 36 | 73 | 461 | .66 |
| 25 | 6 | 40 | 0 | 44 | 84 | 535 | .79 |
| 26 | 6 | 40 | 2 | 43 | 83 | 532 | .79 |
| 27 | 11 | 33 | 12 | 31 | 64 | 412 | .57 |
| 28 | 8 | 37 | 12 | 31 | 68 | 441 | .62 |
| 29 | 10 | 34 | 3 | 42 | 76 | 498 | .72 |
| 30 | 9 | 36 | 13 | 29 | 65 | 430 | .60 |
| 31 | 18 | 19 | 18 | 19 | 38 | 255 | .28 |
| April | | | | | | | |
| 1 | 5 | 41 | 14 | 27 | 68 | 453 | .64 |
| 2 | 6 | 40 | 6 | 40 | 80 | 540 | .80 |
| 3 | 7 | 38 | 15 | 25 | 63 | 427 | .59 |
| 4 | 4 | 41 | 9 | 36 | 77 | 527 | .78 |

The radiation melt potential values thus determined could not be utilized directly in the snowmelt calculations however, because they had to be assimilated with other melt potential factors which were determined for one-quarter day intervals. From a study of daily insolation graphs it was decided arbitrarily to consider that two-thirds of the daily positive radiation melt potential occurred in the interval from 9 a.m. to 3 p.m. and one-sixth occurred in each of the intervals 3 a.m. to 9 a.m. and 3 p.m. to 9 p.m. It was further concluded that the negative melt potential should be equivalent to 36 langleys or 0.18 inches of melt for the period from 9 p.m. to 3 a.m. and that the remainder of the negative melt potential should be equally divided between the 3 a.m. to 9 a.m. period and the 3 p.m. to 9 p.m. period. Using this scheme of division, the melt potential for March 30, 1943 would be subdivided as indicated in Table IV, according to which two-thirds of the .60 inches of melt potential, or 0.40 inches, is assigned to period 2 and the remaining 0.20 inches is equally divided between periods 1 and 3. A total negative melt potential of 0.47 inches is divided so that 0.18 inches is applied to period 4 and the remainder of 0.29 inches is equally divided between period 1 and period 3.

### Total Melt Potential

The total melt potential for any time interval is merely the algebraic sum of the individual melt potential factors. Table V gives the total melt potentials as computed for the snowmelt season of the year 1943.

## Snowmelt Runoff Theory

The streamflow hydrograph resulting from melting snow must reflect the variation in total melt potential. The hydrograph is also a function of a snowmelt unit hydrograph because, like runoff from rainfall, once an increment of flow is started on its path it proceeds until it has passed the measuring station, unless extremely severe freezing conditions follow melting.

By preparing a "relative hydrograph" for each day having a positive melt potential and making these relative hydrographs reflect the daily variation in melt potential as well as the snowmelt unit hydrograph pattern it is possible to divide the daily runoff into the increments which have been contributed from snowmelt potential factors existing on previous days.

To illustrate this procedure in detail numerous examples have been used in the following discussion.

TABLE IV
RADIATION MELT POTENTIAL FOR MARCH 30, 1943

| Period | Positive Melt Potential | Negative Melt Potential | Net Melt Potential |
|---|---|---|---|
| (1) 3am to 9am | .10 in. | -.14 in. | -.04 in. |
| (2) 9am to 3pm | .40 | 0 | .40 |
| (3) 3pm to 9pm | .10 | -.14 | -.04 |
| (4) 9pm to 3am | 0 | -.18 | -.18 |

TABLE V
TOTAL MELT POTENTIAL - 1943

| Date | Period | Melt Potential in Hundredths of an Inch | | | | Rain in Inches |
|---|---|---|---|---|---|---|
| | | Convection | Condensation | Radiation | Positive Total | |
| March | | | | | | |
| 23 | 1 | -6 | -2 | -6 | | |
| | 2 | 28 | -10 | 33 | 51 | |
| | 3 | 22 | -4 | -3 | 15 | |
| | 4 | 2 | -2 | -18 | | |
| 24 | 1 | 2 | -2 | -3 | | |
| | 2 | 16 | 0 | 44 | 60 | |
| | 3 | 18 | 0 | -3 | 15 | |
| | 4 | 0 | 0 | -18 | | |
| 25 | 1 | -4 | -1 | 0 | | |
| | 2 | 22 | 5 | 53 | 80 | |
| | 3 | 30 | 6 | 0 | 36 | |
| | 4 | 14 | 5 | -18 | 1 | |
| 26 | 1 | 8 | -12 | 0 | | |
| | 2 | 18 | -18 | 53 | 53 | |
| | 3 | 8 | -18 | 0 | | |
| | 4 | -22 | -16 | -18 | | |
| 27 | 1 | -20 | -7 | -5 | | |
| | 2 | -14 | -13 | 38 | 11 | |
| | 3 | -6 | -9 | -5 | | |
| | 4 | -10 | -7 | -18 | | |
| 28 | 1 | -32 | -12 | -4 | | |
| | 2 | -8 | -7 | 41 | 26 | |
| | 3 | -6 | -9 | -4 | | |
| | 4 | -10 | -7 | -18 | | |
| 29 | 1 | -12 | -9 | -2 | | |
| | 2 | 22 | -5 | 48 | 65 | |
| | 3 | 18 | 3 | -2 | 5 | |
| | 4 | 36 | 10 | -18 | 28 | |
| 30 | 1 | 16 | 7 | -4 | 19 | |
| | 2 | 70 | 19 | 40 | 128 | |
| | 3 | 58 | 18 | -4 | 72 | |
| | 4 | 58 | 20 | -18 | 60 | |
| 31 | 1 | 6 | 3 | -11 | | |
| | 2 | 66 | 9 | 19 | 94 | |
| | 3 | 30 | 3 | -11 | 22 | |
| | 4 | 14 | -6 | -18 | | .03 |
| April | | | | | | |
| 1 | 1 | 2 | -1 | -4 | | |
| | 2 | 2 | -1 | 43 | 44 | |
| | 3 | 8 | -7 | -4 | | |
| | 4 | -10 | -11 | -18 | | |
| 2 | 1 | -26 | -14 | 0 | | .08 |
| | 2 | -4 | -18 | 53 | 31 | |
| | 3 | -4 | -11 | 0 | | |
| | 4 | -4 | -2 | -18 | | |
| 3 | 1 | -12 | -5 | -4 | | |
| | 2 | 10 | -15 | 39 | 34 | |
| | 3 | 18 | -10 | -4 | 4 | |
| | 4 | 10 | -8 | -18 | | |
| 4 | 1 | 0 | -4 | 0 | | |
| | 2 | 98 | 9 | 52 | 159 | |
| | 3 | 90 | -14 | 0 | 76 | |
| | 4 | 28 | -12 | -18 | 2 | |

## Snowmelt Unit Hydrograph

A trial snowmelt unit hydrograph was determined by isolating the runoff from one day's melt in a manner similar to that used in determining a rainfall unit hydrograph. Base flow was removed from consideration by utilizing the fall recession curve of Fuhriman (1952). In addition, the effect of the duration of the melt potential producing runoff was considered. The resulting snowmelt unit hydrograph, shown on Fig. 4a, is in close agreement with the rainfall unit hydrograph (Beck, 1946), leading to the conclusion that, at least in certain instances, the same unit hydrograph may be used for rainfall and snowmelt runoff. The average daily discharge in cfs for melting beginning at four different times during the day are given in Table VI. Fig. 4b compares the recorded hydrograph with the reconstructed hydrograph for the snowmelt period of 1939 by means of the procedures outlined herein.

## Ice Index Method of Altering Published Data

According to the United States Geological Survey Water-Supply Paper No. 1085 (1947) the runoff records for the Big Eau Pleine River near Stratford, Wisconsin are ". . . good except those for periods of ice effect and those below 10 second-feet, which are fair." The notation "good" ". . . indicates that, in general, the error in the daily records is believed to be . . . less than 10 per cent; 'fair' less than 15 percent;. . ."

Several times during each year actual discharge measurements are made at Stratford and compared with the apparent discharge as determined from the concurrent gage height and the rating table for the station. Frequently a head correction of a few hundredths of a foot is determined from these actual

TABLE VI
AVERAGE DAILY DISCHARGE FOR
SNOWMELT UNIT HYDROGRAPH

| Day | Discharge in cfs for Melt Beginning at: 3 am (Period 1) | 9 am (Period 2) | 3 pm (Period 3) | 9 pm (Period 4) |
|---|---|---|---|---|
| 1 | 2753 | 1603 | 326 | 5 |
| 2 | 2218 | 3068 | 3937 | 3667 |
| 3 | 667 | 868 | 1137 | 1547 |
| 4 | 218 | 282 | 377 | 507 |
| 5 | 97 | 119 | 140 | 168 |
| 6 | 46 | 59 | 68 | 80 |
| 7 | 18 | 22 | 28 | 38 |
| 8 | 1 | 4 | 7 | 12 |
| Total | 6018 cfs days | 6025 | 6020 | 6024 |
| Ratio of "First Day" Discharges (Based on Period (3)) | 2753/326 or 8.44 | 1603/326 or 4.92 | 326/326 or 1.00 | 5/326 or 0.0153 |

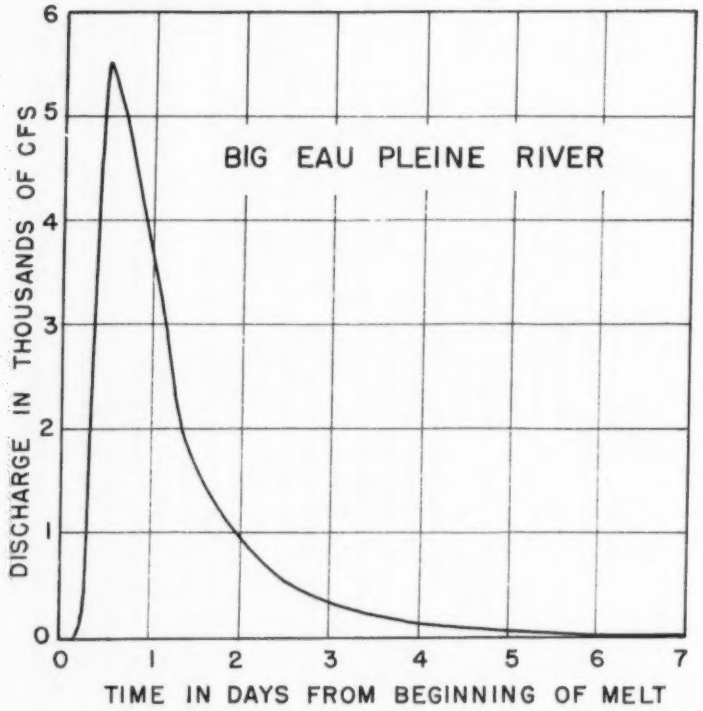


SNOWMELT UNIT HYDROGRAPH

FIG. 4A

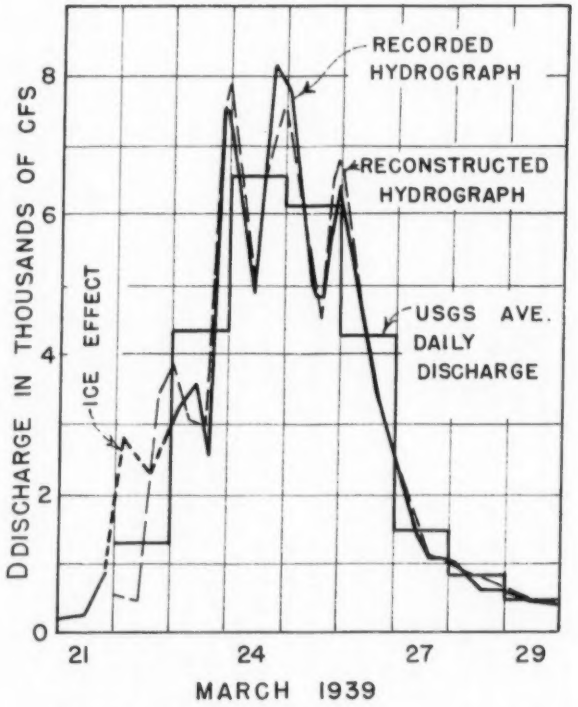


HYDROGRAPH RECONSTRUCTION

FIG. 4B

discharge measurements which correction is then applied to the computed discharges for a period of time as determined by earlier or subsequent discharge measurements. It is quite natural that these corrections should be required as a stream bed tends to erode and redeposit its sediment in a slightly different fashion following each passage of high water. The variations however are slight and no alteration of the rating curve has been necessary since 1948, at which time only minor changes in the discharges were made for gage heights less than 4.5 feet.

During the winter season ice forms on the surface of the stream and the discharge characteristics change from those of open channel flow to those of enclosed flow. During periods of prolonged cold weather the apparent discharge as computed from the recorded gage heights and the rating table will tend to increase markedly, while true discharge as determined by field measurements is actually decreasing. This is explained by the fact that the resistance to flow is markedly increased by the surface contact with the ice, while at the same time, the weight of the ice supported by the water causes an increase in the water level measured in the float well. As an example, an apparent discharge of 110 cfs may be determined from the gage reading at Stratford, while an actual measurement by current meter may indicate that the discharge is 10 cfs.

Usually two or three discharge measurements are made each year during the period when ice effects are noted. The critical period during early snowmelt runoff, however, is not well represented by actual measurements because rising water makes the ice unsafe for measurement operations through the ice while complete cover exists, and floating ice renders the taking of velocity measurements impractical after the break-up begins. Correct discharge values for the early snowmelt runoff season are the most difficult to determine and are the ones most likely to be in error in the published data. The USGS engineers determine the discharge values reported in the Water-Supply Papers from the gage height readings, concurrent air temperatures, reservoir storage and discharge records, and hydrographs of previous runoff. The method of accounting for ice effects presently being used on the Big Eau Pleine River by USGS engineers consists of plotting the apparent discharge, as determined by recording-gage readings, on semi-log paper, along with the actual discharges determined by the winter discharge measurements which are made about two times each winter. A line is then drawn through the measured discharges approximately parallel to the apparent discharge and the discharge values to be recorded are read from this line. Fig. 5 shows the manner in which winter discharge values were determined by this process for the winter 1950-1951. Fig. 6 shows the same discharges plotted on an arithmetic plot for the break-up period of 1951. It will be noted in Fig. 6 that at the higher discharges, the use of the USGS method results in extremely large reductions in discharge for ice effects. It has been deemed advisable, therefore, to alter certain critical discharge values from those given in the Water-Supply Papers for the purpose of this investigation in accordance with the ice index method outlined below.

All winter discharge measurements on the Big Eau Pleine River were analyzed. The gage reading which would have been required to produce the actual discharge as determined by measurement (without ice effect) was obtained from the rating table. This reading was subtracted from the measured gage reading to give the "ice index". It is reasoned that the ice index is equal to the equivalent water depth of the ice cover plus an increment of thickness to

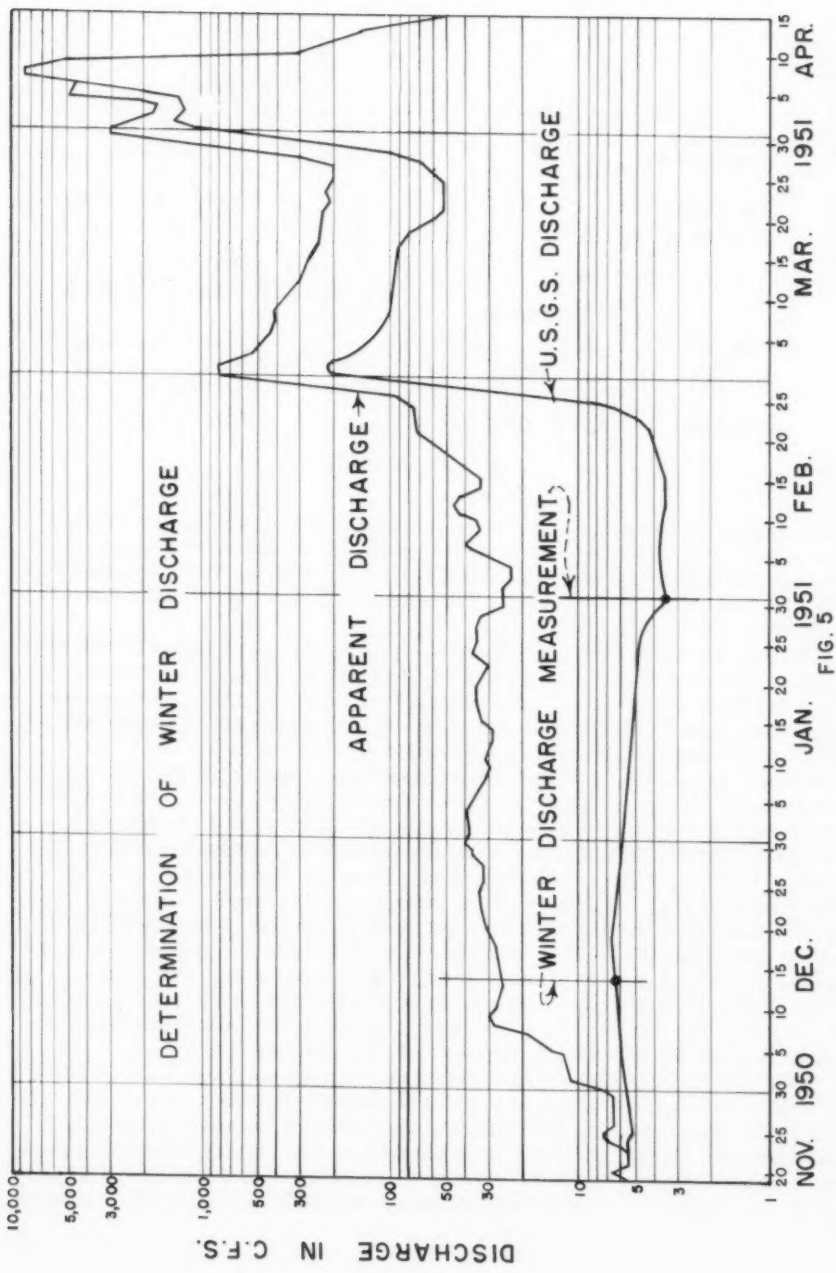
DETERMINATION OF WINTER DISCHARGE
APPARENT DISCHARGE
U.S.G.S. DISCHARGE
WINTER DISCHARGE MEASUREMENT
DISCHARGE IN C.F.S.
10,000
5,000
3,000
1,000
500
300
100
50
30
10
5
3
1
NOV. 1950
DEC.
JAN. 1951
FEB.
MAR. 1951
APR.

FIG. 5

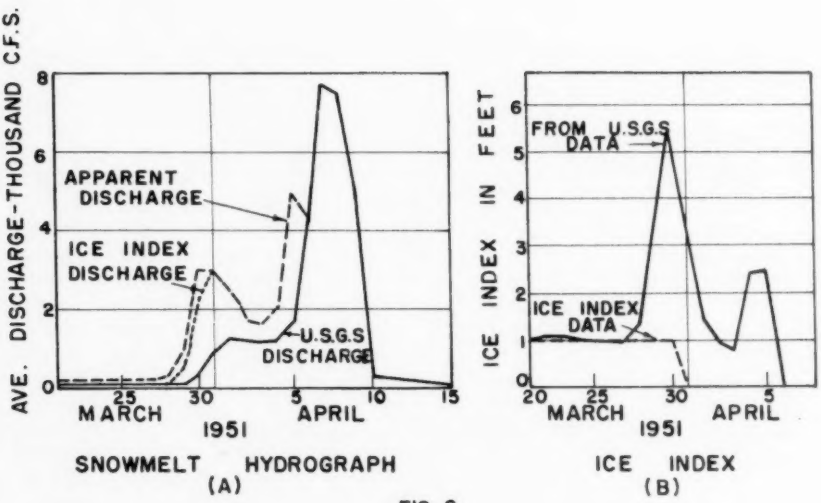


FIG. 6

compensate for the reduction of flow caused by the drag of the water on the ice cover. Values of ice index were computed for all days when winter discharge was measured, and are plotted against the date of the measurement in Fig. 7. The maximum ice index value determined by actual measurement is 1.65 feet.

It is reasoned that the ice indices of Fig. 7 may be applied to the recorded gage heights to determine the probable discharge for those days when only the gage readings are available. For example, on March 17, 1945, the average gage reading of 12.95 feet was recorded. This is equivalent to a discharge of 5890 cfs without ice correction as determined from the rating table. If a maximum ice index of 1.60 feet were considered to apply, the corrected gage reading of 12.95 minus 1.6 or 11.35 feet would provide a flow of 4315 cfs for this date. The discharge reported for this date in USGS Water-Supply Paper No. 1035 is 1500 cfs, which would occur normally with a gage reading of 7.64 feet as determined from the rating table. Thus the computed ice index for this date would be 5.31 feet. Such an index could be correct if an ice jam occurred just below the gaging station and backed up water at the station; or if an ice canopy about 5.31 feet in thickness were formed over the stream at the gaging station for the full channel width. The absence of any obstruction to flow, at the gaging station or downstream, which might cause large ice dams to form leads to the conclusion that such reductions in flow as a result of ice effect are undesirable for the purposes of this investigation.

When published discharge data were examined from all the years of record for which good gage readings are available in the initial snowmelt period, it was found that certain inconsistencies exist, relative to a study by the ice index method. During the days immediately preceding the occurrence of snowmelt runoff, the ice index had a reasonable value between 0.7 and 1.7 feet for all years. During the early snowmelt period the maximum ice effect based on

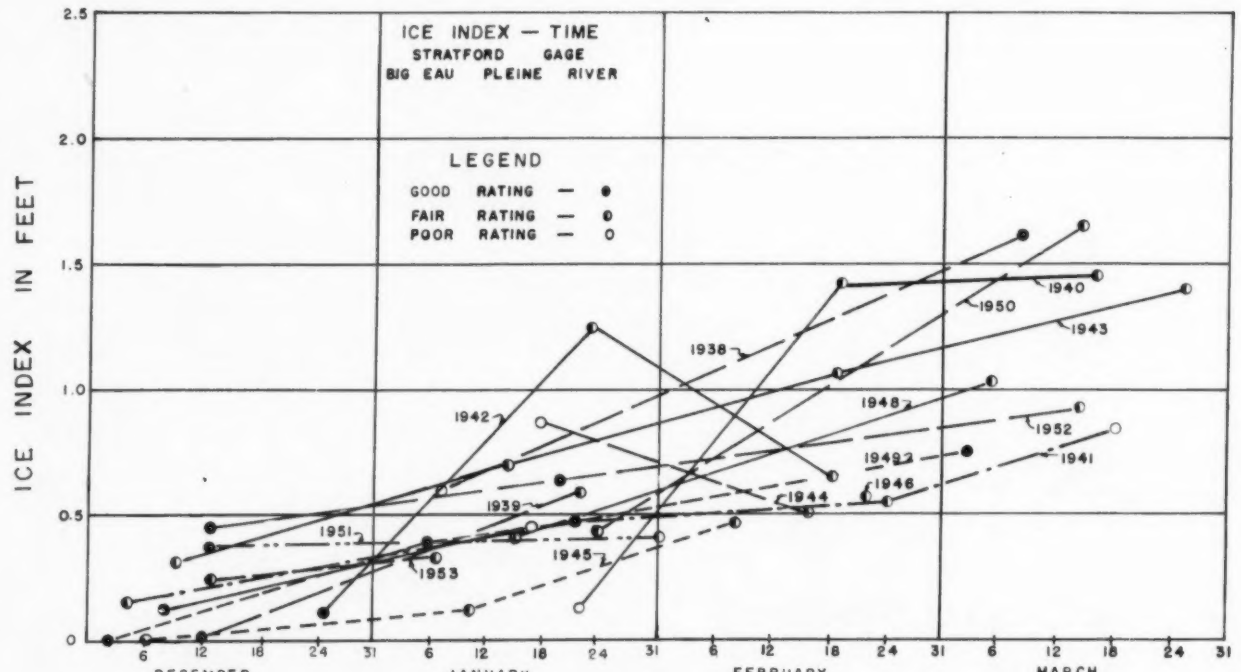
ICE INDEX — TIME
STRATFORD GAGE
BIG EAU PLEINE RIVER
LEGEND
GOOD RATING — ●
FAIR RATING — ◐
POOR RATING — ○
ICE INDEX IN FEET
2.5
2.0
1.5
1.0
0.5
0
1938
1940
1950
1943
1942
1948
1952
1949
1941
1946
1939
1944
1951
1945
1953
6 12 18 24 31 6 12 18 24 31 6 12 18 24 31 6 12 18 24 31
DECEMBER
JANUARY
FEBRUARY
MARCH
TIME

FIG. 7

published discharge data, varied from year to year, at times reading maximum values as high as 7.10 feet as in 1938, and as low as 0.74 feet in 1946. Furthermore, in some years the ice index was considered to become zero on the rising side of the hydrograph, at a discharge of 109 cfs as in 1946, or 8950 cfs as in 1945; and in other years it became zero on the falling side of the hydrograph, at a discharge of 2240 cfs following a peak apparent discharge of 8950 cfs as in 1938. In addition, the ice index for some years was erratic, alternating between low and high values on successive days.

To eliminate these variations, the following rules for reconstituting the average daily discharge for days in the early snowmelt period were adopted.

1. In the hydrograph summation computations the ice index correction at the beginning of snowmelt was assumed to be about equal to that determined from a previous measurement and was never more than 1.65 feet.
2. The ice index was assumed to approach zero on the rising limb of the hydrograph at a gage discharge of less than 5000 cfs.
3. The exact discharge for the last day of ice effect was determined from the hydrograph summation analysis of the total seasonal flow, as outlined later.

## Determination of Daily Melt

The analytical determination of the amount of snowmelt required each day to reproduce the recorded snowmelt hydrograph is a trial and error procedure. The complete analysis for the year 1943 is presented to illustrate the technique developed.

Basically, the method consists of applying a runoff for any given day which will make the total runoff for that day exactly equal to the average daily discharge as determined from the USGS Water-Supply Papers, altered, as necessary, for assumed ice conditions. The runoff so applied for any day is then followed by a sequence of discharges for succeeding days as determined from what has been termed the "relative hydrograph". Thus, the magnitude of first day's runoff, resulting from a given period of melting, is of primary importance because it automatically determines the magnitude of the discharges for succeeding days.

### Relative Hydrograph

The relative hydrograph for any day may be defined as the succession of average daily discharges resulting from melt occurring in the proportions given by the variation in melt potential for that day, and so related that the runoff corresponding to period 2 is equal to one inch. Since the melt potential variation for each day is usually different from that of every other day, it follows that each day will have a different relative hydrograph depending upon its melt potential variation. Table VII lists the melt potential data for 1943 which is necessary for the computation of relative hydrographs, and a summary of the final runoff data computed by the method of hydrograph summation, discussed later. The relative hydrograph computations are tabulated in Table VIII and are determined in the following manner:

From Table VII, beginning with March 25, 1943, it is noted that the melt potentials for periods 2, 3 and 4 are 0.80, 0.36 and 0.01 inches respectively.

TABLE VII
MELT POTENTIAL AND RUNOFF - 1943

| Date | Melt Potential in Inches, Period (1) | (2) | (3) | (4) | Total | Cumulative Total | Runoff in Inches, Total | Cumulative Total |
|---|---|---|---|---|---|---|---|---|
| March 23) | | | | | .63 | .63 | | |
| ) | Ripening Period | | | | | | | |
| 24) | | | | | .75 | 1.38 | .01 | .01 |
| 25 | | .80 | .36 | .01 | 1.17 | 2.55 | .02 | .03 |
| 26 | .01 | .53 | | | .53 | 3.08 | .08 | .11 |
| 27 | | .11 | | | .11 | 3.19 | .22 | .33 |
| 28 | | .26 | | | .26 | 3.45 | .20 | .53 |
| 29 | | .65 | .05 | .28 | .98 | 4.43 | 1.33 | 1.86 |
| 30 | .19 | 1.28 | .72 | .60 | 2.79 | 7.22 | 2.24 | 4.10 |
| 31 | | .94 | .22 | | 1.16 | 8.38 | .58 | 4.68 |
| April 1 | | .44 | | | .44 | 8.82 | .02 | 4.70 |
| 2 | | .31 | | | .31 | 9.13 | .15 | 4.85 |
| 3 | | .34 | .04 | | .38 | 9.51 | .07 | 4.92 |
| 4 | | 1.59 | .76 | | 2.35 | 11.86 | .26 | 5.18 |

TABLE VIII
RELATIVE HYDROGRAPHS - 1943

| Date | Period | Relative Average Daily Discharge - cfs, First Day | Second Day | Third Day | Fourth Day | Fifth Day | Sixth Day | Seventh Day | Eighth Day | Relative Runoff Inches |
|---|---|---|---|---|---|---|---|---|---|---|
| March 25 | 2 | 1603 | 3068 | 868 | 282 | 119 | 59 | 22 | 4 | 1.000 |
| | 3 | 147 | 1772 | 512 | 170 | 63 | 31 | 13 | 3 | .450 |
| | 4 | 0 | 46 | 19 | 6 | 2 | 1 | | | .013 |
| | Total | 1750 | 4886 | 1399 | 458 | 184 | 91 | 35 | 7 | 1.463 |
| 29 | 2 | 1603 | 3068 | 868 | 282 | 119 | 59 | 22 | 4 | 1.000 |
| | 3 | 25 | 303 | 87 | 29 | 11 | 5 | 2 | 1 | .077 |
| | 4 | 2 | 1579 | 666 | 218 | 72 | 34 | 16 | 5 | .431 |
| | Total | 1630 | 4950 | 1621 | 529 | 202 | 98 | 40 | 10 | 1.508 |
| 30 | 1 | 408 | 329 | 99 | 32 | 14 | 7 | 3 | | .148 |
| | 2 | 1603 | 3068 | 868 | 282 | 119 | 59 | 22 | 4 | 1.000 |
| | 3 | 183 | 2215 | 640 | 212 | 79 | 38 | 16 | 4 | .563 |
| | 4 | 2 | 1719 | 725 | 238 | 79 | 38 | 18 | 6 | .469 |
| | Total | 2196 | 7331 | 2332 | 764 | 291 | 142 | 59 | 14 | 2.180 |
| 31 | 2 | 1603 | 3068 | 868 | 282 | 119 | 59 | 22 | 4 | 1.000 |
| | 3 | 76 | 921 | 266 | 88 | 33 | 16 | 7 | 2 | .234 |
| | Total | 1679 | 3989 | 1134 | 370 | 152 | 75 | 29 | 6 | 1.234 |
| April 3 | 2 | 1603 | 3068 | 868 | 282 | 119 | 59 | 22 | 4 | 1.000 |
| | 3 | 38 | 463 | 134 | 44 | 16 | 8 | 3 | 1 | .118 |
| | Total | 1641 | 3531 | 1002 | 326 | 135 | 67 | 25 | 5 | 1.118 |
| 4 | 2 | 1603 | 3068 | 868 | 282 | 119 | 59 | 22 | 4 | 1.000 |
| | 3 | 156 | 1882 | 543 | 180 | 67 | 33 | 13 | 3 | .478 |
| | Total | 1759 | 4950 | 1411 | 462 | 186 | 92 | 35 | 7 | 1.478 |

Referring back to Table VI it will be noted also that one inch of runoff for each of periods 2, 3 and 4 would produce average "first day" discharges of 1603 cfs, 326 cfs and 5 cfs respectively. To combine these discharges in the ratio of the melt potentials listed above, the "ratio of first day discharges" line of Table VI is utilized. The "first day" discharge of period 2 is 4.92 times as large as that of period 3, and the "first day" discharge of period 4 is 0.0153 times that of period 3 for equal runoff, so the "first day" discharge for the relative hydrograph will be a combination of discharges from periods 2, 3 and 4 in the ratio:

$$4.92 \times .80 : 1 \times .36 : 0.0153 \times .01, \text{ or}$$

$$3.94 : 0.36 : 0.000153.$$

For convenience in determining the relative hydrographs the runoff for period 2 was assumed equal to one inch in all cases. Thus the relative "first day" runoff for period 2 is 1603 cfs. Proportionally:

$$\frac{1603}{3.94} = \frac{\text{period 3 discharge}}{0.36},$$

$$\text{or Period 3 discharge} = \frac{1603}{3.94} \ (0.36) = 147 \text{ cfs.}$$

and for period 4 the "first day" discharge is:

$$\frac{1603}{3.94} (0.000153) = 0.062 \text{ cfs}$$

Period 4 computations are carried to at least two significant figures because of the extremely large increase in second day discharges for this period as compared to the first day discharge. Thus, the relative hydrograph for March 25, 1943 is composed of first day average discharges for periods 2, 3 and 4 of 1603, 147 and 0.06 cfs respectively, as shown in Table VIII. For period 2 the average discharges for succeeding days are: 3068, 868, 282 cfs for the second, third and fourth days respectively as determined directly from Table VI, since it was assumed that runoff for period 2 was equal to one inch in all cases. For period 3 the discharges for succeeding days are "f" times the tabulated discharges for period 3 given in Table VI, where:

$$f = \frac{147}{326} = 0.450.$$

Therefore: $0.450 \times 3937 = 1772$ cfs for the second day, and $0.450 \times 1137 = 512$ cfs for the third day, etc. as shown in Table VIII. For period 4 the same process is repeated, with $f = 0.0126$, and the discharges for succeeding days are 46, 19, 6, 2 and 1, as shown in Table VIII. When the above discharges are summed up by days for periods 2, 3, and 4, the relative hydrograph for March 25, 1943 is obtained as indicated by the "Total" line. Thus the relationship between daily discharges as a result of melting occurring on March 25, will be in the proportions given by the relative hydrograph.

The "f" values determined above are equal to the runoff contribution of each period to the relative hydrograph. The total runoff represented by the relative hydrograph, therefore, is: $1.000 + 0.450 + 0.013 = 1.463$ inches. It will be noted that the ratio of runoff per period, 1:0.450:0.013 is exactly equivalent to the ratio of melt potential per period, 0.80 : 0.36 : 0.01 which

was determined originally from the melt potential variation for March 25. Tables VII and VIII list the complete computations for relative hydrographs for the year 1943.

Hydrograph Summation

The process of hydrograph summation, by means of which the daily contributions to the total seasonal snowmelt hydrograph are determined, can also be explained best by the presentation of an example. Therefore, the trial and error procedure is presented below as it was computed for the year 1943.

The average daily discharge for each day of the snowmelt season was tabulated in sequence as shown in Table IX, Trial No. 1. These discharges are: 11, 24, 58 and 204 for March 23 through 26, respectively. Base flow discharges were assumed in accordance with principles not discussed herein. Since a base flow of 8 cfs was assumed for March 23 and the total flow for that date was 11 cfs, there remained 3 cfs which was presumed to have been supplied by melting snows. Since this melting occurred in Period 2 (Table VII), discharges for subsequent days were proportional to the discharges for period 2 listed in Table VI and were 6, 2 and 1 cfs for the second, third and fourth days, respectively. These values placed in Table IX left a deficiency in the discharge for the following day, March 24, of 12 cfs, which was presumed to have been contributed from snowmelt. Subsequent discharges, proportional to period 2 discharges in Table VI of 28, 8, 3 and 1 cfs were computed and listed in Table IX. The deficiency in discharge for March 25 was then 23 cfs, which presumably resulted from melting. The relative hydrograph for melt occurring on the 25th is given in Table VIII, as discussed previously. Since the first day's flow for the 25th of March was 23 cfs, the second day's discharge was:

$$\frac{23}{1750}(4886) = 64 \text{ cfs},$$

and the third day's discharge was:

$$\frac{23}{1750}(1399) = 18 \text{ cfs},$$

the values 4886 and 1399 being the second and third day's relative hydrograph values as given in Table VIII.

The process outlined above was continued until April 1, at which time the summation of discharges was found to exceed the recorded discharge by about 558 cfs. This excess was presumed to be the result of an error in the assumed base flow distribution, or an error in the average daily discharge data. The assumption was made that the discharge value most likely to be in error was the discharge corresponding to the last day of ice effect, which was March 28, 1943. The discharge for March 28, used in the first trial, was 1066 cfs, which was the discharge computed from the gage reading for an ice index of 1.37 feet. Experience with the method indicated that an increase in the discharge for March 28, of about 34 cfs might result in a balance and a second trial was begun using a discharge of 1100 cfs for this date.

Results of the second trial are also shown in Table IX. It will be noticed that all discharges from melt which occurred before March 28 were unaffected by the change under consideration and could, therefore, be lumped together as a summation of previous discharge. The second trial resulted in a discharge

TABLE IX
HYDROGRAPH SUMMATION - 1943

| Date | March 23 | 24 | 25 | 26 | 27 | 28 | 29 | 30 | 31 | April 1 | 2 | 3 | 4 | 5 | 6 | 7 |
|---|---|---|---|---|---|---|---|---|---|---|---|---|---|---|---|---|
| Average Daily Discharge in cfs | | | | | | | | | | | | | | | | |
| TRIAL NO. 1 | | | | | | | | | | | | | | | | |
| Total | 11 | 24 | 58 | 204 | 622 | 1066 | 2270 | 6860 | 9850 | 4820 | 1810 | 1130 | 910 | 1330 | 990 | 750 |
| Base Q | 8 | 6 | 5 | 4 | 0 | | | | | | | | | | | |
| | 3 | 6 | 2 | 1 | | | | | | | | | | | | |
| | | 12 | 28 | 8 | 3 | 1 | | | | | | | | | | |
| | | | 23 | 64 | 18 | 6 | 2 | 1 | | | | | | | | |
| | | | | 127 | 243 | 69 | 22 | 9 | 5 | 2 | | | | | | |
| | | | | | 358 | 685 | 194 | 63 | 27 | 13 | 5 | 1 | | | | |
| | | | | | | 305 | 584 | 165 | 54 | 23 | 11 | 4 | 1 | | | |
| | | | | | | | 1468 | 4458 | 1460 | 476 | 182 | 88 | 36 | 9 | | |
| | | | | | | | | 2164 | 7224 | 2298 | 753 | 287 | 140 | 58 | 14 | |
| | | | | | | | | | 1080 | 2566 | 729 | 238 | 98 | 48 | 19 | 4 |
| | | | | | | | | | | -558 | | | | | | |
| TRIAL NO. 2 | | | | | | | | | | | | | | | | |
| $\Sigma$ of Previous Discharge | | | | | | 761 | 218 | 73 | 32 | 25 | 5 | 1 | | | | |
| | | | | | | 339 | 649 | 184 | 60 | 25 | 12 | 5 | 1 | | | |
| | | | | | | | 1403 | 4261 | 1395 | 455 | 174 | 84 | 34 | 9 | | |
| | | | | | | | | 2342 | 7818 | 2487 | 815 | 310 | 151 | 63 | 15 | |
| | | | | | | | | | 545 | 1295 | 368 | 120 | 49 | 24 | 9 | 2 |
| | | | | | | | | | | 533 | 1020 | 289 | 94 | 40 | 20 | 7 |
| | | | | | | | | | | | -584 | | | | | |

TABLE IX (Cont'd)
HYDROGRAPH SUMMATION - 1943

| Date | March 23 | 24 | 25 | 26 | 27 | 28 | 29 | 30 | 31 | April 1 | 2 | 3 | 4 | 5 | 6 | 7 |
|---|---|---|---|---|---|---|---|---|---|---|---|---|---|---|---|---|
| Average Daily Discharge in cfs | | | | | | | | | | | | | | | | |
| TRIAL NO. 3 | | | | | | | | | | | | | | | | |
| Σ of Previous Discharge | | | | | | 761 | 218 | 73 | 32 | 25 | 5 | 1 | | | | |
| | | | | | | 324 | 620 | 175 | 57 | 24 | 12 | 4 | 1 | | | |
| | | | | | | | 1432 | 4349 | 1424 | 465 | 177 | 86 | 35 | 9 | | |
| | | | | | | | | 2263 | 7555 | 2403 | 787 | 300 | 147 | 61 | 14 | |
| | | | | | | | | | 782 | 1858 | 528 | 172 | 71 | 35 | 13 | 3 |
| | | | | | | | | | | 45 | 86 | 24 | 8 | 3 | 2 | 1 |
| | | | | | | | | | | | 215 | 414 | 116 | 38 | 16 | 8 |
| | | | | | | | | | | | | 129 | 278 | 79 | 26 | 11 |
| | | | | | | | | | | | | | 254 | 715 | 204 | 67 |
| | | | | | | | | | | | | | | 390 | 746 | 211 |
| | | | | | | | | | | | | | | | -31 | |
| TRIAL NO. 4 | | | | | | | | | | | | | | | | |
| Σ of Previous Discharge | | | | | | 761 | 218 | 73 | 32 | 25 | 5 | 1 | | | | |
| | | | | | | 323 | 618 | 175 | 57 | 24 | 12 | 4 | 1 | | | |
| | | | | | | | 1434 | 4355 | 1426 | 465 | 177 | 86 | 35 | 9 | | |
| | | | | | | | | 2257 | 7535 | 2397 | 785 | 299 | 146 | 61 | 14 | |
| | | | | | | | | | 800 | 1901 | 540 | 176 | 72 | 36 | 14 | 3 |
| | | | | | | | | | | 8 | 15 | 4 | 1 | | | |
| | | | | | | | | | | | 276 | 528 | 149 | 49 | 20 | 10 |
| | | | | | | | | | | | | 32 | 69 | 20 | 6 | 2 |
| | | | | | | | | | | | | | 437 | 1230 | | |
| | | | | | | | | | | | | | | -75 | | |
| TRIAL NO. 5 | | | | | | | | | | | | | | | | |
| Total | | | | | | | | | 9850 | 4790 | 1574 | 1033 | 597 | 1089 | 778 | 638 |
| Σ of Previous Discharge | | | | | | | | | 9059 | 2911 | 979 | 390 | 182 | 70 | 14 | |
| | | | | | | | | | 790 | 1877 | 534 | 174 | 72 | 35 | 14 | 3 |
| | | | | | | | | | | 32 | 61 | 17 | 6 | 2 | 1 | |
| | | | | | | | | | | | 236 | 452 | 128 | 42 | 18 | 9 |
| | | | | | | | | | | | | 97 | 209 | 59 | 19 | 8 |
| | | | | | | | | | | | | | 313 | 881 | 251 | 82 |
| | | | | | | | | | | | | | | 241 | 461 | 130 |
| | | | | | | | | | | | | | | | 212 | 406 |
| Base Flow & Rain Runoff | | | | | | | | | | | | | | | | 112 |

summation of 2394 cfs for April 2, which was 584 cfs more than the recorded discharge for this date. It was evident that an over-correction had been applied to the discharge of March 28, and a discharge of 1085 cfs was selected for this date for the third trial.

In the third trial the discharges were reasonable until April 6, at which time the summation of discharges was 31 cfs too large and a fourth trial was undertaken, based on a discharge for March 28 of 1084 cfs.

The change of one cfs in the assumed March 28 discharge was an over-correction and the fourth trial resulted in excessive discharge for April 5 of 75 cfs. Since it was impractical to apply a further correction to the discharge of March 28, the discharge for the second day resulting from melt which occurred on March 30 was changed from 7535 to 7545 and the fifth trial was computed which balanced out satisfactorily. It was assumed that all discharge required for balancing after April 7 was the result of base flow and rainfall runoff.

The flow of 1084 cfs for March 28 is comparable to an ice index of 1.11 feet. Discharges prior to March 28 were computed using an ice index of 1.37, which was determined by actual measurement on March 24. The ice index was zero after March 28.

To compute the runoff attributed to any day, the ratio of the "first day" discharge from Table IX to the "first day" relative discharge from Table VIII was multiplied by the total runoff represented by the relative hydrograph. Thus, on March 25 the runoff was:

$$\frac{23}{1750}(1.463) = 0.02 \text{ inches},$$

and on March 30 the runoff was

$$\frac{2257}{2196}(2.180) = 2.241 \text{ inches}$$

After the daily runoff values were computed they were added cumulatively from the beginning of snowmelt as recorded in Table VII for the year 1943. The positive melt potentials were then added cumulatively for a period beginning two days before the occurrence of snowmelt runoff, as listed in Table VII.

## Precipitation

The occurrence of precipitation during the snowmelt season increases the difficulty of the melt potential-runoff studies many-fold. This is the results of several factors. First, there is no recording precipitation gage within the Big Eau Pleine River Basin. Therefore, the precipitation data, used from adjacent stations, may be grossly erroneous. Secondly, records of snowfall and snow on the ground are available only after October, 1949. Thus it is often difficult or impossible to determine whether the recorded precipitation was rainfall available for immediate runoff, or snowfall for which a significant melt potential would be required in order to produce runoff.

Significant amounts of rainfall occurring in the snowmelt period were handled in two ways. Whenever possible the rainfall was added directly to the melt potential factors for the same period in the analysis. Hourly precipitation values were used for the periods for which they were available, and total precipitation was divided equally for the day for those periods where

hourly data were not available. For some years this procedure would not permit a solution and it was necessary in these cases to consider that all of the rain falling in a given period ran off. Accordingly, the hydrograph of daily values was calculated for each increment of precipitation and their sums subtracted from the total runoff to leave the runoff attributed to melting snow. The years 1942 and 1944 were omitted from further consideration because the precipitation during the snowmelt season was greater than the amount of snowmelt runoff.

## Correlation of Results

As mentioned earlier, if the techniques developed herein are to be considered valid, a reasonable correlation must be evident between the runoff and the melt potential. When the cumulative melt potential for the snowmelt season is plotted against the cumulative runoff, as tabulated in Table VII for 1943, a marked similarity among the curves for the various years is noted. Fig. 8 shows the curves plotted with the occurrences of significant initial runoff at zero on the abscissa scale. It will be noted that the approximate maximum initial rate of runoff is 2 inches over the watershed area for the first 1.5 inches of melt potential, while the minimum initial rate is approximately 1.35 inches of runoff for the first 1.5 inches of melt potential. In all cases the steepest runoff gradient coincides with the earliest portion of runoff, as would be expected, because the snow cover is most extensive in the early melt season. For most years the melting is complete, or nearly so, at a melt potential of 7 inches beyond the occurrence of significant initial runoff. If the curves of Fig. 8 are reconstructed with a common ordiante at a melt potential of 7 inches the curves of Figs. 9 and 10 result. The seven years having the most reliable data are plotted in Fig. 9 and a very good correlation is evident. In Fig. 10 the years of less reliable data are plotted. The snowmelt-runoff equation, represented in Figs. 9 and 10 by the small circles, is:

$$Y = 27.4X - 1.88X^2$$

where Y is the per cent of the runoff at a melt potential of seven inches and X is the cumulative melt potential in inches after the beginning of the runoff.

It was noted from a study of the melt potential runoff data that initial runoff did not occur at a fixed accumulation of melt potential, but varied within rather wide limits.

## CONCLUSIONS

1. The relationship between the cumulative melt potential and the total snowmelt runoff, taken as the runoff at a melt potential of seven inches, may be expressed by the equation:

   $$Y = 27.4X - 1.88X^2$$

   for the Big Eau Pleine Basin, where Y is the per cent of the runoff at a melt potential of seven inches and X is the cumulative melt potential after beginning of runoff.
2. Apparently, factors causing snowmelt may be measured with less than ideal precision at locations somewhat removed from the point of application without losing their effectiveness. This may be due largely to

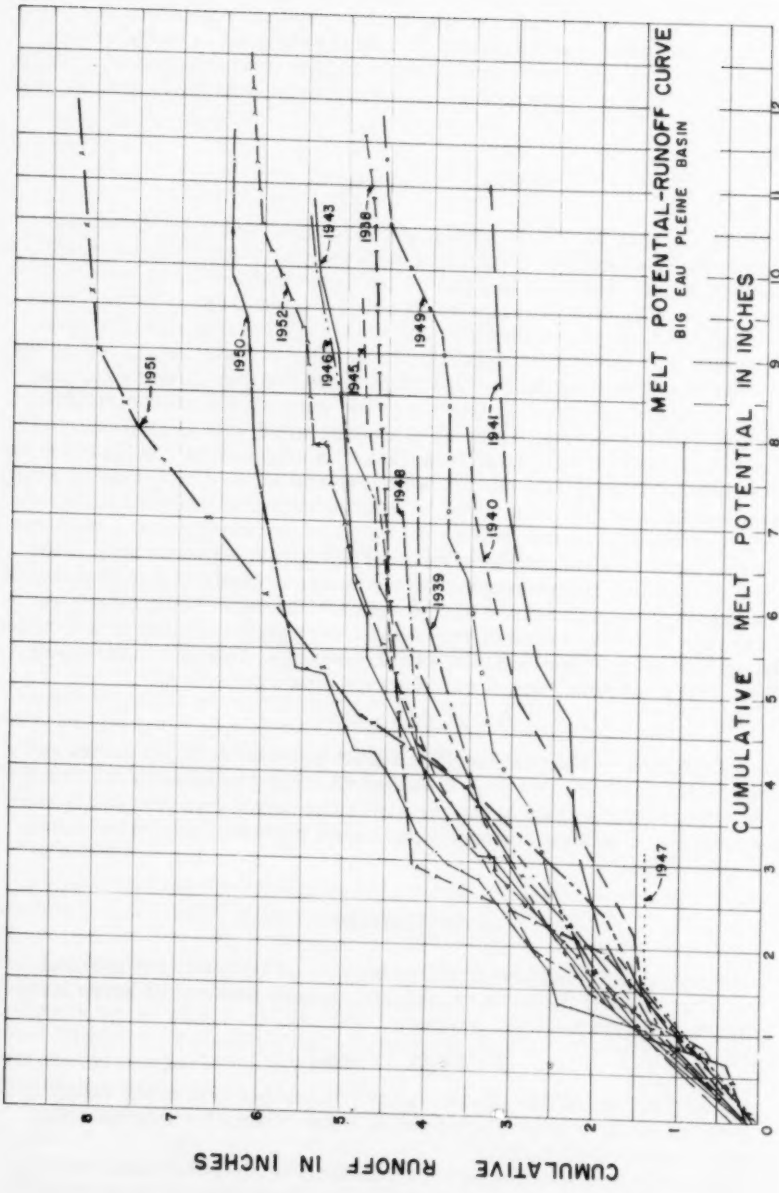
MELT POTENTIAL-RUNOFF CURVE
BIG EAU PLEINE BASIN
CUMULATIVE MELT POTENTIAL IN INCHES
CUMULATIVE RUNOFF IN INCHES
1951
1950
1952
1943
1946
1945
1938
1949
1948
1941
1940
1939
1947
0
1
2
3
4
5
6
7
8
9
10
11
12

FIG 8

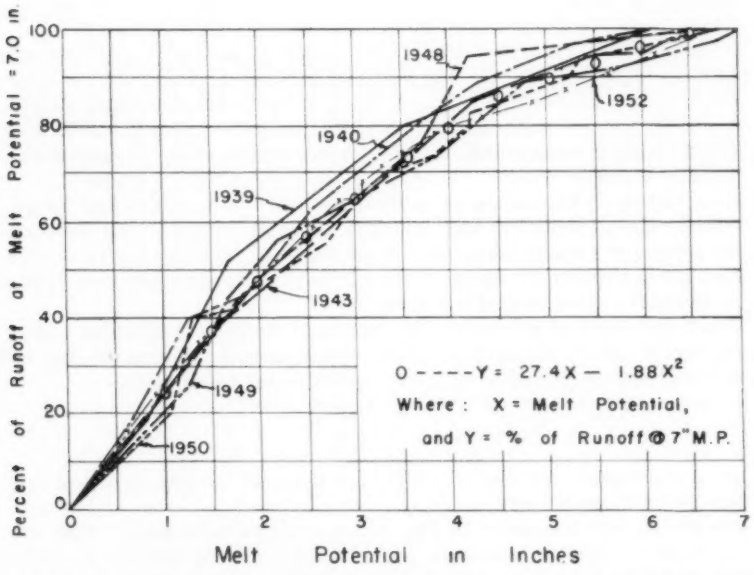


MELT POTENTIAL-RUNOFF CURVES-RELIABLE DATA

Fig. 9

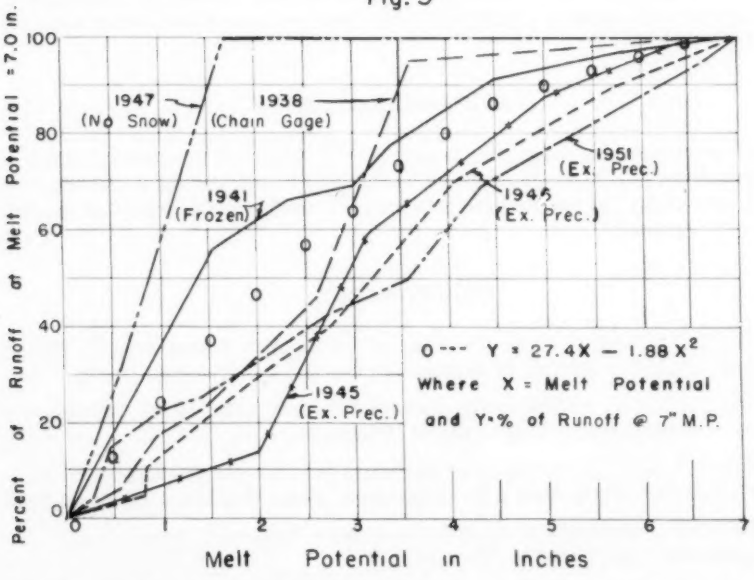


MELT POTENTIAL-RUNOFF CURVES-QUESTIONABLE DATA

Fig. 10

the compensating effect of the various errors which are encountered in Hydrologic data.

3. The general problem of ice effect on discharge rates in the spring breakup requires further study. The assumption seems valid that actual discharge rates for the Big Eau Pleine River at Stratford were higher than the rates published by the U. S. G. S. in its Water-Supply Papers; however, the ice index method presented must be subjected to further study on other rivers before any sweeping claims may be made for its validity in other areas.
4. Rain falling on the snowpack early in the snowmelt season has not produced rates of runoff as high as those produced by snowmelt alone, for the period of record examined. It must be emphasized, however, that rainfall has produced higher rates of runoff than snowmelt in this basin, particularly in the fall of the year.
5. The occurrence of rainfall in the snowmelt season disrupts the normal snowmelt-runoff relationships. This phenomenon requires further study and perhaps more intensive instrumentation on small plots.
6. It appears that the coefficient K in Light's (1944) equation:

$$D = KV(T-32^{0})$$

has a reasonable value of K = 0.002 for the melt conditions of the Wisconsin river valleys.

7. The nomograph presented in Fig. 3 is a useful tool in determining the snowmelt caused by insolation, and is as accurate as the cloud cover data which is used in it. It is believed applicable to latitudes from $40^{0}$ to $50^{0}$.
8. The snowmelt unit hydrograph developed from snowmelt runoff may be considered equally applicable to the study of snowmelt runoff and rainfall runoff.

## ACKNOWLEDGMENT

This research was supported in part by the Research Committee of the Graduate School from funds supplied by the Wisconsin Alumni Research Foundation, and in part by the Research Council of the Graduate School of the University of Wyoming.

## BIBLIOGRAPHY

1. Beck, E. J., "Unit Hydrograph Study of the Big Eau Pleine River", Thesis for the degree of Master of Science, University of Wisconsin, 1946.
2. Fuhriman, D. K., "Forecasting Snowmelt Runoff", Thesis for the degree of Doctor of Philosophy, University of Wisconsin, 1952.
3. Himmel, J. M., "Radiation Heat Exchange Between the Snowpack and its Environment", Civil Works Investigations, Tech. Bull., No. 12, Sept. 1950.
4. Light, Phil., "Analysis of High Rates of Snow-Melting", Trans. Am. Geophysical Union, 22:195-205, 1941.

5. Riter, J. R. and McGinnies, W. G., "Progress in Snowmelt Investigations at the Frasier Experimental Forest" (in: Reports Nos. 1 and 2, Cooperative Snow Investigations, 1949 and 1951).

6. U. S. Department of the Interior, "Surface Water Supply of the United States—Part 5", Geological Survey Water-Supply Papers, Nos. 1035 (1946), and 1085 (1947).

7. Wilson, W. T., "An Outline of the Thermodynamics of Snow-Melt", Trans. Am. Geophys. Union, 22:182-195, 1941.

Paper 1856 November, 1958 HY 6

Journal of the

HYDRAULICS DIVISION

Proceedings of the American Society of Civil Engineers

CONTENTS

DISCUSSION
(Proc. Paper 1856)

Page

Characteristics of a Large Throated Siphon, by J. C. Stevens. (Proc. Paper 1198, April, 1957. Prior discussion: 1417. Discussion closed.)
by J. C. Stevens (closure) . . . . . 1856-3

Transition from Laminar to Turbulent Flow in a Pipe, by M. R. Carstens. (Proc. Paper 1450, December, 1957. Prior discussion: none. Discussion closed.)
by J. M. Robertson . . . . . 1856-5

Flood Frequencies Derived from Rainfall Data, by J. L. H. Paulhus and J. F. Miller. (Proc. Paper 1451, December, 1957. Prior discussion: 1690. Discussion closed.)
by C. O. Clark . . . . . 1856-13
by J. L. H. Paulhus and J. F. Miller (closure) . . . . . 1856-17

Flow Characteristics on the Ogee Spillway, by Robert B. Jansen. (Proc. Paper 1452, December, 1957. Prior discussion: none. Discussion closed.)
by Donald P. Thayer . . . . . 1856-25
by Robert B. Jansen (closure) . . . . . 1856-32

Discharge Characteristics of Rectangular Thin-Plate Weirs, by C. E. Kindsvater and R. W. Carter. (Proc. Paper 1453, December, 1957. Prior discussion: 1616, 1690. Discussion closed.)
by M. R. Carstens . . . . . 1856-39

Air Binding in Large Pipelines Flowing Under Vacuum, by R. T. Richards. (Proc. Paper 1454, December, 1957. Prior discussion: 1690. Discussion closed.)
by R. T. Richards (closure) . . . . . 1856-43

(Over)

Page

Turbulence Characteristics of the Hydraulic Jump, by Hunter Rouse, T. T. Siao, and S. Nagaratnam. (Proc. Paper 1528, February, 1958. Prior discussion: 1690. Discussion closed.)
by A. J. Peterka and J. N. Bradley . . . . . 1856-45
by James M. Robertson . . . . . 1856-47
by Donald R. F. Harleman . . . . . 1856-52
by Philip G. Hubbard . . . . . 1856-55

The Total Sediment Load of Streams, by E. M. Laursen. (Proc. Paper 1530, February, 1958. Prior discussion: none. Discussion closed.)
by R. J. Garde and M. L. Albertson . . . . . 1856-59
by D. C. Bondurant . . . . . 1856-64
by John L. Bogardi . . . . . 1856-74

Eisenhower and Grass River Lock Models, by Martin E. Nelson and Harvey J. Johnson. (Proc. Paper 1582, April, 1958. Prior discussion: none. Discussion closed.)
by Marvin J. Webster . . . . . 1856-81

Water Distribution Design and the McIlroy Network Analyzer, by M. B. McPherson and J. V. Radziul. (Proc. Paper 1588, April, 1958. Prior discussion: none. Discussion closed.)
by Quintin B. Graves and Don Branscome . . . . . 1856-85
by E. Shaw Cole . . . . . 1856-86
by Claud C. Lomax . . . . . 1856-87

Northeastern Floods of 1955: Meteorology of the Floods, by Charles S. Gilman and Kendall R. Peterson. (Proc. Paper 1661, June, 1958. Prior discussion: none. Discussion open until December 1, 1958.)
by H. Alden Foster . . . . . 1856-89

Northeastern Floods of 1955: Flood Hydrology, by Elliot F. Childs. (Proc. Paper 1663, June, 1958. Prior discussion: none. Discussion open until December 1, 1958.)
by Gordon R. Williams . . . . . 1856-91
by H. Alden Foster . . . . . 1856-92

# CHARACTERISTICS OF A LARGE THROATED SIPHON[a]

## Closure by J. C. Stevens

J. C. STEVENS,[1] M. ASCE.—The writer is grateful for Mr. Rice's very illuminating discussion. It is particularly valuable since the laboratory model studies were made by him, at Oregon State College.

Mr. Rice has resurrected the ghosts of the definitions of discharge coefficients and efficiencies of a siphon. Webster's International Dictionary defines the latter thus: "1. Efficient quality, power or action. 2. Mech. The ratio of the energy or work that is got out of a machine, a storage battery, an electrical distributing system, or the like to the energy put in . . ."

In the writer's earlier writings (footnotes 4 and 5) he thought he could settle these moot questions once for all but perhaps that was expecting too much. Mr. Rice concedes that the writer's definition of efficiency there given is the "least objectionable, even though it varies with varying heads on the structure." But how many devices have a constant efficiency? The writer can think of none.

The discharge coefficient will vary with each change of cross-section. For this reason it seemed desirable to fix on one, and the outlet was chosen. It at least offers means of comparing siphons under comparable conditions—for instance, under maximum and minimum heads.

Testing a model under full head is an excellent method of forecasting the characteristics of a projected prototype. Had the laboratory model been strong enough for full-head operation much more valuable data could have been secured in advance of construction. Table III indicates some of the potentialities in this method even crude as the facilities were for testing and coupled with the weakness of the model itself. Such tests render unnecessary the use of controlled atmospheric cabinets for sub-atmospheric pressure models—such cabinets have been built.

The writer cannot agree that the method of correcting the pseudo-energy head of Fig. 5 is necessarily erroneous. Mr. Rice indicates that the maximum value of the alpha coefficient for velocity head is 2.0 and that any higher values would imply a reversal of flow. The writer firmly believes that that was exactly what happened. The highest value in Table VI is 3.5 at the inlet. Here the velocities were moderate but the sharp right-angle turn the water had to make to enter the siphon (Fig. 1) produced marked eddies with pronounced reversals of flow. A value of 3 is indicated at piezometer sets 3 and 4. No. 3 is just below the sharp curve at the end of the crest. Here again marked

---

a. Proc. Paper 1198, April, 1957, by J. C. Stevens.

1. Cons. Engr., Stevens & Thompson Engineers and Leupold and Stevens Instruments Inc., Portland, Ore.

eddies with flow reversals surely obtained and doubtless these continued on to Set No. 4.

The writer will agree that this method of constructing the energy line for water passing through a tortuous siphon has elements of arbitrariness in it. However there are two facts that cannot be ignored. (1) The energy line must slope continuously downstream since energy is being lost continuously, and (2) there is hardly any point within the siphon where the true mean velocity equals Q/A, hence the coefficient alpha is everywhere greater than unity, even though Table VI shows it as 1.00 at piezometer set No. 2. This is in the middle of the long crest where it would naturally be nearer unity than anywhere else in the siphon.

Mr. Rice's velocity traverses of flow in the laboratory model cannot possibly represent what actually occurred in the prototype, with its violent eddies and direction reversals of velocities. It is possible however that had it been practicable to have made such traverses in the high head model a greater conformity to the prototype might have resulted.

## ERRATA

Paper 1198 as printed in HY 2 April 1957 contains errors as follows:

Page 1 under synopsis 3rd line change primary to priming
2, line 16 change floods to boards
line 10 from bottom change cross-section to profile
5, 3rd line after the table change Figs. 1 and 2 to Fig. 2
11, 1st line of the table change 56 in date to 55
Eq. (6) change final zero to letter O
12, Table IV heading col. (1) change M to m
15, Table V 1st col. change 6 to 60.0

# TRANSITION FROM LAMINAR TO TURBULENT FLOW IN A PIPE[a]

## Discussion by J. M. Robertson

J. M. ROBERTSON,[1] M. ASCE.—The subject of laminar-turbulent transition has received little attention in ASCE publications, although it has been discussed in the general fluid mechanics literature since the time of Osborne Reynolds and Lord Rayleigh. This lack of concern of the civil engineer stems from two main causes. Firstly, most theoretical approaches have been in regard to problems (such as boundary layers and laminar-flow airfoils) of primary concern to the aeronautical engineer. Secondly, the experimental information on transition of primary interest to the civil engineer interested in pipe flow was obtained over half a century ago. In fact, Reynolds' classic experiments were conducted seventy-five years ago, while over a hundred years ago G. H. L. Hagen noted a temperature effect on the occurrence of the transition between, what may now be termed, laminar-viscous and turbulent flow.[2] Although Reynolds did not use our present day terminology, his studies did indicate that for "engineering pipes" the critical Reynolds number has the (now) commonly accepted value of 2000 to 2500. This agrees with Hagen's test results (for pipes with square entrances) which have been shown to indicate a critical value of 2200 to 3000. Since the subject appears to be rather hoary, this writer will attempt to justify current interest in the transition problem.

It is usually stated that there is an upper critical Reynolds number above which the flow is always turbulent. Actually there is some uncertainty in this regard. Experimentally, it is observed that as we decrease the disturbance entering with the flow, the critical number increases rapidly. Reynolds himself, in what we now call a "Reynolds apparatus" (transparent pipe with bellmouth entrance from a rather large tank), had little difficulty achieving laminar flow at Reynolds numbers $R = VD/\nu$ of as high as 12,000 to 13,600. Other experimentors have been able to reach even higher values with no great trouble. Thus in 1909 using Reynolds' original apparatus, but taking particular care with the bellmouth and allowing the water in the tank to settle for up to half a day, V. W. Eckman(3) raised the upper critical number to a value of 30,000 to 50,000. According to Table III the author has found laminar flow at Reynolds numbers of about 15,000 to 51,000 depending upon the spot source and other flow factors. These high values are a tribute to his experimental skill, since there is some evidence that a timewise developing flow may be

a. Proc. Paper 1450, December, 1957, by M. R. Carstens.

1. Prof. of Theoretical and Applied Mechanics, Univ. of Illinois, Urbana, Ill.
2. The studies of Hagen, Reynolds and others have been carefully analyzed and presented by L. Schiller(1) and L. Prandtl.(2)

less stable than a steady flow. One wonders how high a Reynolds number he might have reached without turbulence if the disturbance strengths of his spot sources had been further reduced.

The care required to achieve laminar flow at such high Reynolds numbers may appear impractical to the hydraulic designer—however the water in a reservoir often has ample time to become quiescent. Furthermore, laminar-viscous flow may occur even in pumped systems at Reynolds numbers considerably above the accepted critical values. Thus, we have the results reported by the University of Iowa[4] with a system in which oil is pumped continuously through a pipe; it is impossible to obtain turbulent flow even at the upper limit of the pump capacity (R about 7800). The turbulence must be artificially triggered to make it appear in this case. It would appear that appreciable amounts of laminar-viscous flow may well occur in some of our hydraulic structures of clean design.

The author's study of transition is therefore of potential value to designers as well as being of intrinsic interest to fluid mechancians. One has only to glance at the discussions concerning laminar-flow shapes in aeronautical publications to visualize the potential gaines. Fifty to one hundred-fifty per cent increases in aircraft ranges from the use of suction-stabilized laminar boundary layers are suggested. If comparable achievements are possible in some of our hydraulic structures, it might be possible to justify the special construction and precautions needed to achieve the results. Only through fundamental studies such as reported by the author can one obtain the knowledge needed to assess what is possible. Also, we need to be able to tell if our pipe flows may occur with appreciable laminar flow regions. In many cases one may not design for laminar flow but one should consider its likelihood of occurrence. Differences in terms of pressure drop, heat transfer, etc., between a design based on the conventional assumption of turbulent flow (at Reynolds numbers above 2500) and a flow with a considerable laminar-viscous region can be significant.

Study of the laminar-turbulent transition in pipes is of considerable intrinsic interest, since there is some question whether it should occur at all if there is no disturbance. As noted above, the experimental evidence shows no upper limit to the critical Reynolds number as the external disturbances are reduced. One therefore turns to theory to see what says about this question. The author has discussed his observed transition results in terms of the prediction of the small-disturbance theory for the stability of Tollmien-Schlichting waves, but for the case of Blasius flow, i.e., for the laminar-viscous boundary layer on a plane with zero pressure gradient. The result is certainly suggestive, even if not applicable to the present problem. This small-disturbance theory has been quite useful in predicting the instability of laminar-viscous flows. The instabilities and resultant wave length—Reynolds number relations (cf Fig. 9 of the paper) do not immediately indicate transition to turbulence, but they have been found to exist. Although such predictions were long considered of doubtful physical reality, they were first verified for flat plate flows in 1940. The phenomenon of selective amplification of disturbances of the proper wave length and frequency in laminar-viscous flows is now accepted as a prerequisite to transition, except where relatively large disturbances are present to override this occurrence.

Prediction of a critical Reynolds number for pipe flows on the basis of the small-disturbance theory has been a rather elusive thing, considering the practical interest in transition and the available experimental information.

Amongst the early analysis was W. M. F. Orr (1906) who utilized the approaches of Lord Rayleigh (1879 et seq) and O. Reynolds (1895)—in fact the basic relation of the small-disturbance theory is often called the Orr-Sommerfeld equation. Orr found a critical (for instability of the wave disturbances) Reynolds number of 117 for pipe flow. However, more refined analyses have indicated this result to be inaccurate. Thus, C. C. Lin[5] states "no theoretical indication of instability has ever been found for the fully developed parabolic profile in the case of the circular pipe."

Only recently has the apparent dichotomy, between our expectation of a finite critical Reynolds number for pipe flow and the theoretical prediction, been explained. The clarification stems from consideration of the fact that fully developed flow (parabolic velocity profile) in the pipe does not appear full blown at the entrance. Instead it develops in an entrance region whose length depends upon the mean flow Reynolds number. About 0.06 R diameters is required for the entrance length; thus 120, 600 and 3000 diameters are required for the flow to develop at Reynolds numbers of 2000, 10,000 and 50,000, respectively. In this entrance region the flow is of a boundary-layer type with a small favorable pressure gradient. Because of this boundary layer type flow the author has some justification for comparing his results with the stability predictions for Blasius flow. For this latter case the most refined calculations indicate a critical Reynolds number (lowest R value on neutral stability curve of the author's Fig. 9) of $R_{\delta *} = 420$. The boundary layer of the entrance-region flow differs from the Blasius boundary layer due to the pressure gradient.

The possibility that the entrance-region boundary layer may be unstable even though the following Boiseuille flow is stable was investigated by T. Tatsumi[6] in 1952. In terms of his solution for the velocity profiles of the entrance-region boundary layer, his calculations yielded neutral stability curves, i.e., indicated the existence of flows unstable to certain disturbance waves. The minimum critical Reynolds number ($R = VD/\nu$) was found to be 19,400 at a station rather near the entrance, namely at about $x/D = 0.0004$ R (0.67% of the length of the entrance region) or about 7 D from the start of the pipe. For flows at higher Reynolds numbers there is a portion of the entrance region which is unstable and in which small disturbances, if of the proper wave length or frequency, will be amplified. Thus for a Reynolds number of 25,000 the flow is "unstable" (capable of amplifying certain small disturbances) for x/D distances between about 1.4 and 20 as may be seen from study of Fig. A of this discussion. If not enough amplification of the disturbances occurs in this distance and they do not become large enough to cause transition to turbulence, then Tatsumi's analysis would say the flow is stable. It is apparent that the higher the flow Reynolds number (above 20,000) the more opportunity there is for amplification of small disturbances and the greater is the possibility that transition to turbulence will occur. A study of the author's transition data, in terms of the parameters of Fig. A, indicates that the transition Reynolds numbers were generally above the minimum critical value for stability and tended to increase with x/D. However much larger critical x/D values occur.

The author discusses the fact that the disturbances must be considerably amplified after they pass the critical Reynolds number (for neutral stability) before turbulent flow sets in. His discussion is in terms of the stability analysis of the Blasius flow rather than the actual case in hand. It would appear more appropriate to compare the experimental results with the predictions of

the stability analysis of Tatsumi even though this is only for the steady flow case. Actually the comparison should be with neutral stability curves for the profiles calculated from Eq. (3) for the temporally and spacially growing boundary layer. However, neutral stability curves are not easily determined. Since the stability condition is dependent upon the shape of the velocity profile, a suggestion as to which known set of solutions might best apply should be apparent through comparison of the velocity profiles. Lacking this information, it is still possible to glean some useful information from comparison with the Blasius case solution. The remainder of the writer's remarks will follow the author in this regard.

The author's presentation of his transition data in Fig. 10 is interesting and suggestive. However there are several points about the possible neutral stability curves shown that the present writer cannot follow. These points have to do with the wave length $\lambda$ chosen as the basis of calculation for the curves. Thus 2.1 $r_0$ is chosen for spot 2 as "the longest disturbance wave length which originates at the pipe junction." We know very little about the discontinuity presumed to exist at the pipe junction and if we did we still could not predict anything about the wave length of the disturbance which it would produce. Hence, the present writer is forced to conclude that the author chose a wave length which would pass the possible neutral stability curve through the experimental point having the highest transition Reynolds number. The justification for this assumption is that transition is not expected once the disturbance has passed the upper branch of the curve. It is also stated that the appearance of some of the points (actually seven of the nine points for spot 2) below the lower branch of the curve causes no conflict. It is hard to accept this statement, since for points in this region the disturbances would have had no amplification whatsoever. There seems to be no reason why the wave length being amplified should be a unique function of the spot source. Actually it is a function of the boundary layer flow as shown by the neutral stability curve in Fig. 9.

The amplification situation for the simpler Blasius case is clarified through reference to Fig. B, which is nothing but the author's Fig. 9 with some additional information. Some of the amplification contour lines (as found by S. F. Shen[7]) mentioned by the author have been added, together with straight dashed lines indicating the progress of constant wave length disturbances across the amplification ridge. The encircled numbers on some of these dashed lines indicate approximately the total amounts of amplification that have been calculated for these certain wave lengths. The trends of the lines of constant $\lambda$ are quite suggestive of the run lines on Fig. 10. They are inclined straight lines which would pass through the origin, if extended, since as the wave progresses along the flow $\delta^*$ increases and the ordinate and abscissa values increase in constant ratio. Natural transition in the low disturbance flows (free stream turbulence intensity less than 0.3 per cent) is found at $R_{\delta^*}$ values above 2000. In the few cases in which natural Tollmien-Schlichting waves have been measured in terms of their frequency and wave length characteristics, they have been found to occur approximately along the upper branch of the neutral stability curve at Reynolds numbers above 2000. It is apparent that these have been subjected to amplifications of several hundred times at least and that they must cause transition rather quickly since damping sets in after they pass the upper branch of the neutral stability curve. It would appear that amplifications of one hundred or less are inadequate to lead to transition--the amplification occurring at the critical Reynolds number of 420

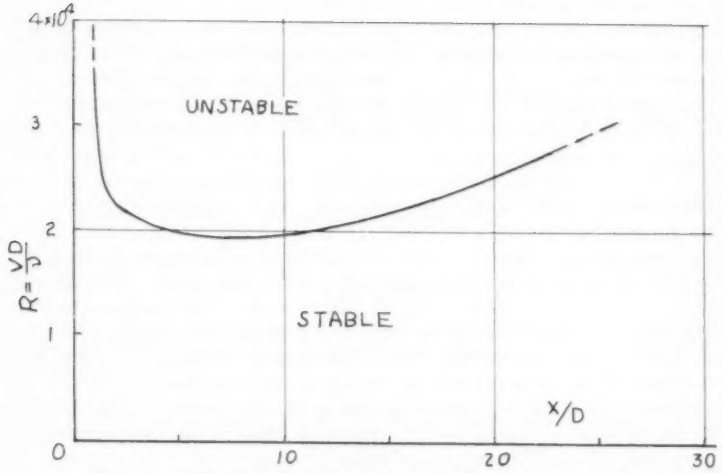


FIG. A STEADY FLOW PIPE NEUTRAL-STABILITY CURVE

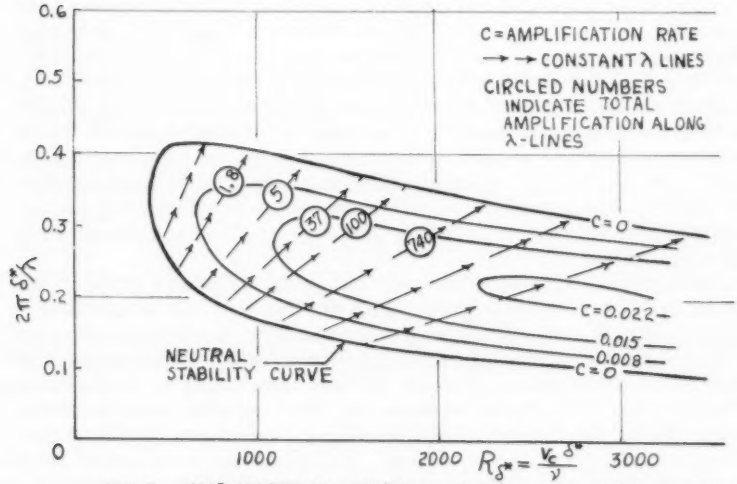


FIG. B AMPLIFICATION CONTOUR RIDGE FOR BLASIUS FLOW

is small indeed. It is not surprising that we find a considerable gap between this critical Reynolds number and that for transition to turbulence.

Attempts to fit the above concepts and results for small disturbance amplification and transition to the results shown in Fig. 10 are not encouraging. Two possibilities suggest themselves as explanation for the poor agreement. The first is that the disturbances causing the transition are not small. The second is that the neutral stability curve for Blasius flow is a poor representation for the actual flow situation. This latter is beyond doubt true, but it behooves one to also check on the former possibility. Information on the effect of roughness elements in causing premature transition has been well summarized by H. L. Dryden.(8) Treating the joint discontinuity as a flat strip element, the important factor telling us whether it will trigger transition is the ratio of the height to the boundary layer disturbance thickness $\delta^*$ evaluated at the location of the roughness element. For turbulence spots 2 and 3, calculations based on the data of Table III indicate that at transition this ratio was of the order of 0.03 to 0.07. Since the change in boundary layer thickness could not have been large in the distance from the pipe joint to the transition location and since Dryden shows that no appreciable effect occurs for ratios below 0.1, it is concluded that indeed the joints were only sources of "small disturbances." In the case of the source for spot 1, the situation is quite different although exact calculation is not possible with the available information. The sand roughness initiating this spot was on the entrance bellmouth where the displacement thickness is extremely thin. The only question in this case is why the author chose to complicate his study with this avoidable source of disturbances and, perhaps, why the sand did not always lead to immediate transition.

The author has been very successful in ferriting out of his rather indirect study considerable information on the occurrence of transition. It is unfortunate that it was not possible to measure the velocity directly. J. Rotta(9) was able to use a hot-wire anemomter to record the velocity fluctuations for transition studies with air flow at Reynolds numbers up to 18,000. No evidence of Tollmien-Schliching waves appear in his results, probably because the hot-wire was located only at the end of the pipe. It would be most enlightening to see how these appear in the regions where their amplification might be expected. Rotta's measurements do give some interesting indications of an intermittent type of laminar-turbulent flow such as noted and discussed by Prandtl and Tietjens.(2)

The writer finds himself at odds with the author in regard to Fig. 7 and the discussion thereof. The turbulence cannot be "diffused into the laminar boundary layer," since it comes from a breakdown of the laminar-viscous flow. Such a breakdown, as opposed to an outside effect, is the whole point of the small-disturbance theory to which we have been trying to tie the transition occurrences. Fig. 7 furthermore shows the turbulent flow after transition as completely filling the pipe cross section where the laminar boundary layer flow did not. This is not necessarily so. Assuming that the laminar boundary layer profile differs only in detail from that for the Blasius case we may take $\delta = 2.9\ \delta^*$ and, except for run 20, $\delta$ is therefore less than one-quarter of the pipe radius. Although the turbulent boundary-layer may well become four times the laminar one in thickness, this does not take place immediately. In flat plate flows the length of the transition region is often found to be as great as that of the preceding laminar flow region. Apparently the simplification of Fig. 7 is satisfactory for the purpose of interpreting the data.

In Table III, it appears that the boundary layer thickness and Reynolds number occurring for transition of spot 2 is less than that for spots 1 and 3 (except for run 20). The author's explanation for this would be appreciated. In terms of the indications that the disturbances which are amplified and then breakdown to turbulence starts from $R_{\delta^*}$ values of about 1000 and hence $2\pi\delta^*/\lambda$ values of about 0.17 the author's discussion of the number of wave lengths between the disturbance source and transition would seem to be in error. For spot 2 it would appear that the distance is only 3 to 15 wave lengths rather than 9 to 40. Also is not the x/D value listed for spot 1 or run 20 in error? Finally, it seems impossible that for spot 1 of run 21, the boundary layer can have a finite thickness at x/D = 0, so this value must also be in error?

## REFERENCES

1. "Stromung in Rohren," by L. Schiller in "Handbuch der Experimental Physik," Vol. IV, Part 4, Leipzig, 1932, pp. 107 et seq.
2. "Applied Hydro and Aero Mechanics," by L. Prandtl and O. G. Tietjens, (German Edition, Berlin, 1931); English Translation, McGraw Hill, 1934, pp. 29-40.
3. "On the Change from Steady to Turbulent Motion of Liquids," by V. Walfrid Eckman, Arkiv for Matematik, Astronomi och Fysik, Vol. 6, No. 12, 1910.
4. "The Iowa Institute of Hydraulic Research," University of Iowa Studies in Engineering, Bulletin No. 30, 1946, pp. 36-37, Fig. 21.
5. "Theory of Hydrodynamic Stability," by C. C. Lin, Cambridge University Press, 1955, p. 98.
6. "Stability of Laminar Inlet-Flow Prior to the Formation of Poiseuille Regime," by Tomomasa Tatsumi, Journal of the Physical Society of Japan, Vol. 7, Sept. 1952, pp. 495-502.
7. "Calculated Amplified Oscillations in the Plane Poiseuille and Blasius Flows," by S. F. Shen, Journal of the Aeronautical Sciences, Vol. 21, Jan. 1954, pp. 62-63.
8. "Review of Published Data on the Effect of Roughness on Transition From Laminar to Turbulent Flow," by H. L. Dryden, Journal of the Aeronautical Sciences, Vol. 20, 1953, p. 477.
9. "Experimenteller Beitrag zur Enstehung turbulenter Stromung in Rohr," by J. Rotta, Ingenieur-Archiv, Vol. 24, 1956, pp. 258-281.

# FLOOD FREQUENCIES DERIVED FROM RAINFALL DATA[a]

Discussion by C. O. Clark
Closure by J. L. H. Paulhus and J. F. Miller

C. O. CLARK,[1] A. M. ASCE.—The criteria for designing structures, dams and bridges, subject to rain and floods can be derived from a look at a small budget from an easy chair, or from the arduous, costly, and sometimes uncomfortable investigation of all data at and all around the scene in all kinds of weather, or from any intermediate combination of observation and non-observation. The consequences of the former, although prevalent, are catastrophic. The mere fact that the subject paper deals with flood frequencies derived from something other than floods, and from data outside of the watershed to which it refers, invites a critical examination as to whether it has really produced the flood frequencies.

The authors have used rainfall data near a site, but outside the subject watersheds, to derive a series of calculated flood flows, which calculated flows are not greatly different in their mean value and variation from, and hence indicate about the same frequency of flooding as, the actual peaks of that same short period. But to reconcile their estimate of normal flood frequency with one observed flood, the authors have to conclude, "data suggest that the 1933 observed flood peak of 11,200 cfs is an unusual event with a return period probably much greater than 100 years".

The writer finds instead that the 11,000 cfs flood is not at all rare, and that it is only luck that there were not two or three as large in the sample period. This fundamental difference in views is attributed to faults of a common statistical process by which judgments about frequency are reached by examination of a small number of observations, and which in this case was probably used with both sets of data, the set belonging to the stream and the set derived from rainfall.

The statistical process is understood to be applicable to some uses with a representative sample of a large population, and has been thought to yield reasonable estimates of size of floods of rare flood frequency when the sample was fairly large and nothing indicated that it was a poor sample, or non-representative, of the whole.

In the record of the subject stream, Codorus Creek, there are several reasons to think that the record is a non-representative sample, some of which reasons involve examination of paths of great storms along the Atlantic coast and noting how few hit Codorus Creek as compared with other places. Hence the data are neither in the rainfall nor the flood experience of a normal

a. Proc. Paper 1451, December, 1957, by J. L. H. Paulhus and J. F. Miller.
1. Cons. Hydr. Engr., Tulsa, Okla.

sample of storm events; both kinds of data, then, are "biased" or unrepresentative. Neither does the trend or scatter of the observed data suggest that the sample may be successfully fitted with a probability curve of a standard type derived from these data alone. This, too, may be correctly said of the record of the stream which the writer introduces to demonstrate that the normal flood experience of the region, and probably of Codorus Creek, is much larger. But neither has this record been used by the writer to select the form of frequency curve which he says is regional in application and applies to Codorus Creek, too. Of the records, either of Codorus Creek or the one introduced, neither is of a sample size sufficient to disprove the form of the applied or indicated frequency. All that is shown is how much small samples can vary from a curve without proving the curve is wrong or right, and without being capable of reliably indicating what curve is right.

Among the streams of this general area is another stream which from an identical quantity of runoff in six hours will produce the same size of peak as the authors assign to Codorus Creek. It is the Passage Creek near Buckton, Virginia, some 90 miles SW of the Codorus Creek, but well within the general area of the problems and basins selected by the authors. There is one significant difference. This stream had its floods; Codorus Creek did not. At least, not in the period 1933-54.

A comparison of the flood experience of these streams with similar flood capacity, but different accidental exposure to opportunity for collecting a record during a specific period, is shown on Fig. 1. The circles and crosses are the experience, and the only facts. The lines are methods of portraying the normal experience of an infinite period of time in relation to these samples. The line attributed to the authors is plotted from Table 4. The lines attributed to the writer are from flood frequency studies made in the subject area about 1942, by James B. Saylor and the writer, for the purposes of the Potomac River Flood Control Survey Report, the essential results of which were published by the District Engineer, Washington District, Corps of Engineers, in his report on that subject to the Chief of Engineers in April 1944. This application is in accord with that study and flood producing capacity of a stream of 87 sq. mi. of drainage area and concentration time of 6 hours. (Data to this effect appear on p. 1484 of Transactions ASCE, 1945, Vol. 110.)

The authors give 74.3 sq. mi. as the watershed of Codorus Creek, and Fig. 5 indicates a time of concentration of about four hours. So the slightly larger drainage area of Passage Creek is to some extent offset by the apparent, but surprising, greater "flashiness" of Codorus Creek. In keeping therewith, the authors have found Codorus Creek capable of producing a flow of 6700 cfs from 1.0 inches of surface runoff uniformly distributed in six hours, and the writer had estimated that Passage Creek could produce 6900 cfs from such an event. On this basis, the streams are selected as essentially of the same flow producing capacity, or as having flood frequencies no more different than the two almost coincident lines on Fig. 1.

Now let us return to the evidence that the larger flood of Codorus Creek is rare. Or to the evidence that because it lies well above a line fitted to the remaining or great majority of points that it should be so regarded.

Except for the two greater values of the flows for Passage Creek, the majority of those data are no greater than the majority of the values for Codorus Creek, and there, too, a line fitted to the majority of the data and extended would indicate a phenomenal rarity to the larger two of the actually observed items.

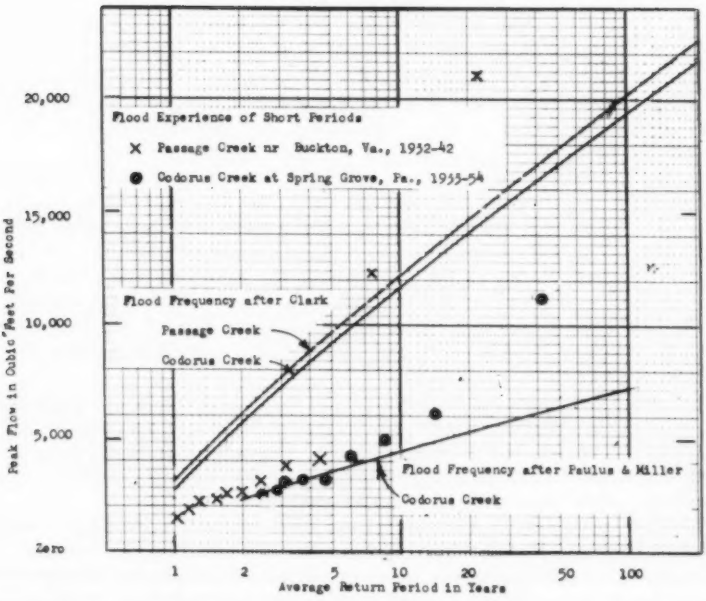


COMPARISON OF STREAMS WITH SIMILAR FLOOD CAPACITY
BUT DIFFERENT ACCIDENTAL EXPOSURE TO OPPORTUNITY

The writer has suggested that there is a pitfall which waits for all of the unwary in frequency calculations from short records, namely that there is no record sufficiently normal to be used, nor a sufficient number of observations to compensate for errors induced by the abnormalities of a few occurrences. What is there to indicate an abnormality in the record of Codorus Creek? First of all, a comparison like that here discussed. But what is there to indicate that it is Codorus Creek and not Passage Creek, or the writer's idea of normal frequency, that is abnormal? Part of that is in the review of the record of this area as a whole.

Such a review shows that few of the great storms of 1930 to 1950 passed very close to Codorus Creek. A further review shows that a storm prior to 1900, probably 1889, not only passed nearby, but created rumors of great floods that persist to this day. Perhaps it was the same storm which sent the Potomac so high that backwater in the gorge below the Falls backed right over the Falls and submerged Delcarlia dam above the Falls and established a high-water mark, there engraved in rock (it was a mark that was discarded as falsely high until a lesser flood of September 1944 demonstrated that the Falls could, indeed, be drowned out, whether the dam could be or not).

Continuing in such a review, the 11,200 cfs flood of Codorus Creek occurred in August 1933, in general a period of drought, but in a storm that established records on a number of nearby Maryland and Pennsylvania streams with short records, but not on any of the streams with moderate length of record at that time. The storm is listed as NA 1-24 among the great storms studied as "Storm Rainfall in the United States", published by the War Department, and one of the bases for preparing Hydrometeorological Report No. 23, a report of the U. S. Weather Bureau on "Generalized Estimates of Maximum Possible Precipitation Over the United States."

The storm maps show 6.8 inches over 10 sq. mi. in six hours as the most intense part of this storm. Report No. 23 gives 24 inches as possible on 10 sq. mi. both there and near Passage Creek. The writer does not consider the 1933 rainfall to be a sufficient approximation of the merely possible as to be even unusual. How then, can the flood be unusual?

For further comparison, the two larger flood items for Passage Creek are for October 1942 and March 1936, Storms SA 1-28 and SA 1-27. In the October center, 6.0 inches is the value given for the maximum 10 sq. mi. in six hours, but it is shown as occurring after 14 inches of prior rain, as compared with 3 inches preceding the maximum rates in the NA 1-24 storm. March 1936 was such a commonly wet month and year that no rare significance can be assigned either to the 2.7 inches of six-hour rainfall or the magnitude of the flow which it produced and which is the second larger on Passage Creek. Compared with these not too rare storms, however, the 1889 storm, SA 1-1, is presumed to have deposited 7.4 inches of water in the same period and area, a wetter season of the year, and somewhat to the northwest of Codorus Creek.

What would Codorus Creek do with 7.4 inches of water in six hours, if one inch of runoff produces 6700 cfs? Fig. 3 indicates that from 2.5 to 5.5 inches would run off. Wouldn't that make 17,000 to 36,000 cfs of flow? What frequency do such flows have? Where would they fit on the suggested normal frequency curves?

Out of some 2500 flood items that lie behind the curves which the writer presents as normal are over a hundred as large as 2 inches of water in 6 hours could produce, and a few are over three times that big. For the basins

the authors list in Table 1 as Nos. 14-19-20-15-18, values of 5.4-4.1-3.3-2.8-2.7 are found in some very short records. In the historical records of the same area, but without any guide as to the total number of items among which they would be found, are values as high as 8 inches of runoff could produce. All are in the area of study of the subject paper, and in the area for which Report No. 23 suggests 24 to 26 inches of rain as being possible on 10 sq. miles in six hours (Values for 100 sq. mi. are not given).

It has been the purpose of this discussion to show that something more than the authors have presented is necessary to derive flood frequency either from rainfall data or from streamflow data, and that without it either or both kinds of data can lead to an erroneous conclusion. There is a wide amplitude of variation in the magnitude of floods which are possible in the subject region. The largest item cannot be discarded from the sample only on the basis of the remaining experience in the same small sample, nor for the convenience or judgment of the calculator. There is nothing needed to explain the wide variations which the writer has presented except measures of accidental proximity to the storm centers and accidental variations of prior wetness and coincidence in the degree of storm intensity with that to which a particular stream is most sensitive. These alone are sufficient to explain wide variations in any small sample, or to explain the extremely long period of time that it would take any one area to experience all of the variations, or even a representative sample, of those which are possible. There are just more possible combinations for hitting a paying combination than there are on a common variety of conventional amusement machines, and as many statistical errors to be avoided in drawing a conclusion on the frequency of outflow as there would be from a similarly small sample of plays on such a machine.

Since none would draw conclusions from a small number of personal observations of action of such a simple machine, what recommends doing so about either rainfall or streamflow observations, either by the authors' procedure, or by any other? Instead, let this profession be built on the processes by which no single observation alters the conclusion by a determinable amount.

J. L. H. PAULHUS,[1] A. M. ASCE and J. F. MILLER.[2]—There certainly can be no argument against the contention that a good relation can be developed between any two sets of randomly selected unrelated items if the items in each set are arrayed in like or opposite order. This fact is so well known that it does not seem to deserve the lengthy treatment given it by Riggs and Benson. The effects of the ranking procedure on correlation had already been explained only a short time before by a Dutch climatologist, C. Levert, in a discussion of "Relation Between Point and Areal Rainfall", published in the Bulletin of the American Meteorological Society, Vol. 38, pp. 618-620, Dec., 1957. However, the subject has no bearing on the authors' paper as correlation was not involved—the objectives of the study being the same as those of any other method of extrapolating streamflow records, namely, the approximation of flood-frequency data and not of individual annual peak discharges. Other comments in the discussion indicated that several important points in the original paper had been misinterpreted.

1. Staff Hydrologist, U. S. Weather Bureau, Washington, D. C.
2. Meteorologist, U. S. Weather Bureau, Washington, D. C.

The second sentence of the discussion implies that a relation was developed between synthesized and observed annual peak discharges and then used to extend the record. The writers did not develop such a relation at any time. The observed and synthesized annual peak discharges were arrayed in like order to facilitate comparison for determining whether frequency analyses of the two would yield similar results. When it was determined that frequency analyses of the synthesized peaks would yield results within 20% of those for the observed, the record of synthesized peaks was extended by means of rainfall data, a rainfall-runoff relation, and a unit hydrograph. At no time was the record of synthesized peaks extended by a relation between observed and synthesized peaks for a specific period.

The objection to the ranking procedure and the suggestion that "the authors' method might have been evaluated by applying it to the latter part of a long flood record and testing the extended results against the known earlier part of the period" are very easily answered. Using the only two basins included in the original study that had records of 30 or more years, the writers have performed the suggested test while showing that the ranking procedure has no bearing on the results.

In the top half of Table 1 are listed in chronological order the observed and synthesized annual peak discharges during the 16-year period, 1938-53, for the Whippany River at Morristown, N. J., (29.4 sq. mi.). The synthesized peak discharges were obtained from runoff computed by applying a rainfall-runoff relation for the Anacostia River, about 175 miles SW of the project basin, to 1938-53 storm-rainfall data from the 2-station network, Plainfield and Elizabeth, N. J., roughly 25 miles SE of the project basin. The 6-hour unit hydrograph used for converting the runoff to discharge was based on data subsequent to 1939, as was the testing and adjusting of the Anacostia River rainfall-runoff relation. Application of the Gumbel method of frequency analysis to the observed and synthesized peak discharges for the 1938-53 period yielded the results shown at the right in the top half of Table 1. The synthesized frequency data are well within the 20 per cent limitation, and the rainfall-runoff relation and unit hydrograph were therefore considered adaptable to the project basin. The arrangement or order of the observed and synthesized peak discharges has absolutely no effect on the flood-frequency data. The discharges could be ranked in like or opposite order or scrambled in any fashion whatever, and the frequency data would remain the same.

The lower part of Table 1 shows the observed and synthesized peak discharges for the 1922-37 period and their frequencies. The same rainfall-runoff relation and unit hydrograph used in synthesizing the annual peak discharges for the 1938-53 period were used to synthesize those for the 1922-37 period, the only difference being that they were applied to the Plainfield-Elizabeth storm rainfall data for 1922-37 instead of 1938-53. Again, the frequency data for the synthesized annual peak discharges are well within 20 per cent of those for the observed.

Table 2 shows the same kind of test applied to synthesized annual peak discharges for the North Branch Raritan River near Far Hills, N. J., (26.2 sq. mi). In this case, a rainfall-runoff relation for the North Branch Raritan River near Raritan, N. J., which includes the project basin, was applied to Plainfield-Elizabeth (about 30 miles ESE) storm-rainfall data for the 1938-53 period to synthesize annual peak discharges for the same period. Data for developing the unit hydrograph and testing and adjusting the rainfall-runoff relation were all from the period subsequent to 1939. The synthesized flood frequency data

TABLE 1

FLOOD FREQUENCIES FOR THE WHIPPANY RIVER AT MORRISTOWN, N. J.

| Water Year | Annual Peak Discharges | | Return Period (yrs) | Flood Frequency | |
|---|---|---|---|---|---|
| | Observed (cfs) | Synthesized (cfs) | | Observed (cfs) | Synthesized (cfs) |
| 1953 | 804 | 920 | 2 | 824 | 772 |
| 1952 | 1360 | 1230 | 5 | 1217 | 1259 |
| 1951 | 938 | 470 | 10 | 1477 | 1582 |
| 1950 | 375 | 380 | 25 | 1807 | 1990 |
| 1949 | 1350 | 610 | | | |
| 1948 | 829 | 900 | | | |
| 1947 | 591 | 420 | | | |
| 1946 | 1020 | 860 | | | |
| 1945 | 460 | 690 | | | |
| 1944 | 640 | 1150 | | | |
| 1943 | 540 | 470 | | | |
| 1942 | 1220 | 1460 | | | |
| 1941 | 679 | 510 | | | |
| 1940 | 1500 | 830 | | | |
| 1939 | 529 | 470 | | | |
| 1938 | 1170 | 1990 | | | |
| Mean | 875 | 836 | | | |
| S. D. | 358 | 443 | S. D. = Standard Deviation | | |
| Mode | 696 | 614 | | | |
| 1937 | 491 | 560 | 2 | 661 | 617 |
| 1936 | 1500 | 1170 | 5 | 990 | 983 |
| 1935 | 467 | 390 | 10 | 1208 | 1225 |
| 1934 | 620 | 600 | 25 | 1484 | 1531 |
| 1933 | 1060 | 750 | | | |
| 1932 | 485 | 430 | | | |
| 1931 | 456 | 400 | | | |
| 1930 | 466 | 420 | | | |
| 1929 | 830 | 430 | | | |
| 1928 | 1100 | 1320 | | | |
| 1927 | 394 | 1140 | | | |
| 1926 | 585 | 1130 | | | |
| 1925 | 680 | 380 | | | |
| 1924 | 830 | 650 | | | |
| 1923 | 600 | 430 | | | |
| 1922 | 700 | 480 | | | |
| Mean | 704 | 665 | | | |
| S. D. | 299 | 333 | | | |
| Mode | 554 | 499 | | | |

being within 20 per cent of the observed, the same rainfall-runoff relation and unit hydrograph were then used to synthesize annual peak discharges for the 1923-37 period from storm rainfall for that period. Again, the synthesized flood frequency data are within 20 per cent of the observed.

Nowhere in the two tests just described would any rearrangement of the order of the observed or synthesized annual peak discharges within any one period have any effect on the computed flood frequencies.

The results of the above tests were satisfactory, considering the short periods of record used for controls and testing—20-year periods should be the minimum and longer periods would be preferable. Generally speaking, this type of test is not a fair one for evaluating the writers' procedure because the off-basin rainfall network does not measure the basin rainfall storm by storm. With the rainfall network fairly well removed from the basin, it is impossible to distinguish between the errors of the synthesizing procedure and sampling errors in the statistical sense. It would be very interesting to see a regional procedure subjected to this same type of test.

The best test of the writers' procedure would be to use a basin with a long streamflow record, say 40 years or longer, and having a rainfall network for 5 to 10 of those years. The basin storm-rainfall data and concurrent streamflow record would be used for selecting or developing a suitable rainfall-runoff relation and for constructing a unit hydrograph. The relation and unit hydrograph would then be applied solely to the storm-rainfall data of an off-basin network to synthesize the annual peak discharges for the entire period of the basin's streamflow record. Comparison of the observed with the synthesized flood frequencies would provide the best possible test of the procedure.

Incidentally, Messrs. Riggs and Benson misinterpreted the purpose of Fig. 6, which was to avoid the necessity of having several unit hydrographs for the same basin. The computed peak discharges were obtained by applying the selected rainfall-runoff relation and unit hydrograph to the basin rainfall actually producing the observed peak discharges. The observed and computed peak discharges were then plotted against each other on a concurrent basis and not after being ranked, as should be obvious from the plotted points of Fig. 6.

In the discussion it was stated that an annual flood peak record of about 15 years is required for applying the writers' procedure. This is not so. The basins used in the study were restricted to those having at least 15 years of streamflow record so that the observed annual peak discharges would serve as a sort of "yardstick" for evaluating the synthesized peaks, as in the above tests. Actually, concurrent measurements of streamflow and of rainfall from an adequate network over the problem basin for a reasonable number of moderate and heavy storms would be the only requirements for application of the technique suggested by the authors. The rainfall and streamflow data would determine the choice and adjustment of the rainfall-runoff relation to be used and permit the development of a unit hydrograph. One or two years of record would suffice in many cases although longer records would, of course, be preferable. Furthermore, the observations need not be continuous but may be made only when major storms or high discharge rates are expected.

There is absolutely no reason why the synthesized and observed peak discharges should correspond on an annual basis—no more so than observed peak discharges for basins being used in developing a regional procedure. If the rainfall network were in the problem basin, agreement between synthesized and observed peak discharges might then be expected. The agreement would

TABLE 2

FLOOD FREQUENCIES FOR THE NORTH BRANCH RARITAN RIVER NEAR FAR HILLS, N. J.

| Water Year | Annual Peak Discharges | | Flood Frequency | | |
|---|---|---|---|---|---|
| | Observed (cfs) | Synthesized (cfs) | Return Period (yrs) | Observed (cfs) | Synthesized (cfs) |
| 1952 | 2010 | 1710 | 2 | 1436 | 1485 |
| 1951 | 1340 | 1020 | 5 | 2443 | 2593 |
| 1950 | 448 | 560 | 10 | 3109 | 3326 |
| 1949 | 1520 | 780 | 25 | 3951 | 4253 |
| 1948 | 1420 | 2260 | | | |
| 1947 | 753 | 860 | | | |
| 1946 | 1430 | 1360 | | | |
| 1945 | 1260 | 800 | | | |
| 1944 | 1140 | 3270 | | | |
| 1943 | 887 | 720 | | | |
| 1942 | 3280 | 3260 | | | |
| 1941 | 1240 | 1370 | | | |
| 1940 | 3410 | 2070 | | | |
| 1939 | 657 | 1000 | | | |
| 1938 | 2700 | 3390 | | | |
| Mean | 1566 | 1629 | | | |
| S. D. | 906 | 997 | S. D. = Standard Deviation | | |
| Mode | 1111 | 1127 | | | |
| 1937 | 1270 | 480 | 2 | 1109 | 1160 |
| 1936 | 1860 | 1960 | 5 | 1747 | 1925 |
| 1935 | 732 | 760 | 10 | 2170 | 2432 |
| 1934 | 2630 | 2170 | 25 | 2703 | 3073 |
| 1933 | 1480 | 1480 | | | |
| 1932 | 1000 | 970 | | | |
| 1931 | 1320 | 770 | | | |
| 1930 | 615 | 870 | | | |
| 1929 | 1040 | 710 | | | |
| 1928 | 1850 | 1790 | | | |
| 1927 | 857 | 1820 | | | |
| 1926 | 1230 | 2740 | | | |
| 1925 | 692 | 440 | | | |
| 1924 | 556 | 1020 | | | |
| 1923 | 750 | 890 | | | |
| Mean | 1192 | 1258 | | | |
| S. D. | 574 | 689 | | | |
| Mode | 903 | 912 | | | |

not be perfect because of inaccuracies in rainfall-runoff relations and unit hydrographs and the probably greater inaccuracies involved in estimating the true volume and the true time and geographical distribution of the rainfall from the network data. In the study described by the writers the rainfall networks were not generally located in the problem basins, because one of the primary objectives was to determine if the rainfall data from one network could be used to synthesize peak discharges for several basins so that the costs of applying the procedure on a per-basin basis would be thus reduced. The only limitation on the use of the rainfall data from a given network to synthesize the peak discharges for a particular basin is that both the network and the basin must have similar precipitation characteristics. Specifically, they must have approximately the same rainfall-intensity frequencies and their intense rainfalls must occur at about the same time of year. It certainly is not required that rainfalls of relative magnitudes over the network and over the basin occur on the same dates.

The reasoning of the writers was that over a long period the basin would have a rainfall record similar to that of the network provided both were in a region of similar precipitation characteristics. This is certainly a better basis for obtaining flood-frequency data than the regional methods mentioned in the discussion. Users of regional methods have to assume that the hydrologic and geologic characteristics, as well as the precipitation characteristics, of the problem basin are the same as those of the basins used in developing the regional method. Of these, the precipitation characteristics are the most conservative and may therefore be interpolated with more confidence than the hydrologic and geologic characteristics for an ungaged basin.

The writers' procedure does make use of causally related data for the problem basin, namely, for adjusting or developing a rainfall-runoff relation and for constructing a unit hydrograph. If any method can be labeled as abandoning the use of hydrologic data causally related, it is the regional method of the usual type. Generally, the only independent parameter is the size of the drainage area. Even if the problem basin has a 5-year record of rainfall and streamflow measurements, the data are usually ignored in regional analysis.

Another advantage of the procedure described by the writers is that it can be adapted to the latest hydrologic characteristics of the basin and might, in some cases, yield more useful results than even the record of observed streamflow. For example, a small basin with 35 years of streamflow measurements has gradually undergone appreciable changes in land use during the first 30 years of record. If the runoff characteristics were seriously affected, the streamflow for the earlier years would not be comparable to that for the last 5 years. A frequency analysis of this record would have little significance in design. Neither would the application of the usual regional method. However, by adapting a rainfall-runoff relation and constructing a unit hydrograph on the basis of the last 5 years of streamflow data, the authors' procedure could reasonably be expected to yield more reliable results than could be obtained from either the streamflow record or the regional method.

The writers admit that there is a great deal of work involved in the application of the procedure, and it would be uneconomical to use it in the design of isolated low-cost structures. However, only about two man-months are required for an experienced person to make the storm-rainfall survey (50-year record), establish the time distribution of the rainfall, adapt a rainfall-runoff

relation, construct a unit hydrograph, convert the rainfall into peak discharge, and make the frequency analysis. The storm survey and time distribution of the storm-rainfall data require about one man-month, so there is a 50 per cent reduction in time required if these two items have already been established for an applicable network. There are certainly many structures for which the expenditure of one or two man-months in obtaining more reliable design data would be justified.

In view of the comments in the discussion, it may appear strange that the writers look upon their procedure as an aid to, as well as a substitute for, regional or generalized methods. The development of regional methods is often hampered by the relatively short streamflow records available, especially for small basins. The writers' procedure would provide 50-year or longer records as a basis for such methods and thus extend their range of reliable application to include design values for longer return periods than is usually possible.

# FLOW CHARACTERISTICS ON THE OGEE SPILLWAY[a]

Discussion by Donald P. Thayer
Closure by Robert B. Jansen

DONALD P. THAYER,[1] M. ASCE.—The author has done a service to the profession in bringing up and proposing a solution for one of the most significant problems confronting the hydraulic designer; i.e., the dissipation of energy by friction on an overflow spillway or steep chute.

The writer is in general agreement with the author as he writes, "It is reasonable to assume that the energy loss on the spillway face is determined by a simple natural law." It is felt that the most logical approach would consist of making a theoretical analysis, taking into account the major factors affecting the phenomenon. Such an analysis should be of immediate use for preliminary design and subsequently should be a convenient framework within which to correlate experimental measurements. From such correlation there should result emprical coefficients bringing the formula into close agreement with experience. By "experimental measurements", the implication intended is measurement of prototype behavior; the writer's observation has been that, for quantitative evaluation of friction losses, conventional models, based upon Froudian similitude, offer little help. More will be said of this later in this discussion.

## Theoretical Analysis

A theoretical analysis of the friction loss on an overflow spillway will be attempted. The well-known Darcy formula will be used for evaluation of the friction head,

$$h_f = f \frac{L}{D} \cdot \frac{v^2}{2g} \qquad (1)$$

where: $f$ = the friction coefficient
$L$ = the length considered
$D$ = diameter of the pipe
$v^2/2g$ = velocity head

The choice of this formula is based upon two considerations: (a) it is dimensionally homogeneous, and (b) it appears to be thoroughly documented by experimental data. It should be noted that this formula is identical, mathematically, with the much earlier Chezy formula; the respective constants appearing in a different form and differing by a constant ratio. For the purpose

a. Proc. Paper 1452, December, 1957, by Robert B. Jansen.
1. Asst. Div. Engr., Div. of Design and Constr., California Dept. of Water Resources, Sacramento, Calif.

of this analysis, however, this formula has two shortcomings: (a) it has been derived for and its use has been limited, almost exclusively, to closed circular conduits, and (b) its friction coefficient f is a function, not of the roughness alone, but of $\epsilon/D$, the relative roughness, where $\epsilon$ = the "absolute roughness", ideally a linear measure of the height of the surface irregularities, but practically an experimentally determined quantity. This formula is often applied to non-circular closed conduits by letting D = 4R, where R is the hydraulic radius, and may, with perhaps somewhat less validity be applied to open conduits.(1)

The channels considered in this discussion will generally be very wide compared to their depth so that without significant error we may say that the depth of flow, perpendicular to the bottom, is equal to the hydraulic radius, R. With this in mind, the Darcy formula may be written

$$h_f = f \frac{L}{4R} \cdot \frac{v^2}{2g} \tag{2}$$

If the hydraulic slope is defined as $s = h_f/L$, then the formula becomes

$$s = \frac{f}{8R} \cdot \frac{v^2}{g} \tag{3}$$

In Fig. 1 consider an elemental prism of the flowing water of weight W, shown cross-hatched, moving down the spillway slope, A-B, from position M to position N. Let the line C-D be the trace of the centroid of the mass as it moves. Measured at this centroidal line, the hydrostatic pressure potential energy of the elemental prism of water is zero and its total energy may be written as the sum of its potential and kinetic energies,

$$E = \frac{Wv^2}{2g} + Wy \tag{4}$$

where: y = distance of the centroid above some datum, as yet undefined, with positive direction upward.

As the mass moves down the slope the change in energy may be obtained by differentiation with respect to L.

$$\frac{dE}{dL} = \frac{Wv}{g} \frac{dv}{dL} + W\frac{dy}{dL} \tag{5}$$

For a frictionless condition, the right-hand member of Eq. (5) would be equal to zero; with friction it is equal to minus the hydraulic friction slope times the weight of the mass,

$$\frac{dE}{dL} = -Ws \tag{6}$$

From geometry of Fig. 1,

$$dL = -dy/\sin\alpha \tag{7}$$

where: $\alpha$ = angle of inclination of line C-D, at the point considered, from the horizontal.

From continuity of flow,

$$R = q/v \tag{8}$$

where: q = specific discharge passing down the spillway.

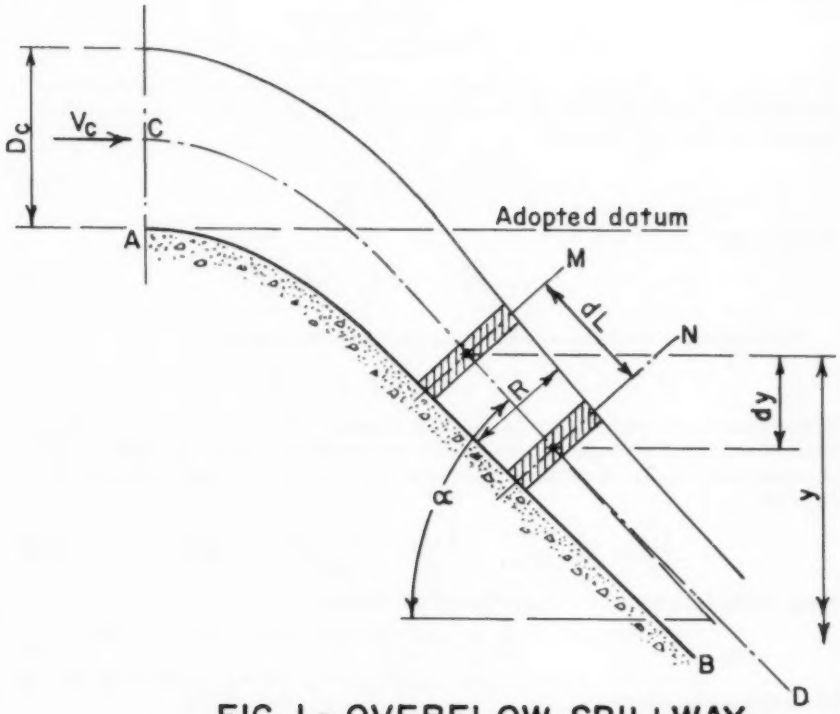


FIG. 1 - OVERFLOW SPILLWAY

Inserting relationships, Eq. (3), (6), (7), and (8) in Eq. (5) and multiplying out dL, gives

$$\frac{Wv}{g}\,dv + W dy = Wf\frac{dy}{\sin\alpha}\cdot\frac{v^3}{8qg} \tag{9}$$

Dividing by W and rearranging

$$-\frac{v\,dv}{g} = \left[1 - \frac{fv^3}{8qg\,\sin\alpha}\right] dy \tag{10}$$

Let

$$B^3 = \frac{fv^3}{qg\,\sin\alpha} \tag{11}$$

Then

$$B^2 = \left[\frac{f}{\sin\alpha}\right]^{2/3} \cdot \left[\frac{1}{qg}\right]^{2/3} v^2 \tag{12}$$

Let

$$F = \left[\frac{f}{\sin}\right]^{2/3} \tag{13}$$

Note that $(qg)^{1/3} = v_c$, the critical velocity, then

$$B^2 = \frac{F}{v_c^2} v^2 \tag{14}$$

Note also, that $v_c^2/g = D_c$, the depth at critical velocity, and substitute this relationship, together with the first differential of Eq. (14) for the left-hand member of Eq. (10) to obtain

$$8 \frac{BdB}{B^3 - 8} = F \frac{dy}{D_c} \tag{15}$$

Integrating

$$8 \int \frac{BdB}{B^3 - 8} = F \frac{y}{D_c} + FC \tag{16}$$

The denominator under the integral sign has the factors

$$[B - 2] \cdot [B + (1 + i\sqrt{3})] \cdot [B + (1 - i\sqrt{3})]$$

These factors become the denominators of partial fractions formed in the usual manner. These partial fractions upon integration and the combination of conjugate complex quantities give as a value of the left-hand member of Eq. (16)

$$\frac{2}{3}\left[\log \frac{(B-2)^2}{B^2+2B+4} - 2\sqrt{3} \tan^{-1} \frac{\sqrt{3}}{B+1}\right] = \Phi(B) \tag{17}$$

Then, using this notation, Eq. (16) may be written

$$\frac{\Phi(B)}{F} = \frac{y}{D_c} + C \tag{18}$$

Eq. (14) may be written

$$\frac{B^2}{F} = \frac{h_v}{h_c} \tag{19}$$

where: $h_v$ = velocity head at any supercritical velocity
$h_c$ = velocity head at critical velocity

It should be noted that the function (B), Eq. (17), is inherently negative, varying from -2.4179 when B = 0, to negative infinity when B = 2.

Eq. (18) and (19) then give dimensionless relationships between y, measured in terms of $D_c$, and $h_v$, measured in terms of $h_c$. These equations have been evaluated for several different values of F and the results plotted in Fig. 3. In all cases the value of C in Eq. (18) has been so chosen that the curve passes through the point ($h_v/h_c = 1$, $y/D_c = +0.5$) thus placing the datum as shown in Fig. 1, at the elevation of the crest where critical velocity is attained. It is recognized that in many cases critical velocity and depth are not attained at the fixed crest. In this case it is a simple matter to compute a critical depth at which the given specific discharge would pass over the given crest or, more precisely, to compute a fictitious crest elevation over which the given specific discharge from the given pool elevation would pass at critical velocity. It is believed that in many cases the former method is sufficiently accurate. In this connection the following relationship may be useful; the equivalent critical depth,

$$D_c' = .314 H C^{2/3}$$

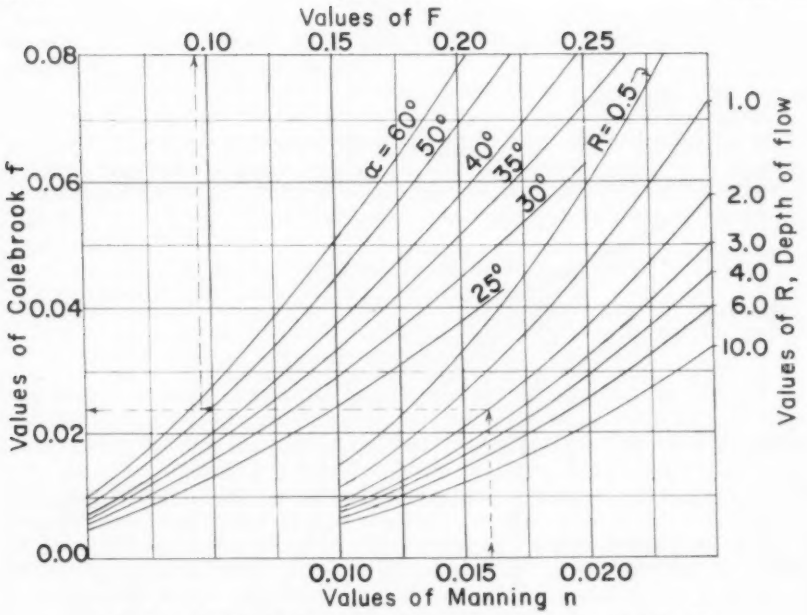


FIG. 2 – DIAGRAM RELATING n, R, f, α, AND F

where: H = head from the given crest to stagnation pool level
C = coefficient of crest, as in $q = C H^{3/2}$

Fig. 3 has been drawn to give a rapid graphical method of obtaining the relationship between Manning n, the Colebrook function for f in the Darcy formula, and F as used in this discussion. The use of this diagram should be self-evident, except for the angle, α, to be used. Theoretically this is the angle the median line of the overflowing nappe makes with the horizontal; actually, at the lower part of the spillway, where the greatest part of the friction loss occurs, this line is nearly parallel to the spillway and the latter angle should be satisfactory. The depth, R, varies continuously throughout the spillway so that a value approximating the mean in the region where the greater part of the friction loss occurs would probably be the best to use.

## Comparisons and Application

For purpose of comparison, three of the points representing velocity measurements at Madden Dam as reported by Mr. Randolph[2] have been plotted on Fig. 3. The correlation is not particularly good, although the trend is in the right direction. It must be pointed out that the plotting may be inaccurate since the values were scaled from Fig. 17 in Mr. Randolph's paper, the writer being unable to find numerical values. Two points from the model study of the Madden Dam, also scaled from this same Fig. 17, are also plotted. These points fall on a much smaller value of F than any of those for the prototype, although the roughness of the model and prototype, as reported by Mr. Randolph were in approximately the correct Froudian relationship

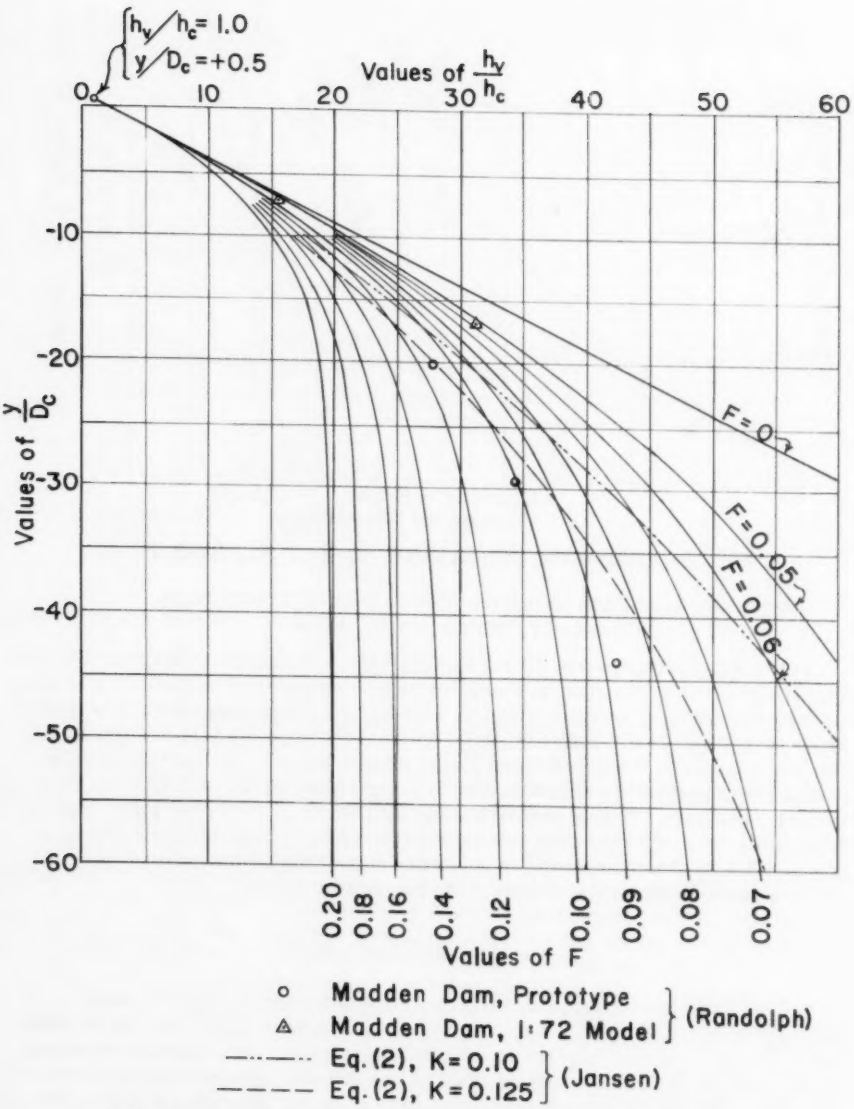


FIG. 3 – FRICTION HEAD LOSS ON SPILLWAYS

(assuming, of course, that the Manning formula is applicable to both). This emphasizes the statement made earlier regarding the inapplicability of model results where friction is concerned.

Curves drawn according to the author's Eq. (2) are also plotted on Fig. 3; one with K = 0.10 and the other with K = 0.125. These curves cut sharply across the F curves indicating considerably discrepancy. It might be pointed out that the author's curves are not asymptotic to a vertical line, indicating no terminal velocity. For practical purposes, with small relative values of y, this should not be considered a serious defect; the point is more theoretical than practical.

The analysis made in this discussion disregards two factors which might have a considerable affect on the spillway velocities:

(a) The friction of the atmospheric air on the overflowing sheet of water.
(b) The effect of entrained air on the friction coefficient.

As the author points out, engineers are not agreed on this point and there are conflicting data. Viparelli[3] states that for calculation of velocity the value of n appropriate for the channel surface should be used. He cites earlier experiments by Mongiardini with flow of an air-water mixture through a closed pipe indicating that for conditions of complete turbulence (Reynolds' number greater than 50,000) the friction coefficient is the same as for water alone. It should be noted that these experiments used a rather small pipe, 20.8 mm diameter. On the other hand, Straub and Lamb[4] show that velocities in an experimental chute computed from the "normal" value of n are considerably less than those measured.

It is believed that more measurements of prototype behavior are needed to clarify this point.

## Future Investigations

No other prototype measurements are available to the writer to compare with his analysis. It would be very helpful if anyone having such data would plot it on Fig. 3 or forward the data to the writer for such purpose.

The lack of reported prototype measurements applicable to this subject is rather unfortunate, and it is hoped that more data comparable to that collected by Mr. Randolph will be collected and reported. It is encouraging to note that the north spillway bay of the Detroit Dam has been arranged to permit such measurements, and it is hoped that data from this source will be made available in the near future.

## REFERENCES

1. Moody, Lewis F., Friction Factors for Pipe Flow, Trans. ASME, Nov. 1944, p. 671 et seq.

2. Randolph, Richard R., Jr., Hydraulic Tests on the Spillway of the Madden Dam, Trans. ASCE, Vol. 103, 1938, p. 1106.

3. Viparelli, Michele, The Flow in a Flume With 1:1 Slope, Proc. Minnesota International Hydraulics Convention, Sept. 1-4, 1953, p. 416.

4. Straub, Lorenz G. and Lamb, Owen P., Experimental Studies of Air Entrainment in Open Channel Flow, Proc. Minnesota International Hydraulic Convention, Sept. 1-4, 1953, p. 435.

ROBERT B. JANSEN,[1] A. M. ASCE.—The subject of head loss on the spillway face is deserving of more attention. Further experimentation and analysis should be directed toward determination of the mechanics of this process of energy dissipation. The rate of energy variation surely must be determined by the relationship of a relatively small number of factors. In the case of an ogee spillway, or any straight spillway with constant slope and roughness, the pattern of energy change obviously is established primarily by conditions at the crest.

For a given spillway slope and roughness, the head loss should be a function of the distance of fall and the rate of discharge. It was on this basis that Eq. (3) was suggested. Application of this formula, with K equal to 0.125, gives results fairly close to the prototype observations on the spillway of the Madden Dam. Since the face of this spillway was reported to be rougher than usual, it was estimated earlier that the value of K for a typical concrete spillway might be closer to 0.10. Recent developments have shown this assumption to be questionable.

The newly published work of Bradley and Peterka(1) contributes to an understanding of this phenomenon. Fig. 15 of their series of valuable papers shows the results of prototype observations on the spillways of Shasta and Grand Coulee Dams. Also presented are curves, drawn from the considerable experience of the authors, which enable the determination of velocity and depth of flow "with a fair degree of accuracy, for chutes having slopes of 0.8:1 or steeper, where computation is a difficult and arduous procedure." The prototype tests cover a range of crest heads from 1.6 feet to 13.6 feet with height of fall as great as 220 feet. These important measurements provide opportunity for comparison with the Madden Dam prototype data, and for further analysis of basic relationships.

The Shasta and Grand Coulee spillways have a face slope of 0.8:1, as compared with the Madden Dam inclination of 0.75:1. All three have drum-gated crests; Shasta with three gates 110 feet by 28 feet, Grand Coulee with eleven gates 135 feet by 28 feet, and Madden with four gates 100 feet by 18 feet.

Since the reported prototype measurements on these three spillways were limited to crest heads not greater than 13.6 feet, there is need for more information on flow at higher heads. No other prototype tests are known to the writer. However, flow at high crest heads is in a range where, at least for relatively low heights of fall, model and prototype results should be in fair agreement. That is, discrepancies attributable to roughness and air entrainment should not enter seriously. It is considered acceptable, therefore, to use the results of model experimentation for comparison in this range. For this purpose, reference is made to two works of the Waterways Experiment Station, Corps of Engineers, Vicksburg, Mississippi. These are Bulletin No. 37(2) and the model studies for Center Hill Dam.(3) Energy losses for large crest heads can be calculated by using the nappe profiles presented in these papers.

---

1. Supervising Hydr. Engr., Dept. of Water Resources, State of California, Sacramento, Calif.

The data from the above various prototype and model tests have been analyzed by the writer in an attempt to establish a generally reliable formula for computing the head loss on the face of an ogee spillway. Logarithmic graphs were used to establish exponents. It was discovered that the head loss varied directly as about the 4/3 power of the height of fall, and inversely as the 1/3 power of the critical depth at the crest. (These are representative values, with emphasis placed on the apparently more consistent Shasta Dam test data. The exponents derived from the Maddem Dam prototype results were 3/2 and 1/2, as reflected in Eq. (3)). These findings lead to the following relation:

$$h_L = J \frac{Z^{4/3}}{D_c^{1/3}} \qquad (10)$$

wherein J is a coefficient, Z is the height of fall from the reservoir level and is equal to the sum of P and H, and $D_c$ is the critical depth at the crest and is equal to $\frac{C^{2/3}H}{g^{1/3}}$.

A value of J = 0.15 yields results which agree well with the prototype and model records now available. As a matter of interest, a value of K between 0.125 and 0.150 in Eq. (3) would give computed losses in good agreement with these same test data. It appears therefore that the suggested reduction of K from 0.125 to 0.100 because of the unusual roughness of the Madden Dam spillway is not justified. A more proper conclusion from the Madden Dam analysis only, in view of present knowledge, would involve a coefficient of 0.125 instead of 0.100 in Eqs. (2) and (3).

Although Eq. (10) is supported by only a meager experimental foundation, it has merits which should be noted. It is simple, easy to apply, and gives apparently dependable results. Use of the term $D_c$ includes the effects of both C and H, which were treated individually in Eq. (3). On the basis of the spillway observations reported to date, Eq. (10) appears to be in a more acceptable form than Eq. (3). It is probably as consistent a criterion as can be offered now.

Mention should be made of the influences of the roughness and the slope of the spillway face. The former should not be cause for great concern. In the construction of a modern concrete spillway, enough attention is usually given to concrete quality and formwork to ensure a uniform roughness. The effect of the slope of the spillway face cannot be determined on the basis of the three prototypes which have been studied. There is not enough difference in their face angles. However, most ogee spillways will fall into a range not much greater than the one in reference (0.75:1 to 0.80:1). To extrapolate the known data into the range of flatter slopes, it might be assumed that the energy loss varies directly with the length of travel along the spillway face, or inversely as the sine of the angle between the face and the horizontal. If the term J in Eq. (10) is assumed equivalent to $\frac{j}{\sin\alpha}$, then the head loss is given by the following expression:

$$h_L = \frac{j}{\sin\alpha} \frac{Z^{4/3}}{D_c^{1/3}} \qquad (11)$$

in which j is a coefficient and $\alpha$ is the angle of inclination of the spillway face with the horizontal.

Eq. (11) is only speculative. The subject of loss on slopes flatter than the usual gravity-dam slopes is beyond the scope of this paper.

It should be noted too that the prototype measurements on which this study is based are limited to values of Z generally less than 200 feet. However, this does not necessarily place a limitation on the applicability of the results. In using Eq. (10), the calculations of energy loss should be performed progressively at intervals down the spillway face until the terminal velocity is reached. This is the point at which the increment in energy loss becomes equal to the vertical increment of fall. Since the velocity head is assumed constant below this level, the incremental head loss beyond the arrival at terminal velocity is taken as equivalent to the increment of fall. This means that Eq. (10) need be applied only in the range where the rate of energy loss is varying; i.e., only down to the point where the terminal velocity has been attained.

Mr. Thayer has made a remarkable contribution to the literature in his theoretical analysis based on the Darcy formula. Essentially, it appears that he has independently accomplished the same result as achieved by Bresse in his method.(4) Bresse performed his integration assuming a very wide rectangular channel and adopting the Chezy formula. Mr. Thayer has used the same assumption, and has employed a formula which, as he states, is mathematically identical with the Chezy relation.

Much has been written about the limitations of the Darcy formula as applied in the way that Mr. Thayer suggests. Admittedly arbitrary premises are involved. Open channels are usually rougher and larger than pipes, with high values of the Reynolds number, corresponding practically to complete turbulence. In this case, the Darcy coefficient "f" would be practically independent of the Reynolds criterion by which it is commonly determined. The belief has prevailed that some other index, such as the Froude number, should be employed for flow with a free water surface.

It would be hard to imagine more dissimilar conduits than an ogee spillway and a small pipe such as that for which the Darcy formula was developed. Any attempt to use the Darcy relation for analysis of a steep spillway would be accompanied understandably by serious doubts. However, comparison of the Thayer results with data from other sources reveals a relatively close agreement for flow with low crest heads. Discrepancies appear at higher heads.

Although Mr. Thayer has performed an analysis closely paralleling the work of Bresse and has suggested a criterion basically the same as the method of Bresse, the new approach has advantages over the earlier work. The Thayer graphs are presented in such a convenient form as to make computation by this means probably more attractive than by the Bresse tables. Mr. Thayer, in his integration of incremental energy losses defined by the Darcy formula, makes unnecessary much of the labor that would be involved in the common step method using the same formula. This is especially true if the energy relation at only a single point on the spillway face is concerned. If the cumulative loss is to be determined at several points, there is less advantage. For practical purposes, the result is the same whether integration is accomplished by the calculus or by small finite steps.

The two graphs of Mr. Thayer provide a rapid means of estimating the energy loss on the spillway face. In using his curves, it is necessary first to estimate the dimension R and to enter the first graph with this trial value to find the factor F. Mr. Thayer states that, "the depth, R, varies continuously throughout the spillway so that a value approximating the mean in the region where the greater part of the friction loss occurs would probably be the best

to use". It would first appear that this assumption would inject a considerable measure of approximation into the Thayer method. However, the writer has found that the suggestion has merit. Also, the extent of trial involved in selecting the value F is not an important handicap. The convenience of the first graph makes the trial a simple matter.

When the sheet of flow is thin, the graphical selection of the proper value of the Thayer factor F becomes rather difficult. In this range, F varies appreciably with small changes in depth. The term F can be expected to vary as much as 100 per cent on a typical ogee spillway. This is well demonstrated by the first graph of Mr. Thayer.

For large heads on the spillway crest, in general the second Thayer graph is too small in scale to yield sufficient accuracy. This is not an unusual disadvantage of a graph prepared for publication. In practice, the plot could be made to a larger scale, or the basic data could be placed in tabular form. However, it is not certain that the method of Mr. Thayer will give acceptable results when the ratio $y/D_c$ is small. More experimental verification is needed in this region.

Table 1 is a compilation of data from the several sources which have been mentioned. The tabulation shows that the energy losses computed from the actual observations on the Shasta spillway prototype are generally illogical for higher magnitudes of the dimension Z. For example, with a crest head of 1.6 feet the listed energy losses from actual measurements on the prototype are 40, 59, 77, 92, 103, and 108 feet corresponding to heights of 70, 90, 110, 130, 150, and 170 feet, respectively. The increments of energy loss are 19, 18, 15, 11, and 5 feet, in the same order. Logic dictates that, since the velocity will continuously increase until the terminal velocity is attained, there should be no decrease in the increments of energy loss in proceeding down the spillway face. The prototype records presented by Bradley and Peterka for Shasta and Grand Coulee spillways manifest a general defect in this respect. In order to eliminate this inconsistency, the writer had adjusted the computed losses for the Shasta spillway by accepting the value of $h_L$ corresponding to the lowest recorded value of Z for each crest head, on the assumption that the accuracy of measurement of flows on the prototype would decrease as the height of fall increased. In making the adjustment, the rate of energy loss was not allowed to decrease. In the case of the Grand Coulee spillway observations, since the initial value of $h_L$ for a crest head of five feet appears obviously too low, the first listed energy loss has been made to conform to the Shasta prototype data. The other adjusted losses shown for the 5-foot crest head fit the loss differentials of the original Grand Coulee measurements, except that again no decrease in the loss rate has been permitted. For a crest head of 13.6 feet, the measured energy loss for the lowest value of Z has been accepted, although it may be slightly high, and an incremental energy loss of ten feet has been adopted from examination of the pattern of the Shasta columns.

The tabulated energy losses on the Madden Dam spillway were taken directly from Fig. 17 of the paper by Mr. Randolph. A general nappe profile (Fig. 8) in Bulletin No. 37 of the Waterways Experiment Station has provided an estimate of losses at crest heads of 20 and 30 feet. Similar data from the model studies of Center Hill Dam, performed at the same laboratory, give approximate losses for flow with 44 feet of head on the crest. These measurements were taken from the original model, which had a face slope of 0.61:1.

Presented also in Table 1 are energy losses determined on the basis of curves drawn in Fig. 15 of the Bradley-Peterka series. This graph shows that the authors themselves have adjusted for the obvious defects in the prototype observations on the Shasta and Grand Coulee spillways.

The last two columns in Table 1 are based on the Thayer method with Darcy coefficients corresponding to Manning n = 0.014, and on the Jansen Eq. (10) with the factor J equal to 0.15. It is believed that Table 1 demonstrates that Eq. (10) offered by the writer gives a fairly reliable estimate of the energy loss on the face of an ogee spillway, on the basis of comparison with the prototype and model observations which have been discussed. As has been stated, the Thayer method when applied to large crest heads is at variance with the other listed references. However, information presently on record does not permit a definite conclusion in this regard. More observations on spillway prototypes are sorely needed.

One avenue of investigation which can be explored, at least as an approximate means of correlation, is application of the law of hydraulic model similitude. For example, disregarding lack of similarity in roughness and in air entrainment, flow on a spillway 200 feet high with a crest head of 20 feet should involve approximately twice the energy loss as on a spillway 100 feet high with a ten-foot head on the crest.

The superposition of the data of the writer on the second Thayer graph would have resulted in a more logical curve if attainment of terminal velocity had been taken into account. As has been stated earlier, the equation defining the energy loss should be applied only down to the point where the terminal velocity has been reached. Eq. (10) is recommended for this purpose, until a more comprehensive formula can be written. It is recognized that this equation is the result of a mere scratching of the surface of this important subject. Certainly a more satisfactory criterion ultimately will be discovered. In the meantime, the procedures herein described may serve as a guide.

The profession is fortunate to have received the outstanding works of Messrs. Randolph, Bradley and Peterka. Their important contributions to the literature have laid the foundation for a broader understanding of spillway hydraulics. In closing this discussion the writer wishes to record appreciation of the notable treatise by Mr. Thayer. The time which he has given to the clarification of the subject matter herein has greatly enriched the paper.

## REFERENCES

1. Bradley, J. N. and Peterka, A. J., "Hydraulic Design of Stilling Basins," Proc. ASCE, Journal Hydraulics Division HY5, October 1957, Paper 1402.

2. Corps of Engineers, U. S. Army, Waterways Experiment Station, Bulletin No. 37, "Hydraulic Models as an Aid to the Development of Design Criteria," June 1951.

3. Corps of Engineers, U. S. Army, Waterways Experiment Station, Technical Memorandum No. 202-1, "Model Studies of Spillway and Bucket for Center Hill Dam, Caney Fork River, Tennessee," August 1946.

4. Bresse, J. A. C., "Mechanique Appliquee," V. 2, Mallet-Bachelier, Paris, 1860.

TABLE 1. - ENERGY LOSS ON SPILLWAY FACE

| H in Ft. | Z in Ft. | C | $D_c$ in Ft. | Loss in Energy Head, $h_L$, in Feet: Shasta | Shasta Adjusted | Grand Coulee | Grand Coulee Adjusted | Madden | W.E.S. Bulletin 37 | Center Hill Model | Bradley-Peterka Graph | Thayer | Jansen |
|---|---|---|---|---|---|---|---|---|---|---|---|---|---|
| 1.2 | 133 | 3.0 | 0.79 | | | | | 131 | | | 110 | 119 | 110 |
| 1.6 | 70 | 3.0 | 1.05 | 40 | 40 | | | | | | 40 | 53 | 43 |
| 1.6 | 90 | 3.0 | 1.05 | 59 | 59 | | | | | | 58 | 72 | 60 |
| 1.6 | 110 | 3.0 | 1.05 | 77 | 78 | | | | | | 77 | 92 | 77 |
| 1.6 | 130 | 3.0 | 1.05 | 92 | 97 | | | | | | 97 | 112 | 97 |
| 1.6 | 150 | 3.0 | 1.05 | 103 | 116 | | | | | | 117 | 132 | 117 |
| 1.6 | 170 | 3.0 | 1.05 | 108 | 135 | | | | | | 137 | 152 | 137 |
| 2.0 | 134 | 3.0 | 1.31 | | | | | 108 | | | 97 | 112 | 94 |
| 4.2 | 136 | 3.2 | 2.87 | | | | | 70 | | | 78 | 85 | 73 |
| 4.6 | 80 | 3.1 | 3.07 | 33 | 33 | | | | | | 30 | 33 | 35 |
| 4.6 | 90 | 3.1 | 3.07 | 40 | 40 | | | | | | 37 | 41 | 42 |
| 4.6 | 110 | 3.1 | 3.07 | 53 | 54 | | | | | | 53 | 58 | 55 |
| 4.6 | 130 | 3.1 | 3.07 | 65 | 68 | | | | | | 67 | 77 | 68 |
| 4.6 | 150 | 3.1 | 3.07 | 73 | 82 | | | | | | 86 | 96 | 82 |
| 4.6 | 170 | 3.1 | 3.07 | 78 | 96 | | | | | | 105 | 115 | 97 |
| 5.0 | 100 | 3.1 | 3.34 | | | 19 | 44 | | | | 41 | 46 | 46 |
| 5.0 | 120 | 3.1 | 3.34 | | | 33 | 58 | | | | 56 | 64 | 59 |
| 5.0 | 140 | 3.1 | 3.34 | | | 48 | 73 | | | | 72 | 82 | 73 |
| 5.0 | 160 | 3.1 | 3.34 | | | 64 | 89 | | | | 90 | 101 | 87 |
| 5.0 | 180 | 3.1 | 3.34 | | | 77 | 105 | | | | 110 | 120 | 102 |
| 5.0 | 200 | 3.1 | 3.34 | | | 89 | 121 | | | | 130 | 139 | 117 |
| 5.0 | 220 | 3.1 | 3.34 | | | 98 | 137 | | | | 150 | 159 | 133 |
| 6.0 | 138 | 3.5 | 4.35 | | | | | 59 | | | 65 | 62 | 66 |
| 7.6 | 100 | 3.3 | 5.30 | 35 | 35 | | | | | | 32 | 25 | 40 |
| 7.6 | 110 | 3.3 | 5.30 | 41 | 41 | | | | | | 37 | 30 | 45 |
| 7.6 | 130 | 3.3 | 5.30 | 52 | 53 | | | | | | 49 | 42 | 57 |
| 7.6 | 150 | 3.3 | 5.30 | 60 | 65 | | | | | | 63 | 55 | 69 |
| 7.6 | 170 | 3.3 | 5.30 | 65 | 77 | | | | | | 79 | 70 | 81 |
| 7.78 | 140 | 3.6 | 5.75 | | | | | 48 | | | 55 | 45 | 61 |
| 10.6 | 130 | 3.5 | 7.68 | 43 | 43 | | | | | | 37 | 29 | 50 |
| 10.6 | 150 | 3.5 | 7.68 | 44 | 55 | | | | | | 48 | 39 | 60 |
| 10.6 | 170 | 3.5 | 7.68 | 39 | 67 | | | | | | 59 | 49 | 71 |
| 13.6 | 130 | 3.5 | 9.86 | | | 49 | 49 | | | | 32 | 19 | 46 |
| 13.6 | 150 | 3.5 | 9.86 | | | 54 | 59 | | | | 39 | 27 | 56 |
| 13.6 | 170 | 3.5 | 9.86 | | | 49 | 69 | | | | 49 | 34 | 66 |
| 20 | 60 | 4.0 | 15.85 | | | | | | 15 | | 13 | 1 | 14 |
| 30 | 90 | 4.0 | 23.78 | | | | | | 23 | | 19 | 1 | 21 |
| 44 | 100 | 4.0 | 34.87 | | | | | | | 23 | 25 | 1 | 21 |
| 44 | 120 | 4.0 | 34.87 | | | | | | | 32 | 27 | 2 | 27 |

# DISCHARGE CHARACTERISTICS OF RECTANGULAR THIN-PLATE WEIRS[a]

## Discussion by M. R. Carstens

M. R. CARSTENS,[1] A. M. ASCE.—The authors are to be commended for the study of rectangular-notch weirs.

The authors have attempted to eliminate the effects of viscosity and surface tension from experimentally determined values of the coefficient discharge of a thin-plate weir by the simple expedient of an effective head and width. The successful elimination of these two effects should result in the coefficient of discharge of potential (irrotational) flow without surface tension. Thus, the equations for the coefficient of discharge for the full-width weir, Eqs. (25), (26), (27), (28), and (29), should be identical for these five series of tests. The small differences in these equations could be attributed to the following causes:

(a) The use of the effective head does not completely eliminate the effect of viscosity and surface tension and the differences in the equations represent differences between the five series of experiments in this regard;
(b) The geometry in each of the five experiments was sufficiently different to account for the small differences; and
(c) The differences are merely an indication of the order of accuracy with which the coefficient of discharge can be experimentally determined.

Since the maximum deviation of the data from each experiment (Figs. 3, 4, 5, and 9) is greater than the deviations between the equations, the writer believes that (c), above, is the explanation for the small differences in Eqs. (25) - (29), inclusive. Therefore, the writer would have combined all the data (reduced to potential flow) shown in Figs. 3, 4, 5, and 9.

Despite the tenuous derivation of Eq. (15) the solution for the coefficient of discharge is amazingly good. Eq. (15) for a full-width weir is

$$q = C_c \frac{2}{3}\sqrt{2g}\left\{\left[h + \frac{V_1^2}{2g}\right]^{3/2} - \left[\frac{V_1^2}{2g}\right]^{3/2}\right\} \qquad (15a)$$

This equation can be placed in the usual form of the discharge equation by factoring the quantity, $h^{3/2}$, from the parentheses.

$$q = C_c \frac{2}{3}\sqrt{2g}\left\{\left[1 + \frac{V_1^2}{2gh}\right]^{3/2} - \left[\frac{V_1^2}{2g}\right]^{3/2}\right\} h^{3/2} \qquad (15b)$$

a. Proc. Paper 1453, December, 1957, by C. E. Kindsvater and R. W. Carter.
1. Prof., Civil Eng., Georgia Institute of Technology, Atlanta, Ga.

The quantity, $V_1^2/2gh$, can be transformed as follows:

$$q = V_1 (h + P)$$

and

$$q = \frac{2}{3} C_d \sqrt{2g}\ h^{3/2}$$

from which

$$\frac{V_1^2}{2gh} = \frac{4}{9} C_d^2 \left(\frac{h/P}{h/P+1}\right)^2$$

Substituting into Eq. (15b)

$$C_d = C_c \left\{ \left[ \frac{4}{9} C_d^2 \left(\frac{h/P}{h/P+1}\right)^2 + 1 \right]^{3/2} - \left[ \frac{4}{9} C_d^2 \left(\frac{h/P}{h/P+1}\right)^2 \right]^{3/2} \right\} \quad (15c)$$

If the theoretical values of $C_c$ for a two-dimensional orifice are utilized in Eq. (15c), the equation can be solved by successive approximation for $C_d$ as a function of h/P. In the following table, the theoretical values of $C_d$ are tabulated for comparison purposes with the best available experimentally determined values, that is, Eqs. (25), (26), (27), (28), and (29). In addition, the experimentally determined values of Kandaswamy and Rouse are tabulated in order to compare the theoretical solution with an experimental solution obtained at larger values of h/P.

The theoretical solution for the coefficient of discharge is within a few per cent of the various experimental solutions throughout the entire range of the weir, that is, $0 < h/P < 10$. The writer cannot agree with the authors' statement,

> "The result is a complex equation which must be modified to make it practicable and adjusted to make it agree with a particular set of experimental data. The fact that a large number of different empirical formulas have been evolved by this procedure is evidence that the "theoretical" equation is inadequate. The obvious reason for the inadequacy is the fact that the basic assumptions are inaccurate."

Rather it appears to the writer, that too many people write empirical equations.

TABLE

Values of the Coefficient of Discharge for a Full-Width Weir

| $\frac{h}{p}$ | Two-Dimensional Orifice $C_c$ | Values of $C_d$ Theoretical | Georgia Tech Data Eq. (25) | Schoder and Turner Data Eq. (26) | Bazin Data Eq. (27) | USBR Data Eq. (28) | Rehbock (1929) Eq.(29) | Kandaswamy and Rouse* |
|---|---|---|---|---|---|---|---|---|
| 0 | 0.611 | 0.611 | 0.602 | 0.600 | 0.608 | 0.608 | 0.602 | 0.61 |
| 0.111 | 0.612 | 0.614 | 0.610 | 0.610 | 0.617 | 0.616 | 0.611 | 0.62 |
| 0.250 | 0.616 | 0.623 | 0.621 | 0.621 | 0.626 | 0.625 | 0.623 | 0.63 |
| 0.429 | 0.622 | 0.637 | 0.634 | 0.636 | 0.644 | 0.636 | 0.638 | 0.64 |
| 0.667 | 0.631 | 0.658 | 0.653 | 0.656 | 0.662 | 0.651 | 0.656 | 0.66 |
| 1.000 | 0.644 | 0.687 | 0.677 | 0.684 | 0.690 | 0.674 | 0.684 | 0.69 |
| 1.500 | 0.662 | 0.733 | 0.714 | 0.727 | 0.731 | 0.706 | 0.726 | 0.73 |
| 2.333 | 0.687 | 0.800 | 0.776 | | | 0.762 | 0.795 | 0.80 |
| 3.200 | 0.708 | 0.86 | | | | | | 0.87 |
| 4.000 | 0.722 | 0.91 | | | | | | 0.93 |
| 5.000 | 0.741 | 0.97 | | | | | | 1.01 |
| 6.000 | 0.757 | 1.03 | | | | | | 1.08 |
| 7.000 | 0.767 | 1.07 | | | | | | 1.14 |
| 8.000 | 0.775 | 1.11 | | | | | | 1.17 |
| 9.000 | 0.781 | 1.14 | | | | | | 1.18 |
| 10.000 | 0.786 | 1.17 | | | | | | 1.18 |

(*) Kandaswamy, P. K., and Rouse, Hunter, "Characteristics of Flow over Terminal Weirs and Sills", ASCE Proc. Paper 1345, August 1957.

# AIR BINDING IN LARGE PIPELINES FLOWING UNDER VACUUM[a]

## Closure by R. T. Richards

R. T. RICHARDS,[1] A. M. ASCE.—The author agrees with Messrs. Templeton and Stelson that air evacuation equipment may be required at vertical drops. This is particularly true of low velocity flow. The equations they have submitted give an interesting comparison of the relative head losses at a vertical and sloping drop. However, the author's observations on large diameter pipelines indicate that at vertical drops preceeded by relatively short radius bends and at water velocities of 6 to 8 feet per second, turbulence appears to reduce air collection to a point where it causes no serious head loss. Such bends may be found, for example, at the majority of steam power plant main condenser discharges. While a few of these condensers become air bound unless continuously evacuated, the majority are self priming. Hydraulic efficiency here is of great importance. A sloping pipe from the same condenser discharge would probably be air bound.

Messrs. Templeton and Stelson close their discussion by appropriately commenting that air binding can be a serious problem in conduits flowing under pressure as well as under the vacuum conditions discussed in the paper. The author's firm has recently investigated head loss problems in two large diameter sloping power tunnels flowing several miles under pressure. The collection of air along the tunnel roof appears to have been a major contributing factor in the observed excess head losses. Air relief taps similar to those described in this paper have been provided on several large diameter sloping pressure pipes designed by the author; however, to date the test data from these pipes is not sufficient to clearly establish the effect of air binding on these particular installations. If continuous air removal is required it can very easily be accomplished by automatic air relief valves. Removal of air from a pipe flowing under vacuum is far more of a problem, especially at pipeline locations where electric power is not readily available for air evacuation equipment.

---

a. Proc. Paper 1454, December, 1957, by R. T. Richards.

1. Civ. Engr., Ebasco Services Inc., New York, N. Y.

# TURBULENCE CHARACTERISTICS OF THE HYDRAULIC JUMP[a]

Discussions by A. J. Peterka and J. N. Bradley, James M. Robertson, Donald R. F. Harleman, Philip G. Hubbard

A. J. PETERKA,[1] M. ASCE and J. N. BRADLEY,[2] M. ASCE.—The authors are to be complimented for accomplishing an investigation which is difficult both in concept and in performance. Their study represents the ultimate approach; to explain the workings of the hydraulic jump by means of its internal mechanics. Although the study is academic in nature, there are certain aspects of the results which help the practicing hydraulic engineer to rationalize the use of stilling basins shorter than the hydraulic jump length.

It is common practice to make the stilling basin floor (usually concrete) shorter than the true length of the hydraulic jump. Hydraulic model tests and prototype verification tests have shown that, within limits, this is a desirable procedure since little in the way of performance is lost and the cost of the stilling basin is reduced appreciably. In analyzing the action in the jump, the authors have shown why it is possible to reduce the apron length to less than the jump length. The drawings in Fig. 13 indicate that most of the losses occur upstream from the end of the roller and that the downstream end of the jump is relatively ineffective in accomplishing hydraulic losses. However, the velocity distribution curves in Fig. 6 show that a redistribution of velocity occurs after the major part of the losses have occurred. For this reason, it is not possible to reduce the apron length as much as appears possible in Fig. 13. For example, in Fig. 13, for $F_1 = 2$, it might be concluded that the apron need extend only about $3d_2$ downstream from the start of the jump. Fig. 6 for $F_1 = 2$, however, shows that at jump length $3d_2$ there is a major redistribution of velocity yet to be accomplished. If the apron were ended at this point, the high bottom velocity might scour an unprotected riverbed. An end sill on the apron would help to redistribute the bottom velocity. Even at the end of the jump, $4.5d_2$, as indicated on Fig. 4, a slight redistribution of velocity is still to be expected according to Fig. 6.

In tests reported by the writers[3] the jump was found to be imperfectly formed for a Froude number of 2, ($d_2 = 2.1d_1$). The total energy loss was only about 7 per cent in a jump measured to be $4.5d_2$ long. Thus, the length of the jump was useful more to redistribute the velocities than to accomplish

a. Proc. Paper 1528, February, 1958, by Hunter Rouse, T. T. Siao, and S. Nagaratnam.

1. Hydr. Engr., U. S. Bureau of Reclamation, Denver, Colo.
2. Hydr. Engr., U. S. Bureau of Public Roads, Washington, D. C., formerly of U. S. Bureau of Reclamation, Denver, Colo.
3. Bradley, J. N. and Peterka, A. J., "Hydraulic Design of Stilling Basins", Journal of the Hydraulics Division, Vol. 83, No. HY5, October 1957.

losses. Nevertheless, the apron length could not be reduced appreciably from the $4.5d_2$ given as the length of jump.

For a Froude number of 4, the writers found the hydraulic jump to have better form since $d_2 = 4.5d_1$. The energy loss was about 40 per cent. The incoming jet showed some instability, tending to flutter from top to bottom of the jump. Surface waves downstream from the jump were more of a problem than scour tendencies. It was found that the apron length could be reduced considerably, however, without changing the jump action. With the addition of chute blocks and an end sill, the apron length was reduced to about $3.6d_2$. For a Froude number of 4, the authors show in Figs. 13 and 6 that most of the losses have already occurred at $3.6d_2$, and only a slight redistribution of bottom velocity will occur downstream from $3.6d_2$.

For a Froude number of 6, the writers found the hydraulic jump to have ideal form, $d_2 = 8d_1$, and the energy loss in the jump was about 55 per cent. The apron length was reduced to $4d_2$ when cute blocks and an end sill were added to the apron; Figs. 6 and 13 help to justify this length reduction.

It is unfortunate that the authors' tests for $F_1 = 8$ could not be completed since these data would probably have shown that the roller occupied more than half the jump length as stated in the conclusions. It was found in the writers' tests that as the Froude number increased, the roller size increased until the roller length became the controlling factor in determining the jump length. The roller length approached the jump length for $F_1 = 8$, $d_2 = 10.7d_1$, and the energy loss in the jump was about 65 per cent. A discharge of 28 second-feet in a flume 4 feet wide produced a jump which was very turbulent and rough and the jump itself surged because the bottom jet did not carry through at all times for the full length of the jump. Bottom jet action was extremely erratic, sometimes penetrating the jump for the full length and at other times, for only a short distance. At times, the jet appeared to jerk horizontally and flutter vertically.

Also, the large difference in conjugate depths resulted in the jump having a steep profile. Slugs of water intermittently rolled down the steep face and fell into the high velocity jet. A surface surge was set up each time a slug made contact with the jet. This was strictly a gravitational effect which an air model may not duplicate. Actually, flow down the face is common to all jumps, but it is usually steady. These findings probably help to explain the difficulty found by the authors in adjusting their air model to obtain good data for $F_1 = 8$. The writers, therefore, suggest that perhaps the agreement between the air model and water model at $F_1 = 8$ was better than suspected by the authors. In the writers' opinion, it would be impossible with presently known equipment to make accurate measurements in a water jump of $F_1 = 8$ having appreciable physical size. In addition, if the air model boundary was set to the jump length, curve of Fig. 4, it is possible that the $d_2$ test length was too short. In the writers' tests, the jump length was found to be considerably longer for the higher Froude numbers than shown in Fig. 4. It is not clear in the description of the water model tests whether the length ratio $Lj/d_2$ was actually measured in the water model or whether the Bakhmeteff-Matzke curve was accepted as the true length of jump. In the air model, the shape of the boundary (the jump profile in a water model) could greatly influence the action within the jump. The jump length given in Fig. 4 for $F_1 = 8$ is $4.2d_2$; the writers' tests showed $6.1d_2$. The reason for the difference is believed to be due primarily to the greater thickness of incoming jet and width of test flume used in the writers' tests. Excessive friction in too small

models can lead to erroneous results. The authors found it necessary to widen their air model to decrease the wall effects noted in the 1-foot duct. This should serve as a warning to other experimenters who are tempted to use very narrow test facilities when wider sections could be used.

JAMES M. ROBERTSON,[1] M. ASCE.—The study reported in this paper is not only of great interest because of the light which it sheds on that most intriguing hydraulic phenomenon—the hydraulic jump—but also because it represents a thorough study of a separated flow which reattached. Many flow situations, besides the jump, occur with a separated zone of flow and a roller-like action of the separated flow on the main stream.

The suitability of air flow in the carefully formed diverging channel as a model of the hydraulic jump is justified by the authors on the basis of expediency and verification of the mean flow pattern. With no intention of deprecating the value and significance of the study, the writer will point out certain aspects of the flow model wherein it cannot have been similar to a jump. Two features of the flow model differed from those of the hydraulic jump; one of these was inherent in the type of model chosen. The presence of a curved rigid boundary rather than the upper free surface of the jump certainly caused some modification in the nature of the flow while the initial mean and turbulence velocity conditions for the model jump differed from those normally expected in open channel flow.

The conditions of flow at the initial station of most hydraulic jumps must be those of fully developed turbulent open channel flow. The probable variations in mean velocity, turbulent shear stress, and turbulence intensity for this situation are sketched in Fig. A. In contrast, the initial conditions tested in the air flow analogy involved relatively thin boundary layers at the upper and lower surfaces with an intervening core of essentially shearless, turbulence—free flow. In the $F_1 = 2$ case for instance, the shear stress curves of Fig. 7 indicate that the boundary layer thickness along the bottom was at most one-quarter of the initial flow "depth" even at relative distances $x/d_2$ of at least 2. Since turbulent boundary-layer behavior in adverse pressure gradients is sensitive to initial flow conditions, the actual flow following this condition must have differed considerably from that in a proper hydraulic jump. In this respect the condition studied would appear to conform closely to a jump following a sluice gate—a situation still of considerable interest.

Since the pressure increases as the flow proceeds in the x-direction (cf. Fig. 5) the writer would expect to note evidence of separation along the "bed" of the channel. That none is in evidence might appear to be due to the existence of an abnormally thin boundary layer along this surface. Further consideration indicates that this explanation does not appear to hold water. The likelihood of turbulent boundary-layer separation occurring has been shown (1) to depend upon the boundary-layer Reynolds number at the start of the pressure gradient and upon the rate of pressure rise. The paper does not give sufficient information to properly determine the initial conditions but it would appear that at the initial station the momentum thickness Reynolds number probably lay between $10^3$ and $10^4$. If so, it is expected (1) that the maximum mean-flow velocity could not be changed by a factor less than 0.76 to 0.69 for the $F_1 = 2$ test and 0.78 to 0.67 for the $F_1 = 6$ test. Actually the

1. Prof. of Theoretical and Applied Mechanics, Univ. of Illinois, Urbana, Ill.

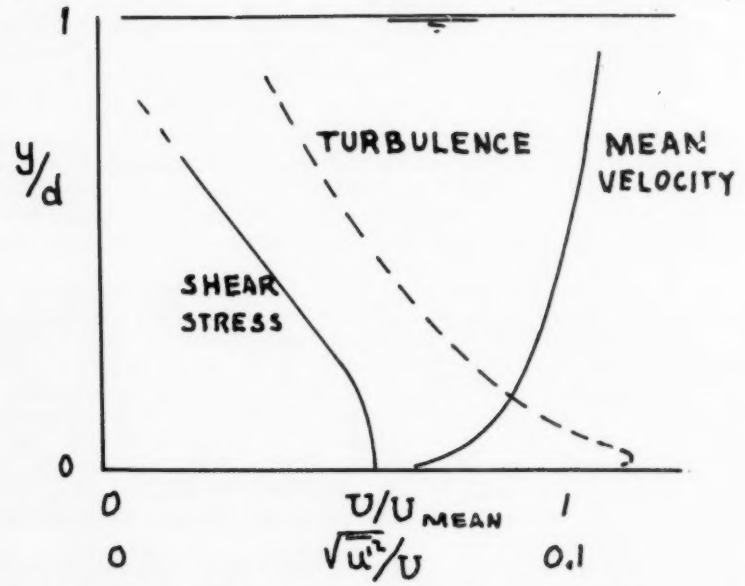


FIG. A VELOCITY AND TURBULENCE VARIATION IN UNIFORM FLOW

apparent reduction in maximum velocity is nearer to 0.50 and 0.12 in the two cases. It is not clear why separation did not occur along the "bed" at an $x/d_2$ location of about 1.2.

The writer's second reservation concerning the "air model" of the hydraulic jump has to do with the upper or "free" surface of the jump and the roller. Since the streamline separating the roller from the main flow and the bed pressure distributions are well verified, it appears that the model is adequate. This mean flow similarity is certainly a necessary condition for similarity, but it is essentially geometric in character. From a dynamic standpoint two other factors enter. The first of these is that in the air model a finite wall shear must have occurred due to the air motion past the rigid upper boundary. In the actual jump no such shear occurs, at least if one neglects air friction. The other divergence of the upper surface from the true hydraulic jump is less simply presented. In the truly-hydraulic jump the surface and its roller appear to be far from steady. Instantaneous views of the upper surface of the jump tend to give the appearance of a breaking wave falling backwards on the oncoming flow. It is felt that the fluctuating nature of the free surface may have a significant effect on the flow at some distance below the surface even though none is apparent in the mean flow characteristics.

The upper boundary, or free surface, differences between the air model and water prototype may be likened to the differences between the outer (distant from the wall) portions of boundary layer and pipe flows. Early boundary layer analyses assumed that the velocity profiles (and by implication, the turbulence pattern) in the two cases were the same if the boundary layer thickness was equated to the pipe radius. More recently careful studies

have indicated significant divergences, both in mean velocity and turbulence characteristics, in the region away from the wall. G. B. Schubauer[2] has shown that this difference in turbulence is completely explained through the phenomenon of intermittency which occurs only at the outer or free stream edge of turbulent flows. As sketched in Fig. B, the division between the turbulently flowing fluid and that outside the boundary layer, does not always occur at the same location, as in the case laminar boundary layers. Instead the interface, between turbulent and non-turbulent flows, fluctuates with time and is conceived of as waves or wrinkles which travel along the outer edge of the layer.

The fluctuating nature of the outer edge of a turbulent boundary layer differs vastly from the situation that obtains at the center of a pipe where the fluid is always turbulent. A velocity indicating instrument with fast time response, when placed in the outer boundary-layer region will see patches of turbulent and non-turbulent fluid pass by. This condition is termed intermittency and the fraction of time that the flow is turbulent is defined as the intermittency factor $\gamma$. Schubauer[2] showed that if we consider only the time when the flow is turbulent in the boundary layer the turbulence in the outer region agrees well with pipe measurements. It is probable that the differences in mean velocity profile are also tied in with intermittency.

Intermittency cannot be immediately applied to our hydraulic jump. Even in uniform open-channel flow, the free edge of our flow is subject to a strong limitation and the air-water interface must inhibit if not eliminate the occurrence of this phenomenon. In the case of the hydraulic jump it would appear that the unsteady roller may result in an intermittency-like behavior. Certainly the upper surface of the roller is rather intermittent in shape and position. The occurrence of air bubbles in this region should also lead to intermittency. As a further bit of suggestive evidence it may be noted that in

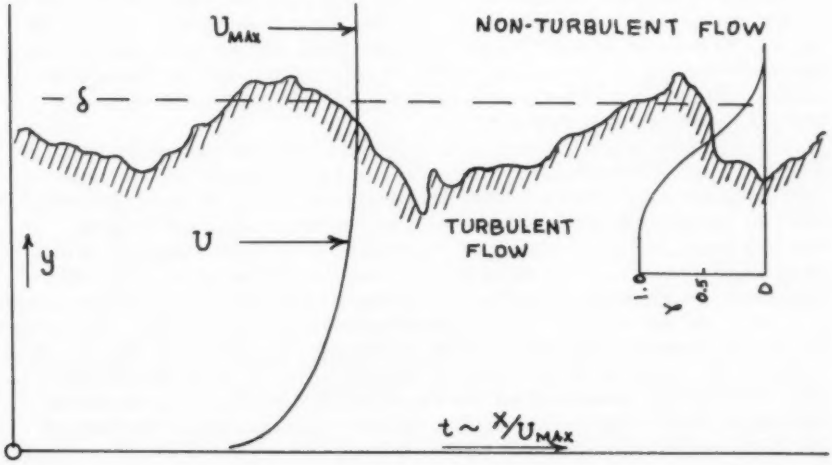


FIG. B DEPICTION OF INTERMITTANCY AT OUTER EDGE OF TURBULENT BOUNDARY LAYER

simple boundary-layer flows the wave or wrinkle length of the free boundary is of the order of two boundary-layer thicknesses. This is of the same order of magnitude as the relative length of the surface roller in the jump.

Although the writer questions whether the authors have adequately "modeled" the hydraulic jump, he agrees that some very suggestive information has been obtained pertinent to the flow behavior in the jump. Actual turbulence studies of a wet hydraulic jump will be needed to ascertain the extent to which the model studied was appropriate.

Aside from its hydraulic jump connotation, the study reported is an extremely valuable piece of basic research. Very few turbulence measurements have been made of separating and reattaching flows. And yet, these are quite common occurrences (in valves for instance). The only comparable study of which the writer is aware was also conducted at the Iowa Institute of Hydraulic Research by A. A. Kalinske(3) and co-workers. The sudden expansion and large angle diffusers studied in that project involved separation and subsequent reattachment. The experimental techniques used were much cruder than in the present instances, but somewhat similar conclusions were reached. Thus Kalinske stated, "the maximum total turbulence energy is a small part of the total energy change taking place" and "the principal loss of energy occurs at the outside of the high velocity stream as it passes into the expansion due to the very high shear developed."

The relatively rapid disappearance of the extra turbulence energy generated in their expanding flow is noted by the authors. Kalinske's sudden expansion results indicate almost as rapid a decay. Since to the observer of the hydraulic jump it still appears quite "turbulent" at its downstream end, where Fig. 10 shows a low level of turbulence, one may question whether to believe his eyes. Another possible explanation may account for this anomaly. In other flow situations (decay of isotropic turbulence) the turbulence energy is dissipated through viscous action in the smaller sized eddies while a relatively small portion of it associated with the large scale eddies, is little effected. In the case of the jump at the downstream station the turbulence level may be low but large eddies could still be quite prominent even though containing little energy. This possibility could be verified through spectrum measurements of the turbulence.

Study of Figs. 6 and 7 should give some idea as to the manner in which a separated and then reattached flow redevelops into a stable pattern again. Following the roller the turbulence levels are seen to be high, but the mean velocity profiles appear to ignore the upper surface. Analysis of mean-velocity data from other studies of reattaching flows have suggested to the writer that a new boundary layer forms along the wall more or less independently of what has gone on before. It may be that the measurements in the jump case did not proceed far enough downstream to indicate this. One of the flow cases analyzed, with the aid of H. R. Fraser, is depicted in Fig. C. This involved the flow of a jet into a partly throttled pipe.(4) Although the pitot tube used was not calibrated for the reverse flows measured, a significant separation zone is apparent. The low values of the momentum thickness $\theta$ and displacement to momentum thickness ratio ($\delta^*/\theta$) found at x/D of about 8 suggest the start of a new boundary layer. Although not at all accurate the wall shear stress variation found in the separated region is of the proper sign and approximate magnitude. In contrast the apparent behavior of the wall shear stress along the upper curved surface in the authors' investigation seems incomprehensible. In the separated zone the flow direction near the

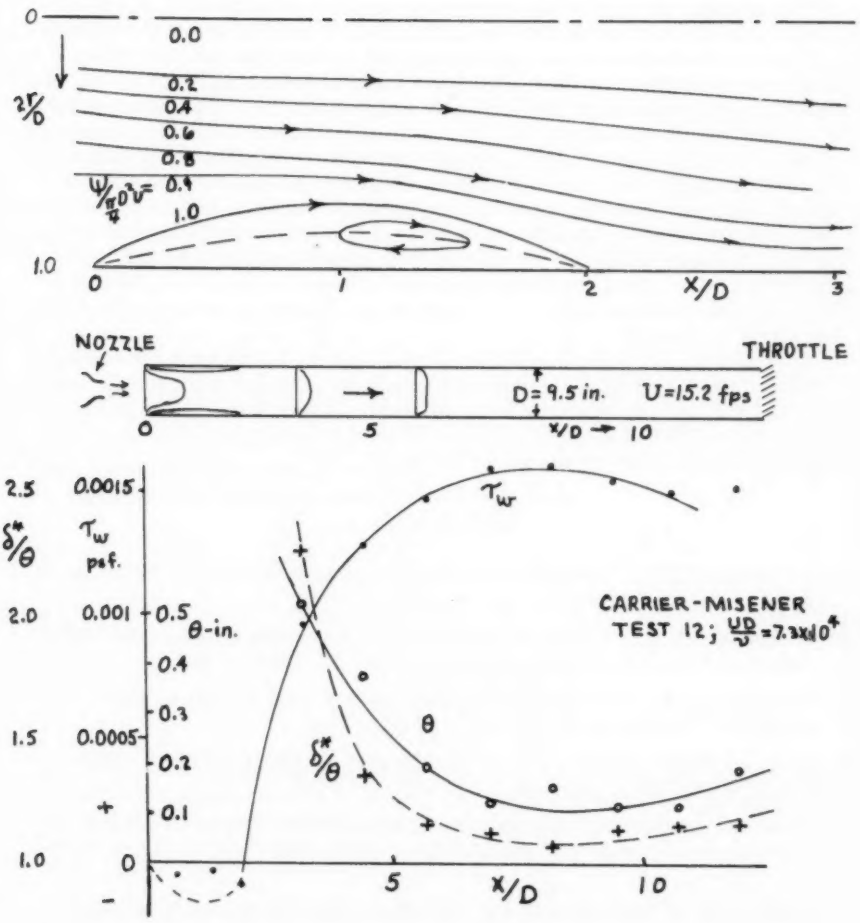


FIG. C FLOW CHARACTERISTICS OF A REATTACHING FLOW IN A PIPE

surface is reversed and yet Fig. 7 indicates a negative wall shear stress within and following the roller.

To calculate the turbulence dissipation the authors utilized the isotropic relation (constant K across and along the flow). They did adjust the value in a bulk fashion for the several Froude number models studied. Certainly K must vary throughout the flow field since the turbulence is far from isotropic and the kind or degree of isotropy can hardly be uniform. P. S. Klebanoff(5) in his very thorough study of the simple boundary layer, measured a majority of the terms appearing in the turbulence dissipation relation. In places some of these differed by a factor of ten from the isotropic values. A transverse integral of the dissipation, based on plausible assumptions for the unmeasured terms, indicated over twice the dissipation calculated with the isotropic relation. It is hard to believe that the more involved pressure gradient and separation flow case in the jump model would come out as close. Therefore the dissipation relations of Fig. 11 must be considered as of suggestive rather than absolute value.

Even within the limitations which it is felt should be placed on the results presented, the paper reports on an extremely valuable and informative study. The writer could only wish for more detailed information on the quantities measured in order that they could be studied independently of the hydraulic jump framework in which the paper is cast.

## REFERENCES

1. Robertson, J. M., "Prediction of Boundary-Layer Separation," Journal of the Aeronautical Sciences, Vol. 24, 1957, p. 631.
2. Schubauer, G. B., "Turbulent Processes as Observed in Boundary Layer and Pipe," Journal of Applied Physics, Vol. 25, 1954, p. 188.
3. Kalinske, A. A., "Conversion of Kinetic to Potential Energy in Flow Expansions," Trans. ASCE, Vol. 111, 1946, p. 355.
4. Carrier, W. H., and Misener, W. S., "Mixing and Equilibrium in Pipe Flow," ASME Paper 53-S-44, May, 1953.
5. Klebanoff, P. S., "Characteristics of Turbulence in a Boundary Layer with Zero Pressure Gradient," NACA Report 1247, 1955.

DONALD R. F. HARLEMAN,[1] A. M. ASCE.—The authors have clearly demonstrated yet another aspect of the universal nature of fluid mechanics by their detailed study of the hydraulic jump by means of an air model.

As a supplement to an otherwise comprehensive treatment the writer would like to set down the explicit equation for the exact depth ratio of the hydraulic jump. This will permit an investigation of the small but systematic deviation of the experimental depth ratio, $d_2/d_1$, from that predicted by the elementary momentum analysis given by,

$$\frac{d_2}{d_1} = \frac{1}{2}\left(\sqrt{1+8F_1^2} - 1\right) \qquad \text{(a)}$$

1. Associate Prof. of Hydrs., Hydrodynamics Lab., Massachusetts Inst. of Technology, Cambridge, Mass.

This deviation is shown graphically in Fig. 4 where the author's hydraulic experiments, together with those of Bakhmeteff and Matzke, are compared with Eq. (a). At a Froude number $F_1 = 6$, for example, the measured depth ratio is five per cent lower than that given by the elementary theory.

The analytical expressions for the hydraulic jump depth ratio taking account of (1) boundary shear, (2) the excess of mean momentum flux due to non-uniform velocity distributions at the beginning and end of the jump and (3) the momentum flux due to turbulence have also been presented by Van Driest.(1) The author's paper, however, permits for the first time a quantitative evaluation of these terms from direct measurements.

The exact equation for the jump depth ratio $d_2/d_1$ can be obtained by evaluating the indefinite integrals of Eq. (13) at the end of the jump where $d = d_2$ and $x = L_j$; Eq. (13) then becomes,

$$\int_0^{d_2} \rho \bar{u}_2^2 dy - \int_0^{d_1} \rho \bar{u}_1^2 dy + \int_0^{d_2} \rho \overline{u'^2_2} dy = \frac{\gamma d_1^2}{2} - \frac{\gamma d_2^2}{2} - \int_0^{L_j} \mu \left(\frac{\partial \bar{u}}{\partial y}\right)_{y=0} dx \qquad (b)$$

(Two typographical errors in the author's Eq. (13) have been corrected, i.e. the dy appearing in the last term should be dx and the sign of the last term should be minus, since the bottom shear acts on the fluid in the same direction as the downstream hydrostatic force.)

Upon introducing the dimensionless coefficients

$$\beta_1 = \frac{\int_0^{d_1} \bar{u}_1^2 dy}{U_1^2 d_1} \qquad \beta_2 = \frac{\int_0^{d_2} \bar{u}_2^2 dy}{U_2^2 d_2}$$

and

$$I_2 = \frac{\int_0^{d_2} \overline{u'^2_2} dy}{U_2^2 d_2}$$

where $\beta_1$ and $\beta_2$ are the momentum flux correction terms for non-uniform velocity distribution and $I_2$ is the downstream turbulence flux correction term ($I_1$ has been assumed equal to zero). After dividing through by $\gamma$ Eq. (b) may be re-written as follows:

$$\beta_2 U_2^2 d_2/g - \beta_1 U_1^2 d_1/g + I_2 U_2^2 d_2/g = \frac{1}{2}(d_1^2 - d_2^2) - \frac{\mu}{\gamma} \int_0^{L_j} \left(\frac{\partial \bar{u}}{\partial y}\right)_{y=0} dx \qquad (c)$$

By introducing the continuity equation, $U_1 d_1 = U_2 d_2$ and defining the Froude and Reynolds numbers as

$$F_1 = \frac{U_1}{\sqrt{g d_1}} \qquad R_1 = \frac{U_1 d_1}{\nu}$$

Eq. (c) may be written as,

$$F_1^2 = \frac{J/2\left[(J+1)(J-1) + S\right]}{\beta_1 J - (\beta_2 + I_2)} \qquad (d)$$

where

$$J = \frac{d_2}{d_1}$$

and

$$S = \frac{2F_1^2}{U_1 R_1} \int_0^{L_j} \left(\frac{\partial \bar{u}}{\partial y}\right)_{y=0} dx$$

Eq. (d) should reduce to the form of the elementary momentum solution of the hydraulic jump if $\beta_1 = \beta_2 = 1$ and $I_2 = 0$ and $R_1 = \infty$ (frictionless flow, $S = 0$). Under these conditions,

$$F_1^2 = \frac{J}{2}(J+1) \qquad \text{(e)}$$

which is in agreement with Eq. (a).

The dimensionless quantities $\beta_1$, $\beta_2$, $I_2$ and S can be evaluated from the author's experimental data for each of the Froude numbers tested ($F_1 = 2$, 4, 6) and the corresponding values of the depth ratio J can be calculated from Eq. (d).

Table I gives the quantities determined from Figs. 7 and 8 of the author's paper. Each of the downstream quantities $\beta_2$, $I_2$ and S were determined at the end of the jump $x/d_2 = 5$.

Table I.

Momentum, Turbulence and Shear Parameters

| $F_1$ | $\beta_1$ | $\beta_2$ | $I_2$ | S | J eq. (d) | J eq.(e) |
|---|---|---|---|---|---|---|
| 2 | 1.01 | 1.02 | .01 | 0.16 | 2.31 | 2.37 |
| 4 | 1.01 | 1.05 | .06 | 1.05 | 5.02 | 5.18 |
| 6 | 1.01 | 1.02 | .15 | 3.60 | 7.70 | 8.00 |

Also given in Table I are the values of the depth ratio $J = d_2/d_1$ from the exact analysis, Eq. (d), and the elementary analysis, Eq. (e). The exact depth ratio is seen to be systematically less than the elementary.

A final verification of the author's measurements and the general validity of Eq. (d) may be demonstrated by comparing the three predicted (exact) values of the depth ratio with Fig. 4 of the author's paper. This comparison is shown in Fig. A and indicates that the predicted values (shown by the dashed line) account for the departure of the experimental depth ratios from the elementary momentum equation for both the hydraulic and air model tests.

The bottom shear S is by far the most important corrective term in the exact equation for the jump depth ratio. In fact, it can be shown that the momentum flux and the turbulence flux corrections tend to cancel each other.

In this respect, the effect of bottom shear is similar to the effect of baffle piers in reducing the downstream depth of a hydraulic jump.(2) In the presence of baffle piers the distributed boundary shear parameter S may be replaced by a term descriptive of the more concentrated force exerted by the piers on the fluid.

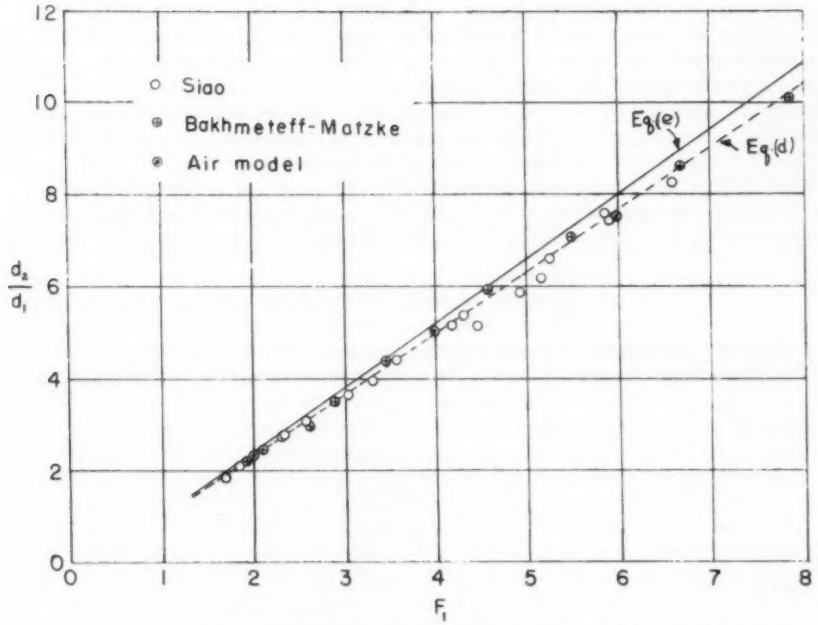


Fig. A. Comparison of Exact and Elementary Momentum Equations for Jump Depth Ratio.

## REFERENCES

1. Steady Turbulent-Flow Equations of Continuity, Momentum and Energy for Finite Systems by E. R. Van Driest, J. Appl. Mech., ASME, Vol. 13, No. 3, September 1946.

2. Effect of Baffle Piers on Stilling Basin Performance, by Donald R. F. Harleman. Journal of the Boston Society of Civil Engineers, April 1955.

PHILIP G. HUBBARD,[1] A. M. ASCE.—As stated by the authors, the analogy between the air-flow system and an actual hydraulic jump may seem to be rather artificial at first glance, so that some engineers may want further verification or at least an evaluation of the applicability of the results. Because of the thoroughness with which the study was conducted and the great importance of the conclusions drawn, it would seem desirable to take advantage of any technique which might supply additional evidence. The hot-film anemometer mentioned in that paper is one such technique, and some exploratory measurements with that instrument are presented herein.

1. Research Engr., Iowa Institute of Hydr. Research, Iowa City, Iowa.

Fortunately, the flume used by Dr. Siao for the measurements in water is a permanent item of equipment at the Institute, so that it was possible to reproduce the conditions of those earlier experiments. In order to obtain representative results in a brief period of time, measurements were made at each Froude number for which results were reported, but only for one representative zone in the flow. The zone chosen was near the downstream end of the roller, where the longitudinal component of turbulence was measured along a vertical line. Although a complete comparison cannot be made on the basis of this one component, it is probably the most representative single parameter. As mentioned by the authors, the total intensity of turbulence is very near equal to twice the intensity of the longitudinal component:

$$\int_0^d \overline{v'^2}\, dy \approx 2\int_0^d \overline{u'^2}\, dy$$

When the measuring instrument was placed in the zone chosen, two pertinent characteristics were immediately evident: The passage of innumerable

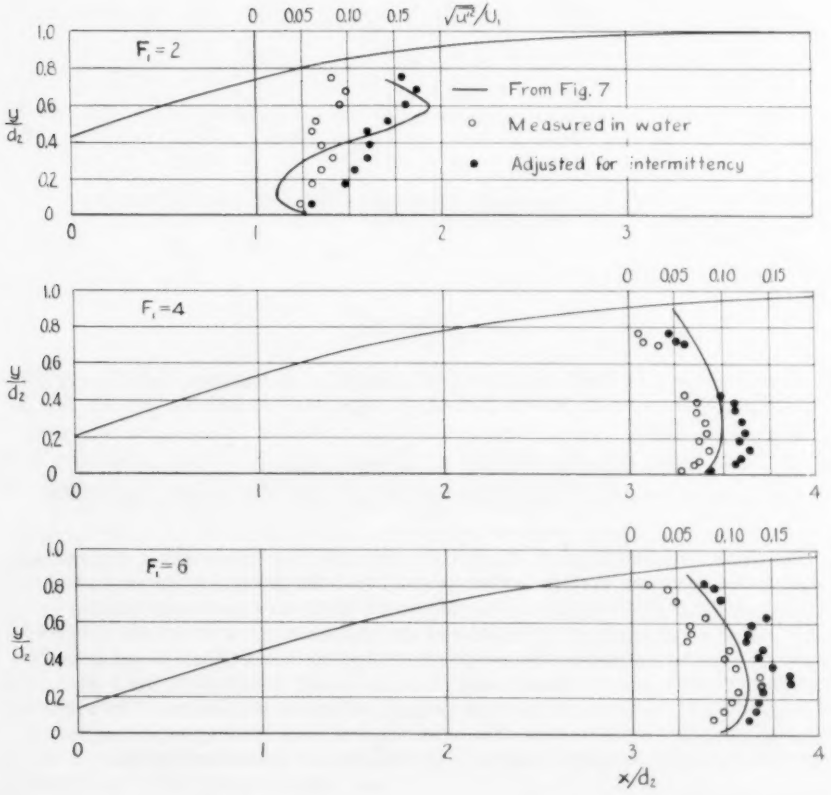

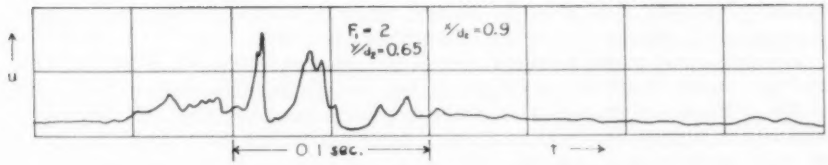


Fig. B. Record of Velocities Inside Roller, Showing Tranquil Intervals

air bubbles past the probe had scarcely any discernible effect on the velocity indications, so that some earlier misgivings were found to be without basis; and the fluctuations were so erratic that only a rough indication could be obtained of either the mean velocity or the root-mean-square deviation of the instantaneous velocity from that mean. Although this problem had been encountered to some extent in the air jump, it was greatly compounded in water. It had been expected that the frequency spectrum of the turbulence would be shifted downward because of the lower velocities used in water, and this shift was expected to cause difficulty because the time constants of the turbulence-analyzing instruments were marginally small. Even when the probable error due to inadequate frequency range in the root-mean-square analyzer was taken into account, however, the measured intensities of turbulence shown in Fig. A were discouragingly below those shown in Fig. 7 of the subject paper.

In order to examine more carefully the variation of the fluid velocity, the output voltage of the hot-film control circuit was connected directly to the deflection terminals of a cathode-ray oscillograph so that no error was introduced by coupling networks. Some typical records obtained in this way have been traced from photographs for reproduction in Figs. B and C, and it is believed that they contain the key to the discrepancy already noted. It was observed that bursts of high-intensity turbulence were interspersed with periods of relatively tranquil flow. Strangely enough, this intermittency existed not only near the upper edge of the boundary layer, but was quite pronounced

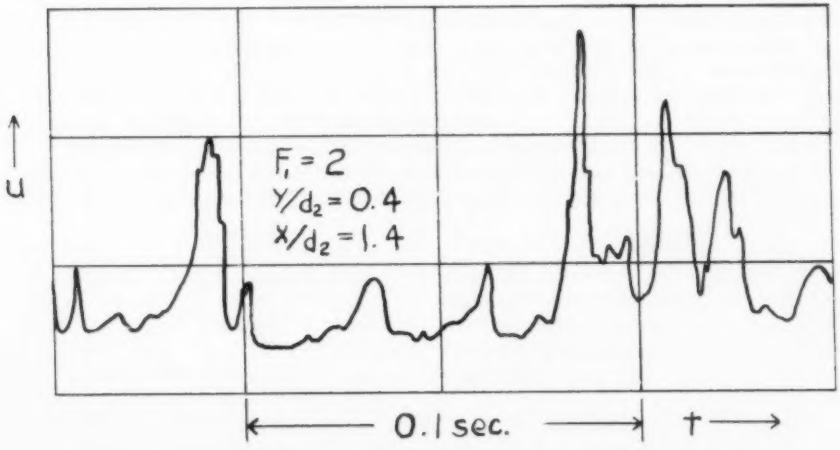


Fig. C. Record of Velocity Immediately Downstream from Roller

inside of the roller. If the data of Fig. A are modified by eliminating the periods of tranquil flow from the record, then the intensity of the remaining fluctuations is slightly higher than that indicated in Fig. 7.

Any evaluation based upon the results reported herein can only be tentative pending a more complete investigation, but two conclusions seem warranted: (1) The diffusion characteristics of the hydraulic jump are probably represented quite well by the results of the subject paper, but those flow characteristics which depend upon the smaller-scale components are probably slightly distorted by the higher indications of the intensity of fluctuation (2) Techniques and possibly definitions will have to be developed especially for flow situations where intermittency may be a factor.

# THE TOTAL SEDIMENT LOAD OF STREAMS[a]

Discussions by R. J. Garde and M. L. Albertson, D. C. Bondurant, John L. Bogardi

R. J. GARDE,[1] J. M. ASCE and M. L. ALBERTSON,[2] M. ASCE.—This paper is a welcome addition to scarce literature on sediment transport in alluvial channels. It will be of use to those who are working in the field, irrespective of the approach in which they are interested—empirical or theoretical.

Broadly speaking, the problem of evaluation of total sediment transport rate in alluvial channels can be handled in one or a combination of the following three ways:

1. Based on the present-day knowledge of fluid mechanics and sediment transport, a theoretical relationship for the total load can be developed.
2. By adding suspended load to the contact (or bed) load, the total sediment transport rate can be determined. Einstein's procedure, and the Modified Einstein's procedure would fall under this category.
3. Based primarily on dimensional analysis and intuition, some empirical relationships can be developed to express the total sediment transport rate as a function of parameters relating hydraulic characteristics of the flow and characteristics of bed material.

Because of time and energy involved, and also because of the inadequate knowledge of sediment transport phenomena, very little work has been done in developing the first method.

Einstein's procedure of finding the total sediment load by adding suspended load to the bed load is quite often used. It is found that the results obtained by Einstein's procedure do not agree with certain data obtained in the field.(8) Therefore, Hembree and Colby(8) have developed a "Modified Einstein's Procedure" to evaluate the total sediment load.

In evaluating the total suspended load by integration of the sediment distribution curves, some important assumptions are made. Following are given the basic equations and the assumptions made in their development:

| | Equation | Assumptions |
|---|---|---|
| 1. | $\tau = (\upsilon + \epsilon_m)\frac{d}{dy}(\rho v) = \rho\epsilon_m \frac{dv}{dy}$ | That the density $\rho$ of the fluid-sediment suspension is independent of y and that the kinematic viscosity $\nu$ is relatively insignificant compared with the eddy viscosity $\epsilon_m$. |

a. Proc. Paper 1530, February, 1958, by E. M. Laursen.

1. Graduate student, Colorado State Univ., Fort Collins, Colo.
2. Director of Research Foundation and Prof. of Civ. Eng., Colorado State Univ., Fort Collins, Colo.

| | Equation | Assumptions |
|---|---|---|
| 2. | $\frac{dv}{dy} = \frac{1}{ky}\sqrt{\tau_0/\rho}$ | That the logarithmic distribution of velocity is applicable and that the Karman universal constant k has a constant value. |
| 3. | $\omega c + \epsilon_s \frac{dc}{dy} = 0$ | That the sediment transfer coefficient $\epsilon_s$ is equal to the momentum transfer coefficient $\epsilon_m$. |
| 4. | $\epsilon_m = \epsilon_s = ky\sqrt{\tau_0/\rho}\ \frac{D-y}{D}$ | |

At present, work is being done at Colorado State University on the evaluation of total sediment load by adding suspended load to contact load. Thus far, this method has been found to have serious limitations because in a dune regime one does not know how to predict accurately either the concentration of suspended load at a given elevation or the exponent z in the actual sediment distribution curve. Furthermore, if one assumes a general law of velocity distribution as

$$\frac{V}{V_*} = \frac{2.3}{K} \log_{10} \frac{y}{K_s} \qquad (1)$$

in which v is the velocity at a distance y above the bed

k is the Karman universal constant

$K_s$ is some length parameter

V* is the shear velocity

it is found that both k and $K_s$ depend on the flow regime—such as plane bed or dune bed—and other flow parameters.

Therefore, for immediate use, at least some empirical relationships are necessary for predicting the total load. With this view in mind, the writers carried out certain preliminary investigations in 1956. The results of these investigations are summarized in the following paragraphs.

While studying the sediment transport through pipes,(1) the writers found by dimensional analysis the following relationship to be applicable:

$$Re\sqrt{f} = \phi\left(\frac{D}{d}, C_t\right) \qquad (2)$$

in which D is the diameter of the pipe

d is the diameter of sediment particles

$C_t$ is the concentration of total sediment load expressed in per cent by weight

f is the Darcy-Weisbach resistance coefficient and

Re is the Reynolds number $= \frac{VD}{\nu}$

For smooth pipes (as compared to standard corrugated, or helically corrugated pipes), for a given value of $\frac{D}{d}$, it was possible to obtain plots as shown in Fig. 1.

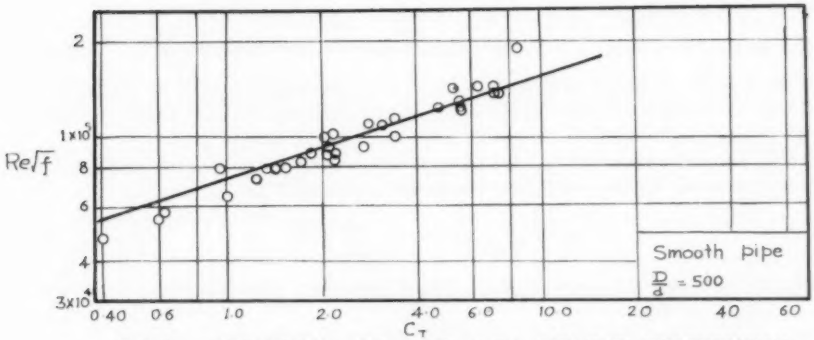


FIG. 1 VARIATION OF $Re\sqrt{f}$ WITH SEDIMENT CONCENTRATION.

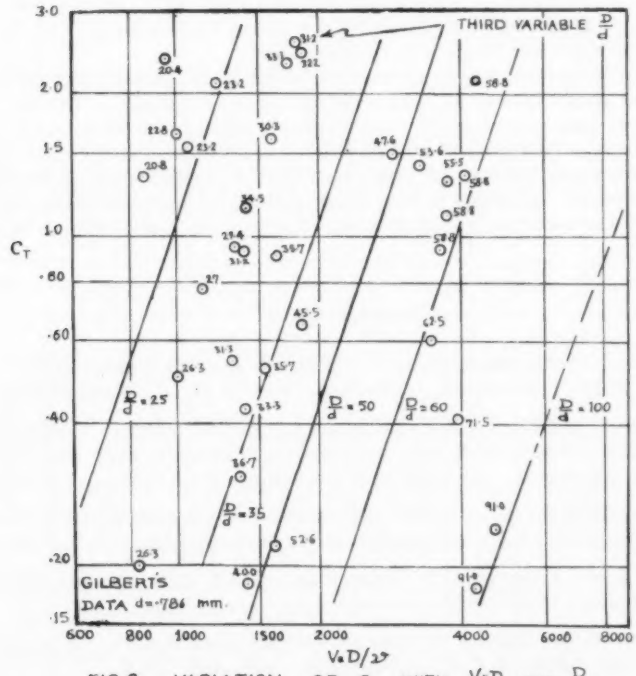


FIG. 2 VARIATION OF $C_T$ WITH $\frac{V_* D}{\nu}$ AND $\frac{D}{d}$

Although open-channel flow differs from pipe flow because of the existence of a free surface, it is reasonable to assume that a similar relationship should exist for the transport of sediment in alluvial channels. Therefore, $\frac{V_* D}{\nu}$ (which is proportional to $Re\sqrt{f}$) was plotted against $C_t$. A typical variation of $\frac{V_* D}{\nu}$ with $C_t$ and $\frac{D}{d}$ is shown in Fig. 2 using Gilbert's data.

For each set of data, a definite relationship existed between $\frac{V_* D}{\nu}$, $\frac{D}{d}$ and $C_t$. Plots were made for flume data from various sources such as Kalinske and Hsia,(3) Brooks,(5) Barton and Lin,(6) and Gilbert.(4) The range of size of bed material included in the study was from 0.011 mm to 1.71 mm.

Using standard techniques, it was possible to express the total sediment transport rate $C_t$ by the following empirical relationship:

$$\left( \frac{V_* D}{\nu} \cdot \frac{1}{C_t^{1/3}} \right) = \left( \frac{D}{d} \cdot \frac{1}{\psi} \right)^{3/2} \qquad (3)$$

in which $\psi$ is a function only of size of bed material. This functional relationship is shown in Fig. 3.

Fig. 4 shows Eq. (3) plotted for the various data already mentioned. (Laursen's data for 0.04 mm and 0.10 mm are also included.) There is an average scatter of 40 to 50 per cent. Possible causes for this scatter are that, in the development of Eq. (3) neither the influence of flow regime (such as dune bed or plane bed) nor the influence of the Froude number on the total sediment transport are taken into consideration.

The investigations under progress at Colorado State University by the writers have shown that k, $K_s$, and z depend on the condition of the bed and, therefore, the rate of suspended load transport should depend on the flow regime. Similarly, Tsubaki and others(7) have shown that under conditions of equal tractive force the contact load is smaller if ripples exist on the bed than if the bed is plane. Therefore, flow regime at least should be taken into consideration in the development of formulae for transport of sediment in alluvial channels.

## BIBLIOGRAPHY


1. Garde, R. J. Sediment Transport Through Pipes. Colorado A & M College, Fort Collins, Colo. Oct. 1956. Report No. CER No. 56RJG 19.
2. Garde, R. J. Effect of Alluvial Channel Characteristics on Total Sediment Load. 1956. Unpublished Report of Special Studies in Irrig. Eng. under Dr. M. L. Albertson. Colorado A & M College, Fort Collins, Colorado.
3. Kalinske and Hsia. Study of Transportation of Fine Sediments by Flowing Water. University of Iowa. Studies in Engineering, Bulletin No. 29, 1945.
4. Johnson, J. W. Laboratory Investigations of Bed Load Transportation and Bed Roughness. USDA. Soil Conservation Service, 1943.
5. Brooks, N. H. Mechanics of Streams with Movable Beds of Fine Sand. Proceedings, ASCE, Vol. 81, Separate No. 668, Apr. 1955.
6. Barton and Lin. A Study of the Sediment Transport in Alluvial Channels. Colorado A & M College, Fort Collins, Colorado. March 1955. Report No. 55 JRB 2.

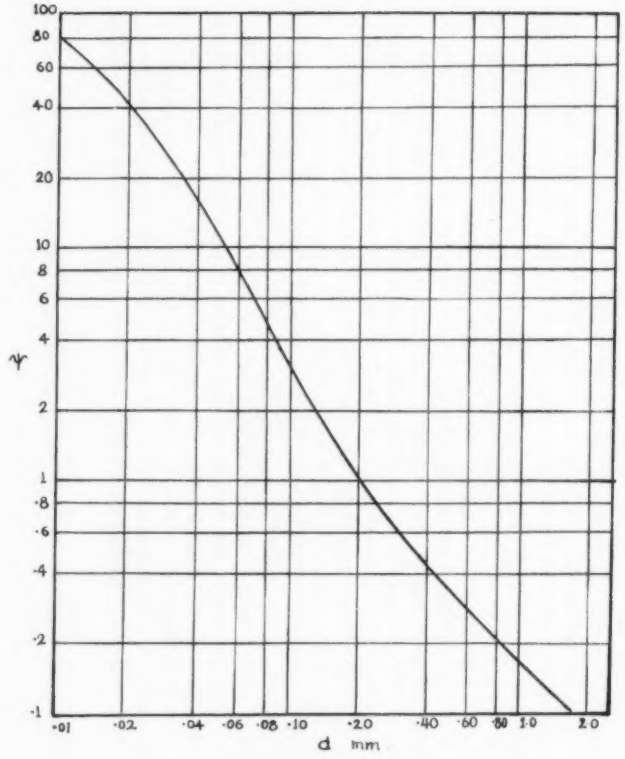


FIG.3 VARIATION OF $\Psi$ WITH d.

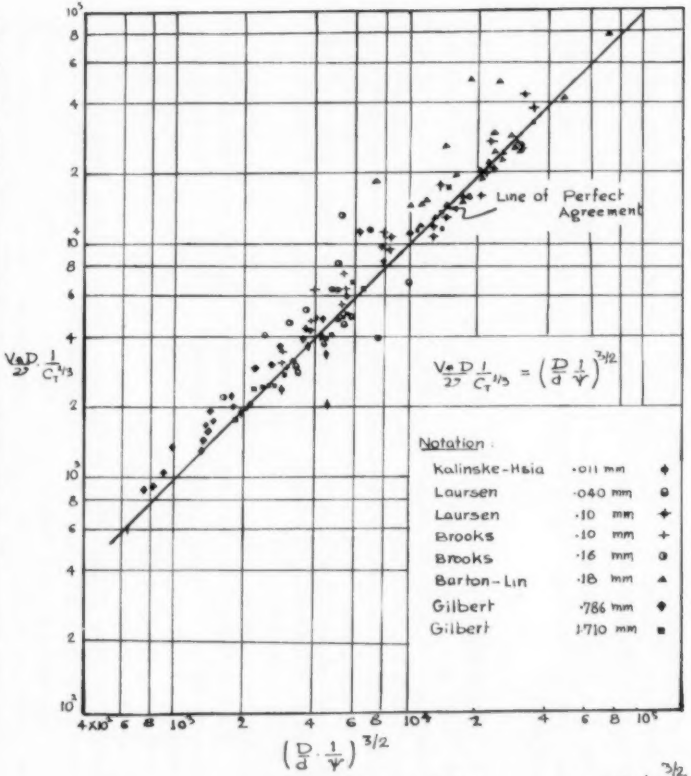


FIG. 4 VARIATION OF $\left(\frac{V_s D}{\nu} \frac{1}{C_T^{1/3}}\right)$ WITH $\left(\frac{D}{d} \frac{1}{\Psi}\right)^{3/2}$.

7. Tsubaki, Kawasumi, and Yasutomi; On the Influence of Sand Ripples Upon the Sediment Transport in Open Channels. Reports of Research Institute for Applied Mechanics, Kyushu University, Japan, Vol. II, No. 8, 1953.

8. Colby and Hembree. Computations of Sediment Discharge, Niabrara River near Cody, Nebraska. Geological Survey Water Supply Paper No. 1357, 1955.

D. C. BONDURANT,[1] A. M. ASCE.—There are several formulae available for the computation of sediment transport. Unfortunately, data available for the development of these formulae have seldom extended to the range of large streams, and it has been found that their use in respect to such streams requires a liberal application of experienced judgment. The writer's primary objective in reviewing this presentation was, thus, to determine its values and limitations in respect to streams such as the Missouri River. It is concluded that the form of the author's equation can be very useful but that some revision of the curve of $\Gamma(\sqrt{\tau_o/\rho}/\omega)$ is indicated.

Data for the purpose of the review were available from measurements made in the Missouri River in connection with the sediment investigations of the Missouri River Division, Corps of Engineers. Of the more than 400 sets of measurements of vertical distribution of velocity and suspended sediment, 76 were selected to provide the maximum range of data. Within these data, stream depths ranged from 7 feet to 22 feet, velocities from 3 fps to 9 fps, and discharges from 25,000 cfs to 90,000 cfs. Stream widths approximated 1,000 feet and slopes were from 0.8 to 0.9 foot per mile. From 6 to 8 verticals were occupied at each range, and the ranges occupied were in 4 separate reaches located at (1) River Mile 640, above Omaha, Nebraska, (2) Mile 614.1, 2-1/2 miles above the mouth of the Platte River, (3) Mile 608.2, 3-1/2 miles below the mouth of the Platte River and (4) Mile 365.6, below Kansas City, Mo. and 14 miles below the mouth of the Kansas River. Reaches were as nearly straight as could be found, and were unobstructed. Measurements were made from a boat held in place on a tag-line.

Figs. 15, 16, and 17, respectively show typical plots of velocity, suspended-sediment, and bed-material. Velocities were measured with a Price-type current meter; suspended sediment samples were obtained with a U. S. P-46 (point-integrating) sampler; and bed-materials samples were obtained with either a B.M.-48 or B.M-54 sampler or both. The B.M. instruments sample only the top one-inch (approximately) of the bed, and are so constructed that the sample is effectively protected against washing or contamination.

Fig. 18 shows a comparative plot of the average suspended sediment concentrations at the three upstream reaches as determined from the samples and as computed by the author's method. The measured concentrations are four times as large as the computed; however, the relationship is reasonably consistent. Furthermore, the measured and computed size distributions were in excellent agreement. Additionally, four points provided by Mr. J. C. Pyle of the U. S. Army Engineer District, Little Rock, Arkansas, showed almost exactly this same relationship of four. These latter points represented discharges of 25,000 cfs, 73,000 cfs, 135,000 cfs, and 190,000 cfs in the Arkansas

1. Head, Sediment Section, U. S. Army Engr. Div., Missouri River.

| POSITION NO. 4 | POSITION NO. 5 | POSITION NO. 6 |
|---|---|---|
| D = 10.4' | D = 10.7' | D = 9.2' |
| $\bar{U}$ = 3.48 | $\bar{U}$ = 3.77 | $\bar{U}$ = 4.10 |
| N = 1.25 | N = 0.54 | N = 0.52 |

NOTE: CONNECTED POINTS REPRESENT SIMULTANEOUS READINGS OF TWO METERS, ONE SUSPENDED 1.75 FEET ABOVE THE OTHER.

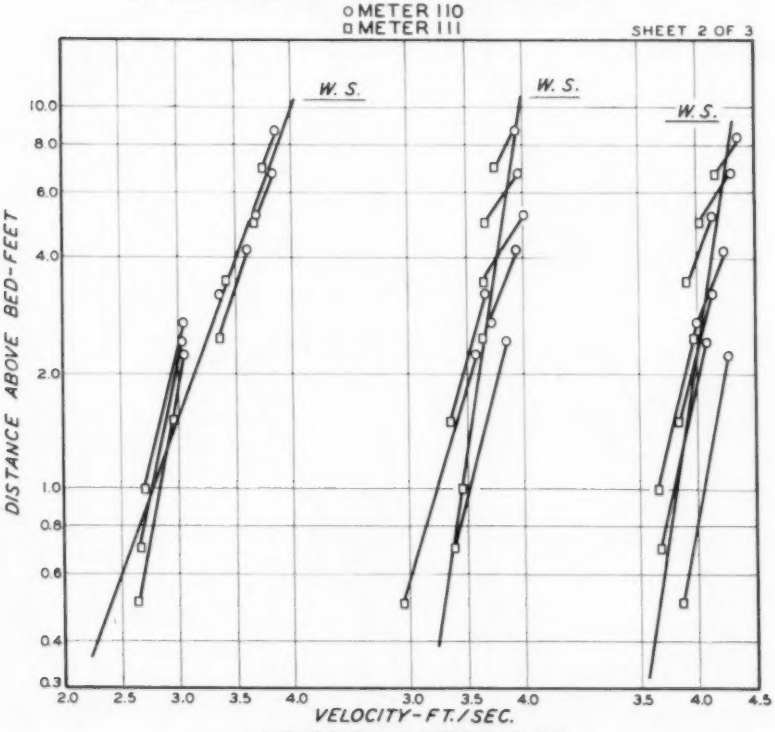


VELOCITY DISTRIBUTION
MISSOURI RIVER KANSAS CITY
18 OCTOBER 1954

FIG. 15

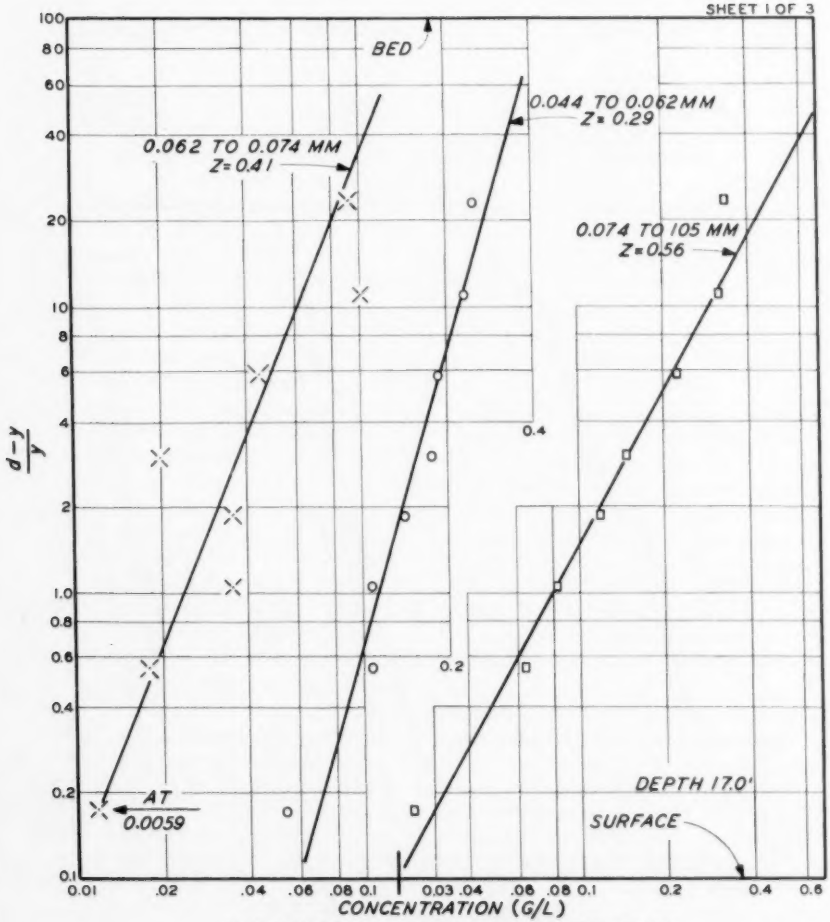


SUSPENDED SEDIMENT DISTRIBUTION
MISSOURI RIVER MILE 614.1
25 MAY 1954
STATION 35 + 20

FIG. 16

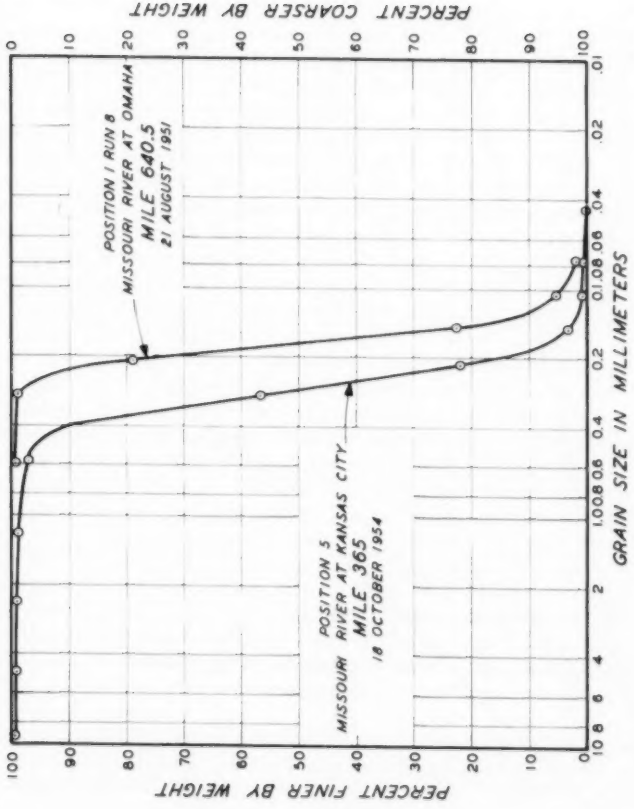


FIG. 17

MECHANICAL ANALYSIS BED SURFACE MATERIALS

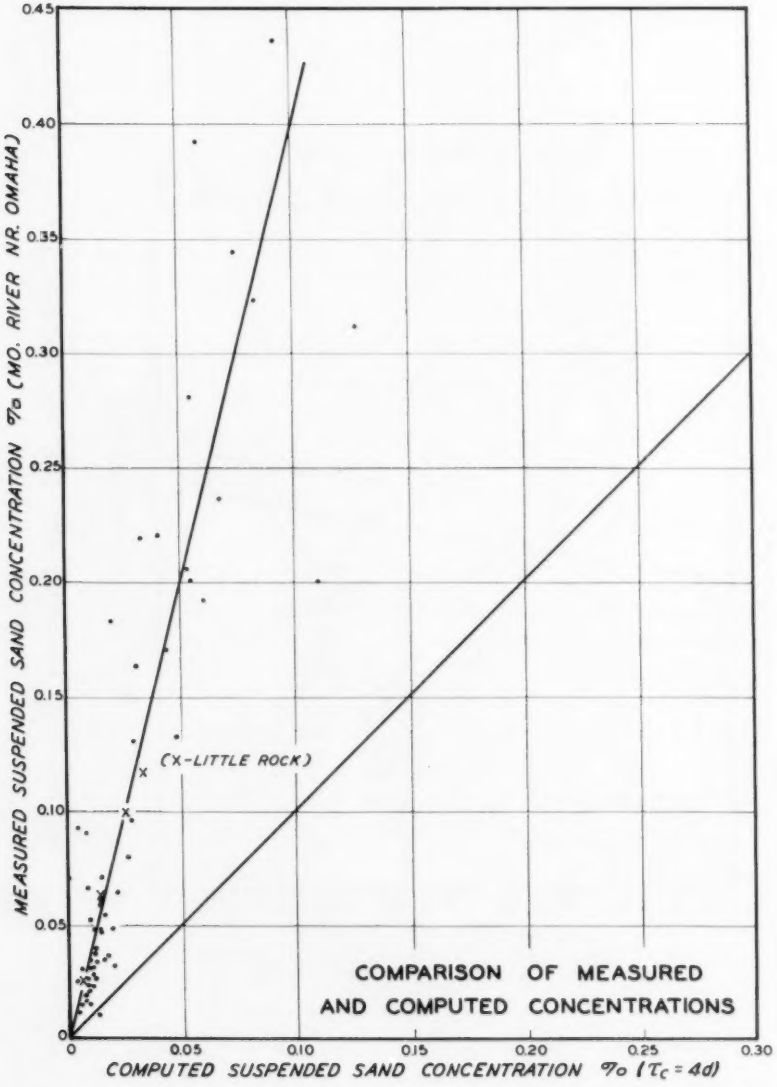
MEASURED SUSPENDED SAND CONCENTRATION % (MO. RIVER NR. OMAHA)
COMPUTED SUSPENDED SAND CONCENTRATION % ($T_c$ = 4d)
(X-LITTLE ROCK)
COMPARISON OF MEASURED
AND COMPUTED CONCENTRATIONS
0
0.05
0.10
0.15
0.20
0.25
0.30
0.35
0.40
0.45

FIG. 18

River. The writer has no information as to the magnitude of other factors involved.

On the basis of the consistency indicated in Fig. 18, it appeared that further computations might be unnecessary. However, the bed-materials in the Kansas City reach, as may be noted in Fig. 17, are substantially larger than those of the upstream reaches, thus they provided an opportunity to extend the range of the data used. With these data the consistency of the relationship deteriorated rapidly, the ratio varying from 10 to 100 and indicating the need for a more basic review.

Inspection of the computations revealed that the values of $(\sqrt{\tau_o/\rho}/\omega)$ associated with the larger bed-materials of the Kansas City reach caused the corresponding function values for the major size fractions to be much smaller than appeared reasonable. Accordingly, re-computations were made to derive values of the function corresponding to the measured data.

Figs. 19 and 20 show plots of $f(U_*/w)$ computed for the upstream reaches and Kansas City reach respectively. Since all the writer's plotted data use the symbol "$U_*$" for the more formal $\sqrt{\tau_o/\rho}$, that symbol will be used for this discussion. It may be seen that the points plot with a reasonably limited scatter except for those points representing the two smaller size fractions and a few points representing the largest sizes in the respective samples. These deviations point to a systematic error in the data in respect to these fractions, and investigations made subsequent to the analyses of the samples indicated that such error did exist.

The samples were analyzed by sieves, for reasons outside the scope of the present discussion. Fall velocities at various temperatures were later determined by an extensive investigation involving both individual grain drops and analyses of individual sieve fractions by the visual accumulation tube method. It was noted that the smaller size fractions periodically contained quantities of heavy magnetic minerals and, if the fraction represented only a small percentage of the total sample, the average specific gravity of the fraction might be as much as 2.85 and in a few cases greater than 3. Had these points been corrected for the higher fall velocity which would have resulted from the presence of these minerals, they would have been moved to the left and would have been essentially in line with the other points.

The less consistent variations for fractions of the larger sizes were found to be due to low density agglomerated particles. They were present only in sufficient quantity to affect a fraction which was less than about one per cent of the total sample.

It might be well to note here also that the percentages pertaining to the size fractions of the bed-material samples were read from the plotted curves rather than from the original laboratory records. Inspection of the computations showed that the possible error thus introduced was negligible insofar as the concentration computations based on Missouri River data were concerned; i.e., those fractions for which the error of reading might be appreciable were of themselves such a small portion of the whole that a reading error of even several hundred per cent would make little difference in the over-all result. Time did not permit a return to the original analyses for the function computations.

Fig. 21 shows individually the lines drawn as the approximate average of the plotted points for the upstream reaches and the Kansas City reach. The spread between these lines is not excessive, however, they are roughly parallel, indicating a systematic difference. A third line on this figure indicates an

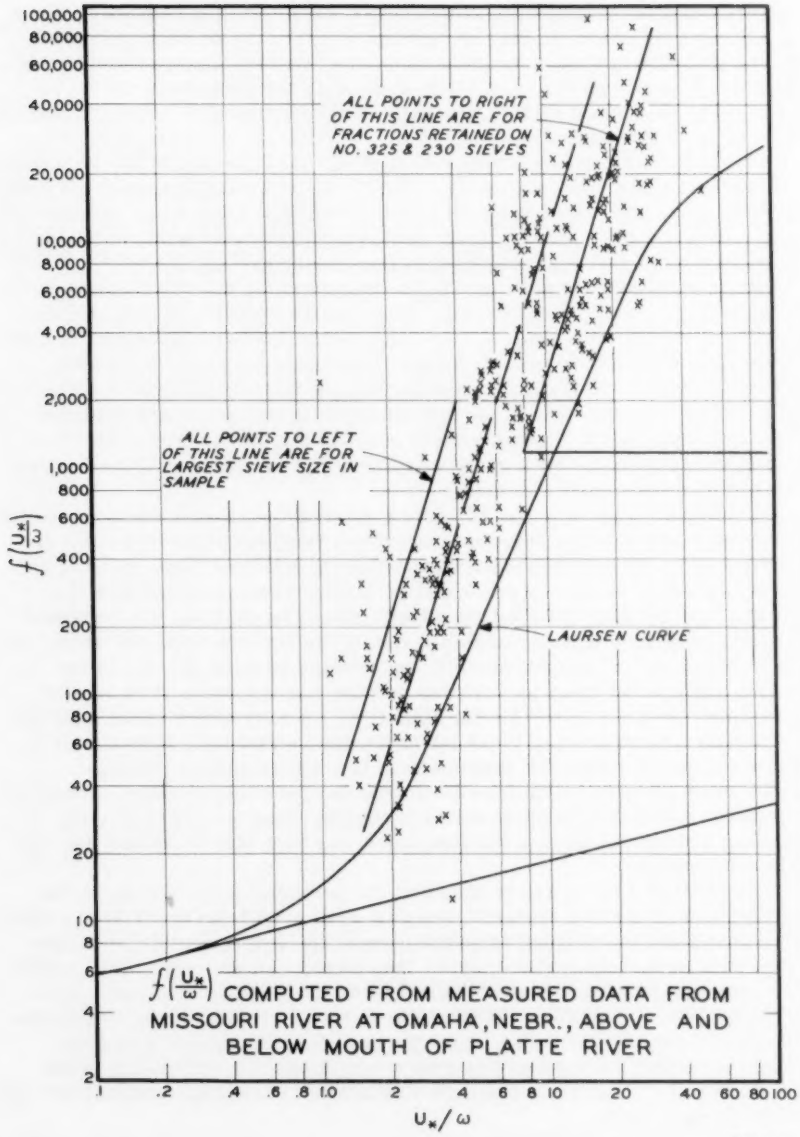
ALL POINTS TO RIGHT OF THIS LINE ARE FOR FRACTIONS RETAINED ON NO. 325 & 230 SIEVES
ALL POINTS TO LEFT OF THIS LINE ARE FOR LARGEST SIEVE SIZE IN SAMPLE
LAURSEN CURVE
$f\left(\frac{U_*}{\omega}\right)$ COMPUTED FROM MEASURED DATA FROM MISSOURI RIVER AT OMAHA, NEBR., ABOVE AND BELOW MOUTH OF PLATTE RIVER
$f\left(\frac{U_*}{\omega}\right)$
$U_*/\omega$
100,000
80,000
60,000
40,000
20,000
10,000
8,000
6,000
4,000
2,000
1,000
800
600
400
200
100
80
60
40
20
10
8
6
4
2
.1
.2
.4
.6
.8
1.0
2
4
6
8
10
20
40
60
80
100

FIG. 19

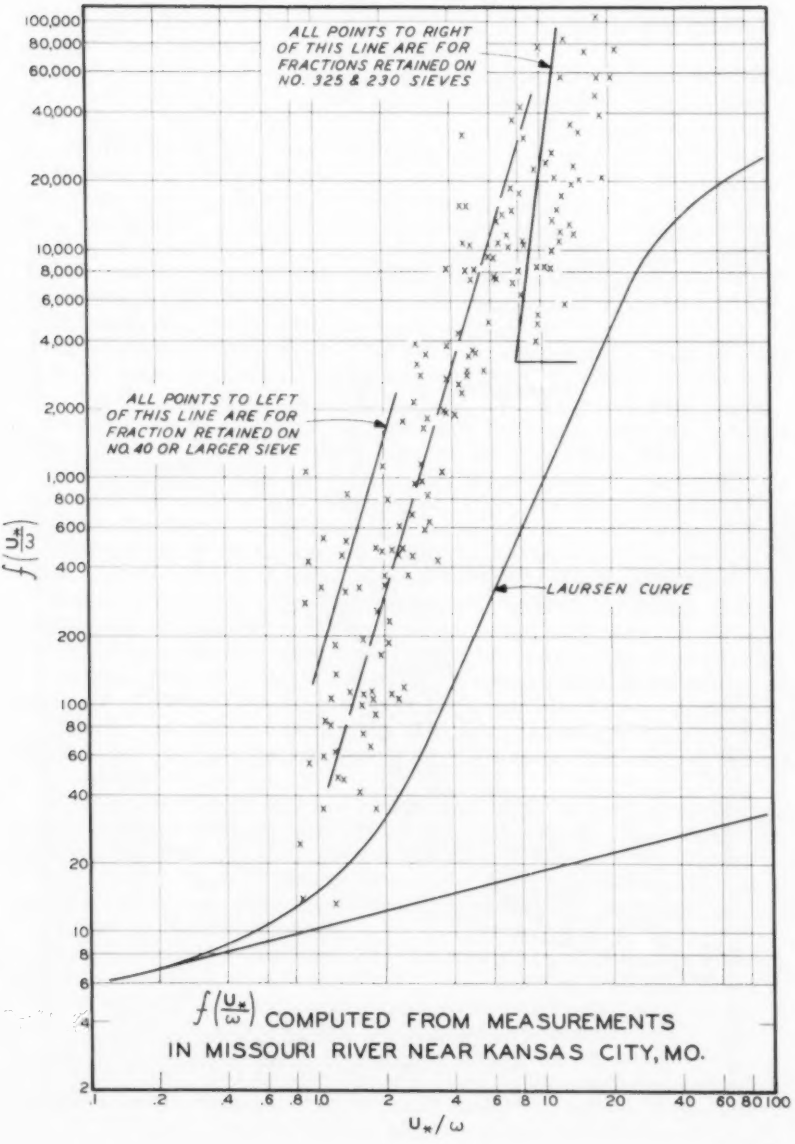
ALL POINTS TO RIGHT OF THIS LINE ARE FOR FRACTIONS RETAINED ON NO. 325 & 230 SIEVES
ALL POINTS TO LEFT OF THIS LINE ARE FOR FRACTION RETAINED ON NO. 40 OR LARGER SIEVE
LAURSEN CURVE
$f\left(\frac{U_*}{\omega}\right)$ COMPUTED FROM MEASUREMENTS IN MISSOURI RIVER NEAR KANSAS CITY, MO.
$f\left(\frac{U_*}{\omega}\right)$
$U_*/\omega$
100,000
80,000
60,000
40,000
20,000
10,000
8,000
6,000
4,000
2,000
1,000
800
600
400
200
100
80
60
40
20
10
8
6
4
2
.1
.2
.4
.6
.8
1.0
2
4
6
8
10
20
40
60
80
100

FIG. 20

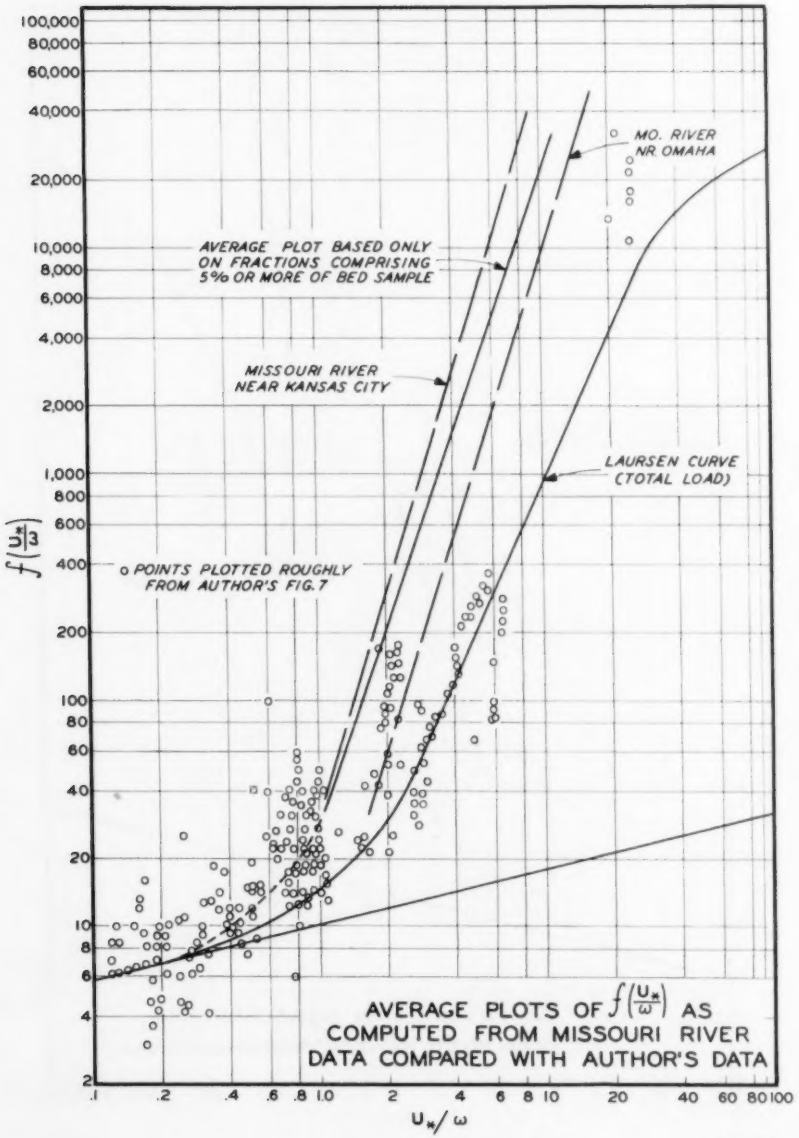


AVERAGE PLOTS OF $f\left(\frac{U_*}{\omega}\right)$ AS COMPUTED FROM MISSOURI RIVER DATA COMPARED WITH AUTHOR'S DATA

FIG. 21

average for all points representing fractions which were more than 5 per cent of the total respective samples, but this line is not presented as a recommended mean. The difference between the lines for the upper and lower reaches is believed to result primarily from the limits used to determine the average concentrations from the measured data.

If one assumes that the logarithmic distribution of concentrations extends to y = 0, the concentration at that point becomes infinite; thus, one must assume a limit at which y equals some real value. For purposes of prior computations, this limit had been adopted as y = 2d with an arbitrary maximum of 480 g/1 which was not to be exceeded at that level. The average concentrations thus determined were used for the present computations. Insofar as the three upper reaches were concerned, these averages were reasonably consistent with averages shown by depth-integrated samples (which could not extend closer than 0.5 foot to the bed). In the Kansas City reach, where the material was larger and thus necessarily concentrated more heavily near the bed, the difference was substantial.

Experiments of Einstein and Chien[26] indicate that the logarithmic distribution of suspended sediment begins to break at the level where the total concentration approximates 100 g/1. Inspection of the computations for average concentrations at Kansas City indicates that assumption of any limiting value below 480 g/1 would reduce most of the computed average concentrations, and assumption of a value below 350 g/1 would reduce all of them. This would move the computed values of $f(U_*/w)$ for the Kansas City data to the right, more nearly approximating the position for the upstream data.

Time has not permitted recomputation of the data to verify, quantitatively, the variations above discussed. Even with these variations, however, the Missouri River data provide a consistent plot within their range, without excessive scatter, and verify the form of the author's equation. A plot of the author's data (roughly scaled from Fig. 7), included in Fig. 21, indicates that the average lines from the Missouri River computations fit the author's data for lower values of $U_*/w$ as well as or better than the curve necessarily constructed by the author to fit his data for the higher values of $U_*/w$. For the higher values of $U_*/w$ the Missouri River results deviate sharply from those of the author.

The Missouri River data are sharply restricted in their range in respect to both sediment size and slope of the energy gradient. The writer does not, thus, suggest that a function derived from these data be given arbitrary precedence over a function derived from other data. It is to be hoped that other readers will further augment the available information to permit the author to provide an integrated result.

In considering the fit of the Missouri River data, it is well to remember that all pertinent factors in these data represent measured values in which the correct values of other functions, such as roughness or turbulence, are implicit. It has been found that equally valid computations can be made with the theoretical type of equations (for example) if the measured values of k (or $\beta$k) are utilized. The author's function has the advantage that velocities can be more simply measured than k values; thus, in cases where the velocity can be adequately established, this function should be the more valuable. In

26. H. A. Einstein and Ning Chien, Effects of Heavy Sediment Concentration Near the Bed on the Velocity and Sediment Distribution. University of California Inst. of Engr. Research Series No. 33, Aug. 1955.

cases where velocity must be computed from assumed roughness factors, the necessary dependence upon judgment and the possible variations in results would be about the same as for other available formulae.

JOHN L. BOGARDI.[1]—All credit is due the author for his successful investigations into the subject of sediment transportation. In keeping with the latest concepts, bed-load and suspended load are not separated in the treatment, and the possibility for relationships of a more general nature is opened thereby. Numerous aspects of this complex problem are elucidated by clear and logical reasoning. The writer fully agrees with every statement made by the author and only wishes to contribute a few additional remarks.

In the writer's view, the relationship shown in Fig. 7 applies to the sediment-transporting capacity of the stream rather than to the actual rate of sediment transport. Quite obviously, the actual rate of transport will depend on a number of factors besides the transporting capacity, e.g. also on the availability of sediment in the stream. It follows that the actual rate of transport in natural streams is governed also by the hydrological conditions of both the watercourse and the catchment area drained thereby. The writer interprets the excellent agreement between predicted and actually observed rates of transport on the Niobrara River as an indication of the fact that hydrological conditions of the watercourse, as well as sediment supply, are such as to enable the stream to carry sediment in an amount equal to its transporting capacity. A rate of transport in excess of the transporting capacity and observed on Mountain Creek is, as mentioned also by the author, due probably to artificial flash floods. Consequently, the author is fully justified in arriving at the conclusion that the prediction of the so-called wash load is not feasible.

Relationships (8) and (9) published by the author gave the writer the opportunity to extend his investigations, conducted on the basis of results published by Liu(1) and by Albertson, Simons, and Richardson,(2) to total sediment transport. In his paper Liu established a definite relationship between $U_*/w$ and $U_*d/\nu$ for the state of incipient ripple formation. Albertson and his collaborators have further shown the existence of a similar relationship between the two above dimensionless invariants also for the beginning of movement, the development of dunes, transition, and antidunes, respectively. The writer investigated the significance of the channel stability factor

$$b = \frac{d}{hS} = \frac{gd}{U_*^2}$$

used in Hungary since 1942. This factor, being formally a Froude number, was named, following the example set by Albertson and in analogy to the shear-velocity Reynolds number, the shear-velocity Froude number. Using the channel stability factor $b = 1/Fr_*$ the writer succeeded in defining numerically various regimes of movement by a single parameter $\beta$. Investigations of the writer, conducted using data and results published by Albertson and his collaborators, showed a relationship between the parameter $\beta$ and the shear-velocity Froude number that can be expressed as

$$\beta d^N = b = \frac{d}{hS} = \frac{gd}{U_*^2} = \frac{1}{Fr_*}$$

1. Asst. Prof., Technical University, Budapest. Head, Experimental Section of the Scientific Research Inst. of Hydroeconomy.

Since for all regimes N was 0.882 = constant, the parameter

$$\beta = \frac{gd}{U_*^2 d^{0.882}} = \frac{g d^{0.118}}{U_*^2}$$

defines uniquely the bed formation. The relationship between the particle size d and $1/Fr_*$ is shown in Fig. 15. It is to be seen from the figure that the parameter $\beta$ (of the dimension $cm^{-0.882}$) in effect defines uniquely the bed formation.

A number of important conclusions can be arrived at from Fig. 15. Ripples, for instance, cannot develop unless the particle size is smaller than approximately 2 mm, and even for these particle sizes only if $66 < \beta < 322$.

Fig. 15 relates to a water temperature of 20° Centigrade and to a sediment having a specific gravity $\nu_1 = 2.65$ gr/cc. For other temperatures, e.g. for a temperature of t° Centigrade,

$$\beta_t = \beta_{20} \frac{\nu_{20}^2}{\nu_t^2} = \frac{1}{Fr_* d^{0.882}} \frac{\nu_{20}^2}{\nu_t^2}$$

wherein $\nu_{20}$ and $\nu_t$ denote the kinematic viscosity of water at 20° and t° Centigrade, respectively.

For sediments having any arbitrary specific gravity $\nu_1$

$$\beta_{\gamma_1} = \beta_{2.65} \frac{(\gamma_1 - \gamma)}{1.65\gamma} = \frac{1}{Fr_* d^{0.882}} \frac{(\gamma_1 - \gamma)}{1.65\gamma}$$

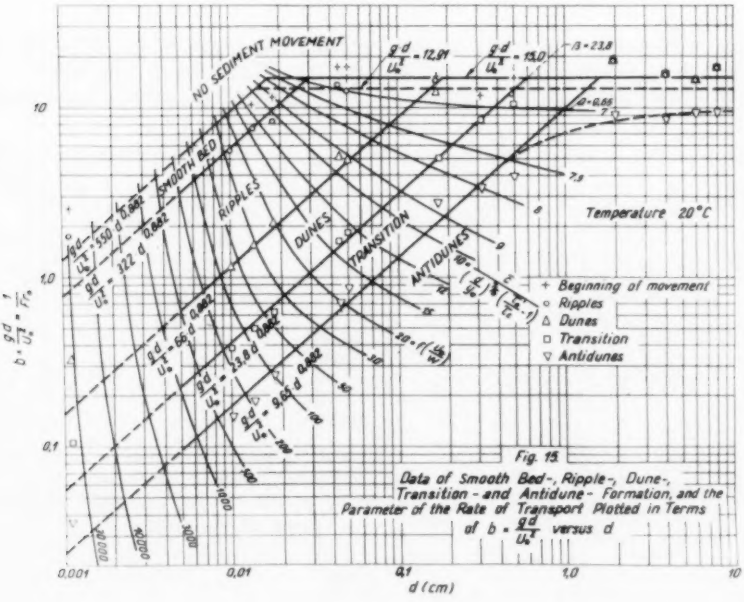


Fig. 15. Data of Smooth Bed-, Ripple-, Dune-, Transition- and Antidune- Formation, and the Parameter of the Rate of Transport Plotted in Terms of $b = \frac{qd}{U_*^2}$ versus d

The interrelation between $U_*$ and d can also be determined from that established for $\beta$ and $Fr_*$. Thus

$$U_* = \left(\frac{\mu}{\beta}\right)^{1/2} d^{\frac{1-N}{2}}$$

Since, however, $\frac{1-N}{2} \approx 0.0582$ = constant for every bed configuration, introducing the parameter

$$\varepsilon = \left(\frac{\mu}{\beta}\right)^{1/2}$$

of the dimension $cm^{0.9418}\ sec^{-1}$, results in the relationship

$$U_* = \varepsilon d^{0.0582}$$

This relationship, derived also on the basis of data published by Albertson, is shown in Fig. 16. As can be seen from the figure, the configuration of the bed is uniquely defined for any arbitrary particle size by the parameter

$$\varepsilon = \frac{U_*}{d^{\frac{1-N}{2}}} = \frac{U_*}{d^{0.0582}}$$

It should be noted that all sorts of bed configurations are uniquely defined similarly to parameters $\beta$ and $\epsilon$ by the parameter

$$\alpha = \frac{d}{Re_*^{\,n}} = \frac{d}{\left(\frac{U_* d}{\nu}\right)^{0.945}}$$

The parameter $\epsilon$ is also related to a water temperature of 20° Centigrade and to a sediment having a specific gravity $\gamma_1 = 2.65$ gr/cc. For water temperatures and sediments having a specific gravity other than mentioned

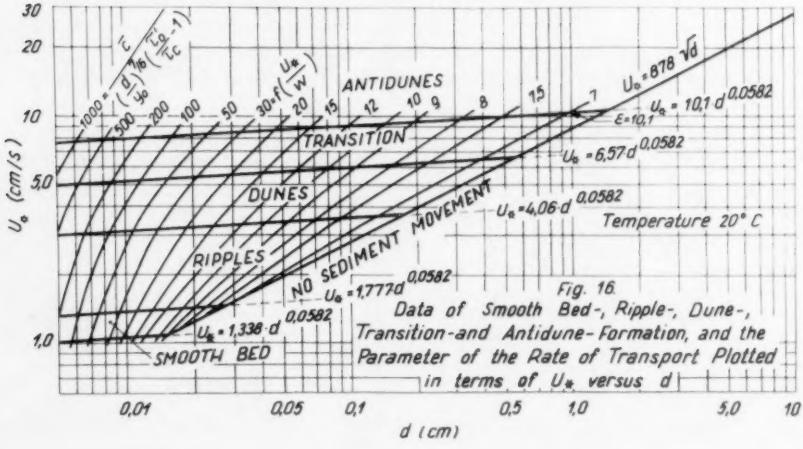


Fig. 16. Data of Smooth Bed-, Ripple-, Dune-, Transition-and Antidune-Formation, and the Parameter of the Rate of Transport Plotted in terms of $U_*$ versus d

above, the parameter can be determined from the following two equations:

$$\varepsilon_t = \varepsilon_{20} \frac{\nu_t}{\nu_{20}}$$

$$\varepsilon_{\gamma_1} = \varepsilon_{2.65}\left(\frac{\gamma_1 - \gamma}{1.65\gamma}\right)^{-1/2}$$

Details pertinent to the above investigation are to be found in the writer's discussion of Liu's paper.

In the writer's opinion, if Fig. 7 presented by the author actually expresses the relationship between the sediment-load parameter corresponding to the transporting capacity of the stream and $U_*/w$, the variation in the sediment-load parameter

$$\frac{\bar{c}}{\left(\frac{d}{y_0}\right)^{7/6}\left(\frac{\tau_0'}{\tau_c} - 1\right)}$$

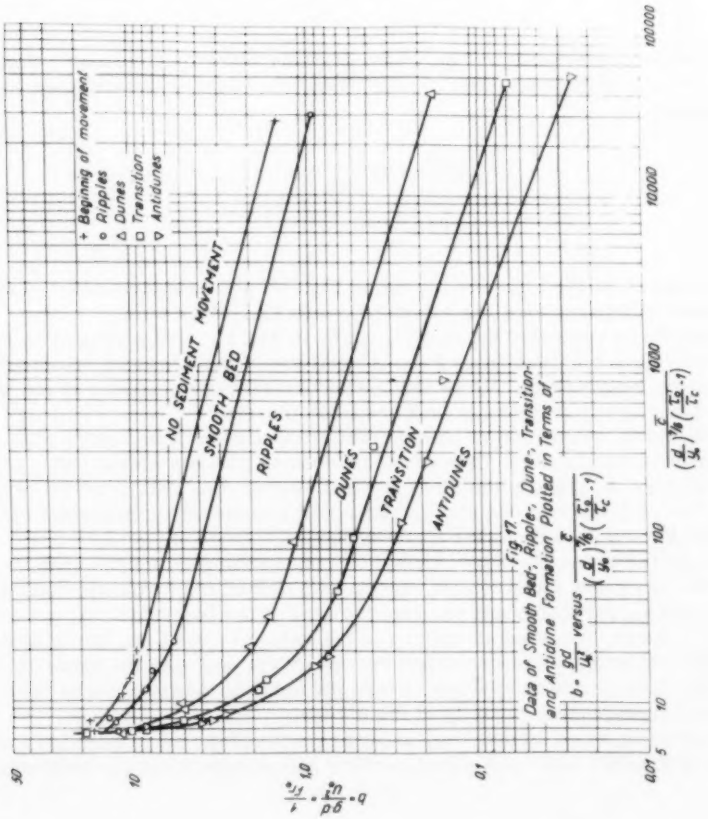


Fig. 17. Data of Smooth Bed, Ripple-, Dune-, Transition- and Antidune Formation Plotted in Terms of $\frac{\bar{c}}{\left(\frac{d}{y_0}\right)^{7/6}\left(\frac{\tau_0'}{\tau_c} - 1\right)}$ versus $\frac{gd}{U_*^2}$

can also be entered into Figs. 15 and 16.

Values of $U_*/w$ can be established for all five bed configurations in the case of several particle sizes from Fig. "A" published by Albertson and his collaborators;[2] moreover, values of $U_*d/\nu$ can also be determined. The latter lends itself readily to the computation of values of $U_*$ and subsequently of those of the parameter $gd/U_*^2$. For each value thus determined, those of

$$\frac{\bar{c}}{\left(\frac{d}{y_0}\right)^{7/6}\left(\frac{\tau_0'}{\tau_c}-1\right)}$$

pertaining to various $U_*/w$ values can be correlated using Fig. 7 published by the author.

The relationship between

$$b = \frac{gd}{U_*^2}$$

and

$$\frac{\bar{c}}{\left(\frac{d}{y_0}\right)^{7/6}\left(\frac{\tau_0'}{\tau_c}-1\right)}$$

can thus be represented in Fig. 17 for particle sizes in Albertson's Fig. "A". Thereafter, relying upon Fig. 17, the isometric chart of the sediment load parameter

$$\frac{\bar{c}}{\left(\frac{d}{y_0}\right)^{7/6}\left(\frac{\tau_0'}{\tau_c}-1\right)}$$

can be traced in Fig. 15. Finally using Fig. 15, the isometric chart of the sediment load parameter can be entered into Fig. 16 as well.

It should be remembered that Figs. 15, 16 and 17 were prepared on the basis of values obtained from Fig. "A" and Fig. 7 published by Albertson and the author, respectively, as no numerical values were available to the writer. Some discrepancy may easily be introduced thereby.

It should be noted further that the writer completed Albertson's Fig. "A" by extrapolating Shield's curve towards smaller particle sizes, and, on the basis of Fig. 15, slightly modified at the diameter d = 0.0011 cm the curve characterizing the five bed configurations by transferring observation points of Kalinske and Hsia to higher $U_*/w$ values.

The writer considers Figs. 15 and 16 very useful for design purposes, since for any given watercourse, having established the hydraulic radius (water depth), the slope, and the particle size of the bed-material, parameters $\beta$ and $\epsilon$ may be computed directly, and the value of one of the two is alone sufficient to define uniquely the bed configuration, and also the value of the sediment-load parameter, which in turn permits the computation of the total sediment-transporting capacity of the stream.

It should be noted further that no accurate limiting values have been determined towards large and small particle sizes in deriving the relationships

and in constructing the figures. These are felt to require further study and experiments. For example, the line representing the formation of antidunes in Fig. 15 is likely to join that representing the limiting condition of a smooth bed through a curved transition instead of a definite point of intersection. Similarly, the determination of relationships for values smaller than 7 and higher than about 1000 to 3000 of the sediment-transport parameter is likely to require further investigation.

The number of particular and general conclusions that can be arrived at by means of the relationships described above and by Figs. 15, 16, and 17 constructed therefrom is great. It is, however, the intention of the writer to devote a special paper to these problems.

## REFERENCES

1. Liu, H. K., "Mechanics of Sediment Ripple Formation", Proceedings of ASCE, Hydraulics Division, Vol. 83, No. HY 2, April, 1957.
2. Albertson, M. L., Simons, D. B., Richardson, E. V., "Discussion of Sediment Ripple Formation" by H. K. Liu, Proceedings of ASCE, Hydraulics Division, Vol. 84, No. HY 1, February 1958, Part I.

# EISENHOWER AND GRASS RIVER LOCK MODELS[a]

Discussion by Marvin J. Webster

MARVIN J. WEBSTER,[1] M. ASCE.--The authors state that the degree of surging and consequently the magnitude of force imposed upon a craft in the lock chamber reaches a minimum value when the manifold system of ports or laterals occupies the approximate middle third of the lock chamber walls. Tests performed by the Bonneville Hydraulic Laboratory, Bonneville, Oregon, in a 1:25-scale model of The Dalles navigation lock, Columbia River, and in the prototype furnish additional data to substantiate this statement.

The Dalles lock has a culvert system in which seven lateral culverts from each wall culvert are located in the middle third of the lock chamber (see Fig. 9). Model and prototype tests showed very low hawser forces on a commercial tow of 2780 tons.(1)

The tests in the prototype were made in December 1957.[2] The tow consisted of two barges and a tug having a total displacement of 2780 tons. Instrumentation for the tests was developed and constructed at the Bonneville Hydraulic Laboratory. The bridles for holding the tow in position were constructed of 5/8-in. cable and connected to the floating mooring bits, as shown in Fig. 10. The tow was centered over the lateral culverts. The longitudinal forces were measured with two 20,000-lb-capacity dynamometers, one at each end of the tow. No attempt was made to measure transverse forces in the prototype because of the difficulty of constructing a suitable bridle to measure transverse forces and because previous tests in the model on larger size tows showed that transverse forces were less than the longitudinal forces. Tests were made in the 1:25-scale lock model prior to the prototype tests and, although the displacement was simulated, the shape of the model tow differed from that of the prototype.

Results of the tests during filling for a lift of 84.6 ft in the prototype and 86.0 ft simulated in the model are shown in Fig. 11. The maximum lift of The Dalles lock is 90.5 ft. The test results show low hawser forces during filling operations on the tow used in the tests and good correlation between the model and prototype for filling. An emptying test in the prototype with the same tow showed a maximum longitudinal force of 1.1 ton. An emptying test was not made in the model. Hawser forces also were measured on the same tow in the McNary navigation lock, which has a culvert system similar to The Salles, for a lift of 87.9 ft (maximum lift is 92.0 ft). The maximum

a. Proc. Paper 1582, April, 1958, by Martin E. Nelson and Harvey J. Johnson.

1. Chf., Hydr. Design and Lab. Section, U. S. Army Engr. District, Portland, Ore.

2. On a tow furnished through the courtesy of the Tidewater-Shaver Barge Lines, Portland, Oregon.

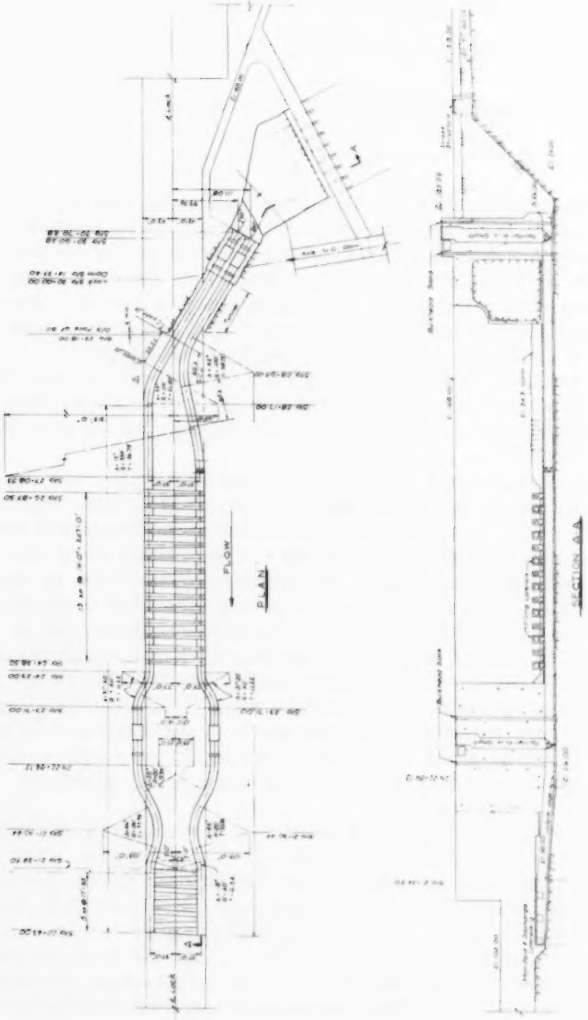


THE DALLES DAM
NAVIGATION LOCK
FILLING & EMPTYING SYSTEM

Fig. 9

Fig. 10

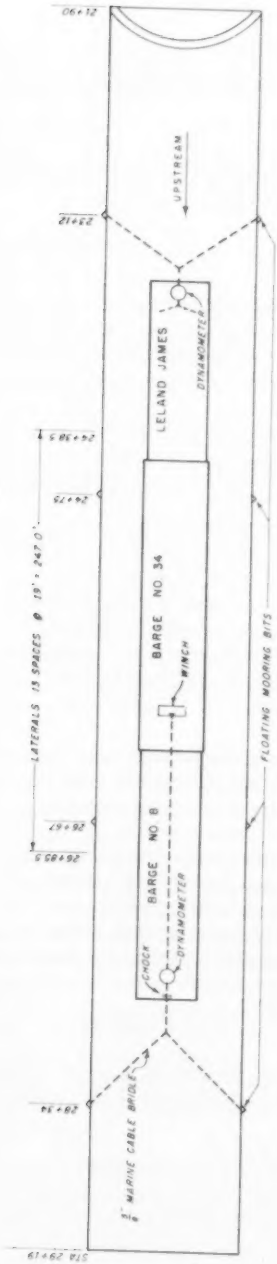


THE DALLES LOCK
BARGE MOORING POSITIONS

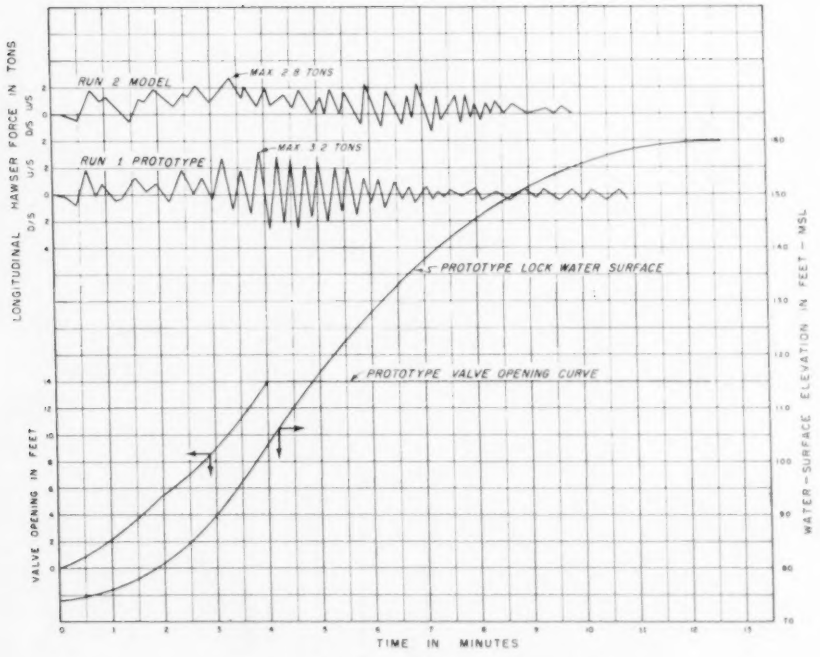


HAWSER FORCE MEASUREMENTS
THE DALLES LOCK
FILLING

longitudinal force measured during filling was 1.7 tons. The filling valves open in 7.6 min and the lock filling time is 15.0 min at McNary compared with 4 min and 12.5 min at The Dalles, which probably accounts for the lower hawser forces at McNary.

The writer wishes to acknowledge the use of material for this discussion from the U. S. Army Engineer District, Portland, Oregon. Instrumentation for the tests was developed and constructed under the supervision of C. Robert Grim, Head of the Electronics Unit under the general supervision of Harry P. Theus, Chief, Bonneville Hydraulic Laboratory and the writer.

## REFERENCE

1. Memorandum Report 1-1, Prototype Hawser Forces, The Dalles and McNary Locks, Bonneville Hydraulic Laboratory.

# WATER DISTRIBUTION DESIGN AND THE McILROY NETWORK ANALYZER[a]

---

Discussions by Quintin B. Graves and Don Branscome, E. Shaw Cole, Claud C. Lomax

---

QUINTIN B. GRAVES,[1] M. ASCE and DON BRANSCOME,[2] J. M. ASCE.— The authors have presented an interesting approach to the design of water distribution systems with particular emphasis on the advantages of the McIlroy Network Analyzer in providing a visualization of the hydraulics of a water distribution system.

This paper and a paper by the writers on "Digital Computers for Pipeline Network Analysis" were presented at the October, 1957 ASCE Convention, but before different divisions and were published simultaneously in the Proceedings.

It is obvious, as the authors point out, that by visual inspection of the system as set up on a McIlroy Analyzer design changes will be quickly indicated and may be easily adjusted at "Inflow rates well below the design rates". This is an advantage for the McIlroy Analyzer over the electronic digital computer primarily in those cases where changes in the distribution of inflows or outflows are indicated. In the case of the electronic digital computers, computations on the basis of the largest rates of demand usually will prove to be advantageous. This may not be required in the case of the McIlroy Analyzer.

No doubt, improvements in the techniques of utilizing the McIlroy Analyzer have been made since its first introduction, and more probably will be made with continued use. Also, improvements in programming for digital computer analysis of distribution systems will be made. It has been evident from "long hand" calculations with the Hardy Cross Method that convergence of the process does not always occur. Usually, by changes in the initial flow assumptions for the network it is possible to obtain rapid convergence. The writers are in agreement with the authors in regard to the use of "electric service power-system calculating boards with linear resistors".

One of the advantages of electronic digital computers over other types of analyzers is their wide distribution throughout the United States. One of the costs to occasional users of McIlroy Analyzers is that of travel and associated expense for those who do not have one available for use locally. For most users of digital computers, such costs will be substantially reduced due in part to the greater number of such computers available. As greater use is

---

a. Proc. Paper 1588, April, 1958, by M. B. McPherson and J. V. Radziul.

1. Prof. of Civ. Engr., Oklahoma State Univ., Stillwater, Okla.
2. Sales Engr., Aluminum Co. of America, Pittsburgh, Pa.

made of digital computers for water distribution analysis, many improvements in programming will be made thus enhancing their value.

The authors mention that 50 to 60 punched cards will be required for basic instructions, regardless of the size of the network being studied. It is possible to reduce the number of basic instructions required by using an interpretive programming system. For most networks only 30 to 40 punched cards will be required for the basic instructions.

The authors, in discussing Fig. 6, state "A revised storage rate requires a new storage curve". The writers are of the opinion that this would be more intelligible if the statement read, "A revised uniform pumping rate requires a new storage curve."

Values of the Hazen-Williams coefficient "C" are not accurately known for many small water distribution systems. In such cases the variation in voltages or currents, which has been mentioned to the writers by some users of the McIlroy Analyzer are of little or no concern. In those few cases where basis information is more accurate, a variation of 5 per cent or greater may be significant.

The authors' statement that "(However, a 2.00 power rather than 1.85 power is involved)" in reference to the electronic digital computer programs is no longer valid as programs are available utilizing the 1.85 power.

The authors hold that "an error in programming or data instructions is not evident until the run is made and the analysis is completely summated and checked, . . ." In general after a program is once checked out all errors should be eliminated and would not introduce errors when applied to other water distribution systems. Errors in data may occur for any given case, however automatic machine checking of data such as the summation of inflows and outflows at a junction may be included in a program prior to the analysis of the system.

The authors are to be highly commended for this fine contribution to the literature on water distribution system design.

E. SHAW COLE,[1] M. ASCE.—The authors have made an important contribution in water distribution design and have shown how complicated problems can be solved readily by use of the McIlroy Analyzer. The writer has been privileged to work with them on some of their problems and has used the analyzer on a number of design problems for other systems. He believes the authors have presented thoroughly the advantages of the analyzer, as well as the limitations in its use, but would like to mention several points that may not be apparent to the casual reader.

The importance of accurate field data is mentioned. This should be obvious and was recognized by Dr. McIlroy at the outset of his work in developing the analyzer. Unless the C-Value is reasonably accurate, the answers given by the analyzer may be seriously in error, but accurate field data implies more than determination of C-Values.

Frequently, water distribution systems do not function as intended, due to closed valves or obstructions that reduce carrying capacity far below the most conservative estimates. Some water works designers may not appreciate the difficulties of maintaining distribution systems at peak efficiency, but

1. Pres., The Pitometer Associates, New York, N. Y.

the discovery of major difficulties is becoming more frequent every year. The increasing complexity of our systems and the lack of responsibility, or complete records of the field operations, are major causes for this condition.

The problem of determining the quantity of equalizing storage necessary to permit uniform pumping is most interesting and illustrates the advantage of the analyzer. In many water works systems, uniform pumping is not practical and pump units are added or subtracted periodically as the load changes. The pump changes may only occur a few times during a twenty-four hour period but this can be sufficient to make effective use of the existing storage. For medium size systems, the cost of pumps is relatively much less than storage, particularly if elevated, and it would be interesting to have a study made of the economics of variable pumping under various conditions vs. uniform pumping.

CLAUD C. LOMAX,[1] A. M. ASCE.—This paper is a welcome addition to the literature on the analysis of fluid distribution networks. Use of the McIlroy analyzer to study the effect of demand ratio and pumping station outages, and to balance pumpage and storage demonstrates its versatility. As engineers become more familiar with the potential of this instrument, increased use for other than the routine head loss and flow rate determinations can be anticipated. The R. L. Albrook Hydraulic Laboratory of the Division of Industrial Research, Washington State College, has had such an analyzer since 1951. This analyzer has been used for high and low pressure gas and for water distribution networks. The usual analysis has been determination of head losses and/or flow rates for present and future demands. Unusual problems include analyses for Anchorage and Fairbanks, Alaska to insure all pipes had the minimum flow required to prevent freezing. The distribution of cooling water for Priest Rapids turbines was also analyzed. The City of Spokane included the pump characteristics as influenced by the system pressure. Bend, Oregon used this analyzer to assist in selecting a location and water surface elevation for a reservoir being added to their system. The City of Los Angeles used the analyzer to study drawdown characteristics of their reservoirs. Pressure drops and distribution of bleed air for B-52 jets were checked.

Other possible uses include economic studies related to pump selection, reservoir size and location, and main size. Stagnation potential of reservoirs can be evaluated. Leaks and blocking can be pinpointed when a few field pressures have been taken. Hazen-Williams C values can be determined or confirmed from field data for a badly tuberculated system. In time of disaster this analyzer could be invaluable in re-routing gas and/or water for the most efficient use of the remaining system. A booster pump which will raise pressure at a selected point in the network has been added to the R. L. Albrook Laboratory's installation.

The authors' comparison of the digital computer and McIlroy analyzer confirms several of the conclusions of this Laboratory. The great value of the analyzer over a digital computer in presenting an immediate and visual analysis of a system should be emphasized. While such a picture is very useful to the engineer, it is also valuable in helping administrative personnel, fire

1. Associate Hydr. Engr., R. L. Albrook Hydr. Lab., State College of Washington, Pullman, Wash.

chiefs and water superintendents understand the distribution systems. The analyzer is probably a better design tool than the digital computer since the effect of changes are easily and quickly evaluated.

There are disadvantages to the McIlroy analyzer which are not easily solved. The number of pipe sections which can be included are limited by the available Fluistor sockets. The identical pipe sections which can be placed on the analyzer are limited by the Fluistor stock, and it is not practical to maintain a large stock of identical Fluistors for several pipe sizes. Solution of the Darcy equation takes more time, and a trial and error fitting of the Fluistors is necessary.

A program for the IBM 650 digital computer to supplement the McIlroy analyzer has been developed by the R. L. Albrook Hydraulic Laboratory and the Computing Center at the State College of Washington. It is believed that the computer will be better for system analyses when there are few changes anticipated and when (1) the Darcy equation is used, (2) the piping system consists of many identical sections, (3) the number of pipes greatly exceeds the analyzer capacity and/or (4) great accuracy is required. The combination of the analyzer and the computer will provide complementary rather than competitive services.

The possibilities of the digital computer and the analyzer have not been fully developed. As increased use of each continues it is hoped future comparisons will be made. There seems to be an established need for each. Factors influencing the selection of one or the other are not clearly established at this time.

# NORTHEASTERN FLOODS OF 1955: METEOROLOGY OF THE FLOODS[a]

Discussion by H. Alden Foster

H. ALDEN FOSTER,[1] M. ASCE.—Hydraulic engineers and hydrologists are particularly interested in the effects of hurricanes or other large cyclonic disturbances on the production of floods; hence it may be in order to point out certain lessons that may be learned from the authors' analysis of the storms of 1955.

One interesting fact is the extreme magnitude and expanse of the forces involved in such cyclonic storms. Thus, the total volume of water carried over the continent in one 24-hour day of hurricane Connie is given as 562,000 square-mile inches, or about nine cubic miles,—a lot of water even if spread over a large land area. Also, during a single week in the life of such a hurricane, a large portion of the atmosphere over the tropical Atlantic Ocean could be drawn into the storm pattern. Evidently, hurricanes mean not only excessive winds but also immense volumes of water that may be released to the streams and rivers in a short period of time.

There is an extreme variation in location of the tracks of these tropical storms. They originate over the open ocean far south of the northeastern states, but during their travels may end up almost anywhere in this area. Their intensity is maintained largely because atmospheric conditions near the North Atlantic coast during late summer or early fall may at times be similar to those commonly occurring in tropical regions where these storms originate.

The travel paths of hurricanes are quite unpredictable for more than a day or two in advance. These paths are controlled by the general tendency of all atmospheric masses in motion to curve to the right in the northern hemisphere, but they are also strongly affected by atmospheric conditions in their vicinity, such as occurrence of high or low pressure centers or troughs.

The storm may pass over the open ocean throughout its journey to the northern latitudes, in which case it is most likely to cross the coastline of Long Island or southern New England. Or it may pass inland south of Cape Hatteras, and wear itself out while passing northward more or less parallel to the coastline. Where the storm track crosses the coastline, exceptionally high tides may be expected, not necessarily at the location of the path of the center or "eye" of the storm but more likely some distance ahead of this location,—that is, further north or east.

The precipitation rates caused by a hurricane are not necessarily a function of the wind velocity. Even after the storm has grown old and is about to

a. Proc. Paper 1661, June, 1958, by Charles S. Gilman and Kendall R. Peterson.

1. Prin. Assoc., Parsons, Brinckerhoff, Hall & MacDonald, New York, N. Y.

expire, it may still carry an immense load of moisture in the circulating atmosphere and is quite capable of dumping this water in places where it can cause severe floods.

Theoretically, the major portion of the precipitation should take place ahead of and somewhat to the right of the eye of the storm, although topographic or orographic influences may tend to affect this tendency; or the air masses carrying excessive quantities of moisture may be deflected from their natural paths by atmospheric conditions in the general vicinity. As a result, the track of the storm does not necessarily indicate the location of the maximum total precipitation during the storm. For instance, the total precipitation for Connie was generally to the right of the track, while for Diane most of the precipitation in southern New York and New England appears to the left of the track. This seems to be due to the fact that, on August 16 when Diane was moving northward over Virginia, the precipitation was mostly located far to the northeast, from Pennsylvania all across southern New England. By the next day, Diane had made an abrupt turn to the right and passed south of the area where the rain had mostly fallen the day before. If Diane had not changed her course so abruptly but had followed a track eastward near the southern boundary of Massachusetts, the precipitation in southern Connecticut might have been considerably increased by bringing in some of the water which actually must have fallen over the ocean south of Long Island in the right-front quadrant of the storm as it moved along.

This discussion brings up the important question as to whether the storms of 1955 produced the maximum precipitation that may ever be expected in the affected areas. Studies made in 1955 by Dr. A. A. Koch under the writer's supervision show that no storm of record in these Northeastern states has yet closely approached the maximum possible value for precipitation. It is quite possible that greater precipitation and more severe floods may occur in these areas in the future, though the probability of occurrence of such floods may be very small. On the other hand, the maximum possible storm tides have been approached on several occasions at certain locations on the coast of southern New England, although other Atlantic coastal regions have not yet experienced the greatest possible storm tides.

It is interesting to note in a news report of August 23, 1958, that the Weather Bureau has started a comprehensive study of storm tides along the 3,000 miles of the Atlantic coast, from Texas to Maine. It is to be hoped that such a study will show whether the probability of occurrence of hurricanes in this region may be greater in the future than indicated by past records.

# NORTHEASTERN FLOODS OF 1955: FLOOD HYDROLOGY[a]

Discussions by Gordon R. Williams and H. Alden Foster

GORDON R. WILLIAMS,[1] M. ASCE.—Ample evidence is given in this paper that floods resulting from extraordinarily large concentrations of precipitation are hydrologically and hydraulically a different phenomenon from floods having recurrence intervals of 10 years or less. No longer should engineers and mathematicians compile frequency relations on the assumption that all floods comprise a homogeneous statistical population. The writer has previously emphasized this point.(1) For river basins with areas of less than about 4,000 square miles in rolling or mountainous country, the major floods often define frequency curves which have steeper slopes than the curves for ordinary floods. These relations are particularly pronounced in many California(2,3) streams and elsewhere.(4) Rowe(3) has used the term bilineal frequency curve. Curves with this characteristic are also common in New England streams.(5) Unfortunately the number of points available to define the upper curves are too few so the problem of determining reliable recurrent intervals for rare floods is not solved.

The most promising approach to frequency determinations is the regional or composite frequency curve method that has been adopted by the U. S. Geological Survey(6,7) and others.(3) Briefly this method uses the mean annual flood or the 5-year flood as an index to evaluate the magnitudes of floods of equal frequency. Within similar physiographic regions, floods of equal frequency have quite similar magnitudes when expressed as ratios to an index flood. Thus it is possible to use the sum total of flood experience in a region to develop a composite dimensionless frequency curve and to obtain more reliable estimates of the frequencies of major floods than can be obtained by a single record. Dalrymple, in another paper in this symposium, has used the ratio to the mean annual flood to indicate the relative magnitudes of the 1955 floods.

Correlations between index floods and size of drainage area are improved by introducing factors such as the lagtime for the unit-hydrograph(8) or a factor which is a measure of average basin slope.(7)

At least two conclusions can be drawn from this paper. One is that the conservative meteorologic, hydrologic, and hydraulic design criteria(9,10) that have been used in the past by the Federal engineering organizations are now justified. Modifications to the criteria will be inevitable as operating experience is accumulated but the basic conservatism must be retained. The second conclusion is that experience and judgment in hydraulic engineering cannot be replaced by stereotyped design procedures.

---

a. Proc. Paper 1663, June, 1958, by Elliot F. Childs.

1. Prof. of Hydr. Eng., Massachusetts Inst. of Technology, Cambridge, Mass.

REFERENCES

1. Williams, Gordon R., Discussion of "The Estimation of the Frequency of Rare Floods," Jour. of Hydr. Div., Proc. ASCE, vol. 83, June 1957, pp. 1283-11 to 1283-12.

2. Todd, D. K., and Ateshian, K. H., "Estimation of Flood Peaks in Sierra Nevada Mountains, California," Div. of Civil Eng., Univ. of Calif., Series 102, Issue No. 1, Nov. 1, 1956.

3. Rowe, R. R., Long, G. L., and Thomas, C. R., "Flood Frequency by Regional Synthesis," Trans. Am. Geophys. Union, vol. 38, No. 6, Dec. 1957, pp. 879-884.

4. Potter, W. D., "Upper and Lower Frequency Curves for Peak Rates of Runoff," Trans. Am. Geophys. Union, vol. 39, No. 1, Feb. 1958, pp. 100-105.

5. Franceschi-Ayala, L. E., "Flood Frequency Studies," Master's thesis, Dept. of Civil and San. Engr., Mass. Inst. of Tech., June 1957.

6. Dalrymple, Tate, "Regional Flood Frequency," Research Rept. No. 11-B, Highway Research Board, Dec. 1950.

7. Bigwood, B. L., and Thomas, M. P., "Connecticut Flood Planning Session, Part I, Basic Magnitude and Frequency Relation," Ann. Rept., Conn. Soc. of Civil Engrs., 1957, pp. 76-92. See also "A Flood-Flow Formula for Connecticut," U. S. Geol. Survey Circular 365, 1955.

8. Mitchell, W. D., "Floods in Illinois: Magnitude and Frequency," Div. of Waterways, State of Illinois, 1954.

9. Bernard, Merrill, "Primary Role of Meteorology in Flood Flow Estimating," Trans. ASCE, vol. 109, 1944, pp. 311-382.

10. Hathaway, G. A., and Cochran, A. L., "Flood Hydrographs," Chapt. 5, pp. 140-207, in "Engineering for Dams" by Creager, Justin and Hinds, 1945.

H. ALDEN FOSTER,[1] M. ASCE.—Mr. Childs' paper brings out very clearly the fact that hydrological knowledge is never complete or final. The basic data for design of hydraulic structures need to be continually revised to conform with new experience. Nature always demands the last word in such matters.

The writer will confine his comments to the portions of the paper dealing with questions of probability or frequency of floods.

The author refers to the "probable maximum precipitation" which is used as a basis for deriving the "maximum possible flood". This seems to involve some confusion of ideas, although the latter expression has been commonly used in the past by the Corps of Engineers. It does not seem advisable to place any finite limit to future flood magnitudes. In any case, the "probable maximum precipitation" should be used to estimate the "probable maximum flood".

1. Prin. Assoc., Parsons, Brinckerhoff, Hall & Macdonald, New York, N. Y.

The difficulties of combining extraordinary floods with the "run-of-the-mill" variety when preparing a probability curve from a particular flood record were recognized by Allen Hazen nearly 30 years ago.(1) It is closely related to the question of "sampling errors" and "confidence limits".(2,3) Any sample record of 25 years or more is likely to have one or more extreme values well outside the general trend of the rest of the sample. The writer has been unable to develop any method by which the floods caused by extraordinary storms, such as hurricanes, could be separated from the record, because some of the smaller floods may have been produced by hurricane storms at a considerable distance from the gaging station which would cause excessive floods in other locations.

In preparing a flood-probability curve, one or two floods that obviously do not conform with the general trend should be ignored in selecting the curve-of-best-fit. This curve should only be used for such purposes as determining the mean annual flood damage where omission of the extreme floods would have relatively small effect on the results because of their obviously small probability. Of course the hurricane floods should not be ignored in spillway design, but here they should be supplemented with estimates of the "maximum probable flood". The probability of the latter is necessarily small, but we are not concerned with whether it is the 1,000-year flood or the 100,000-year flood; as long as we are convinced that it may occur sometime, or even be exceeded, we cannot afford to ignore it.

These remarks do not include the so-called "historical floods". It should be generally possible to include them in the probability study by the methods described in the ASCE "Hydrology Handbook", page 102ff. See also (4).

The following comments are quoted from a report(5) on the Northeastern Floods of 1955 prepared under the supervision of the writer:

> "Climatic Changes.—The great increase in precipitation and stream discharge in the 1955 floods as compared with previously recorded storms indicates that the storms of August 1955 were of a very exceptional nature. From a statistical standpoint, it appears that they would have a probability of occurrence much smaller than would be indicated by theoretical studies based on previously available records. Two alternative inferences may be drawn from this situation:
>
> (1) The 1955 storms were the result of atmospheric conditions of a most unusual character, following the simultaneous occurrence of a number of unfavorable controlling factors that normally would not be expected to occur together; or
> (2) There have been changes in general climatic or atmospheric conditions in recent years that tend to increase the frequency and intensity of storms of this type along the North Atlantic seaboard.
>
> "If the first inference is accepted, it would be possible to make a reasonable estimate of the probability of occurrence of such storms in the future, for use in determining the effect of the 1955 floods on the mean annual flood damage to be expected on rivers in the area under consideration. If the second inference holds, however, any estimates of flood probability based on previous records would have to be revised to include the effect of the assumed changes in meteorological conditions. . . . The recent apparent changes in climate affecting the paths of hurricanes along the North Atlantic seaboard cover too short a time period to

justify the assumption of any long-term major climatic changes in this region. Nevertheless, the possibility of such cyclic variations in climate should not be neglected in estimating flood probabilities.

"Probability of Occurrence of 1955 Floods.—If the question of climatic change is eliminated from consideration, the excessive magnitude of the 1955 storms must be treated as due to an unusual combination of most unfavorable controlling factors, but excluding any additional factors that have not been effective during the period of record. As a result, if we have prepared a suitable probability curve representing the previously recorded floods, the 1955 floods should be located on the same curve. But since these floods are so much larger than any previously observed, such a method of plotting will result in assigning a very low value of probability to them. If the present hurricane situation is assumed to be the result of climatic changes, the question of determining the probability of occurrence of the 1955 floods becomes much more difficult. Such a change would have to be assumed as commencing not earlier than 1938, the year when the first severe hurricane in more than 100 years struck the Long Island coastline. The intervening period of 17 years (between 1938 and 1955) is much too short to permit any reasonable estimate of probability for the recent storms. All of this brings out the difficulties of estimating mean annual flood losses in any locality by statistical methods, even if the problem of errors of sampling could be satisfactorily taken care of."

Although the 1955 floods in many places were exceptionally large in comparison with previous recorded floods, their effect on the determination of the Mean Annual Flood Loss for any particular property may be relatively small. Studies referred to above indicated that, for a number of properties in the City of Waterbury, Conn., the addition of the 1955 floods to the record available for 1930-1953 would have increased the estimate of mean annual flood losses for those properties by less than 3 per cent.

## REFERENCES

1. Allen Hazen, "Flood Flows", John Wiley, 1930.
2. L. R. Beard, "Estimation of Flood Probabilities", ASCE Sept. No. 438, May, 1954.
3. G. N. Alexander, Discussion of "Technical Problems of Flood Insurance", by H. Alden Foster, ASCE Proc. Sep. No. 1348, Aug. 1957, pg. 15.
4. "Review of Flood Frequency Methods", Trans. ASCE, Vol. 118, 1953, pg. 1224.
5. "Studies of Floods and Flood Damage, 1952-1955", privately printed by American Insurance Association, 116 John St., New York City.

## PROCEEDINGS PAPERS

The technical papers published in the past year are identified by number below. Technical-division sponsorship is indicated by an abbreviation at the end of each Paper Number, the symbols referring to: Air Transport (AT), City Planning (CP), Construction (CO), Engineering Mechanics (EM), Highway (HW), Hydraulics (HY), Irrigation and Drainage (IR), Pipeline (PL), Power (PO), Sanitary Engineering (SA), Soil Mechanics and Foundations (SM), Structural (ST), Surveying and Mapping (SU), and Waterways and Harbors (WW) divisions. Papers sponsored by the Board of Direction are identified by the symbols (BD). Societies and order coupons, refer to the separate issue of "Civil Engineering." Beginning with Volume 82 (January 1956) papers were published as Journals of the various Technical Divisions. To locate papers in the Journals, the symbols after the paper numbers were followed by a numerical designating the issue of a particular Journal in which the paper appeared. For example, Paper 1443 is identified as 1443 (HY 6) which indicates that the paper is contained in the sixth issue of the Journal of the Hydraulics Division during 1957.

### VOLUME 82 (1956)

NOVEMBER: 1426(EM4), 1427(EM4), 1428(SM4), 1429(SM5), 1430(SM4)[c], 1431(ST8), 1432(ST8), 1433(ST8), 1434(ST8), 1435(ST8), 1436(ST8), 1437(ST8), 1438(EM4), 1439(SM4), 1440(ST8), 1441(ST8), 1442(ST8)[c], 1443(HY6), 1444(SU2), 1445(SU2), 1446(SU2), 1447(SU2), 1448(SU2)[c].

DECEMBER: 1449(HY6), 1450(HY6), 1451(HY6), 1452(HY6), 1453(HY6), 1454(HY6), 1455(HY6), 1456(HY6)[c], 1457(PO6), 1458(PO6), 1459(PO6), 1460(PO6)[c], 1461(SA6), 1462(SA6), 1463(SA6), 1464(SA2), 1465(SA6), 1466(SA6), 1467(AT3), 1468(AT2), 1469(AT2), 1470(AT2), 1471(AT2), 1472(AT2), 1473(AT2), 1474(AT2), 1475(AT2), 1476(AT2), 1477(AT2), 1478(AT2), 1479(AT2), 1480(AT2), 1481(AT2), 1482(AT2), 1483(AT2), 1484(AT2), 1485(AT2)[c], 1486(SU2), 1487(SU2), 1488(SU2), 1489(SU2), 1490(SU2).

### VOLUME 83 (1957)

JANUARY: 1494(SM1), 1495(SM1), 1496(SM1), 1497(IR1), 1498(IR1), 1499(IR1), 1500(IR1), 1501(IR1), 1502(IR1), 1503(IR1), 1504(IR1), 1505(IR1), 1506(IR1), 1507(IR1), 1508(ST1), 1509(ST1), 1510(ST1), 1511(ST1), 1512(ST1), 1513(WW1), 1514(WW1), 1515(WW1), 1516(WW1), 1517(WW1), 1518(WW1), 1519(ST1), 1520(EM1)[c], 1521(HY1)[c], 1522(ST1)[c], 1523(WW1)[c], 1524(HW1), 1525(HW1), 1526(HW1)[c], 1527(HW1).

FEBRUARY: 1528(HY1), 1529(PO1), 1530(ST1), 1531(ST1), 1532(HY1), 1533(SA1), 1534(SA1), 1535(SM1), 1536(SM1), 1537(SM1), 1538(PO1), 1539(SA1), 1540(SA1), 1541(SA1), 1542(SA1), 1543(SA1), 1544(SM1), 1545(SM1), 1546(SM1), 1547(SM1), 1548(SM1), 1549(SM1), 1550(SM1), 1551(SM1), 1552(SM1), 1553(PO1), 1554(PO1), 1555(PO1), 1556(PO1), 1557(PO1)[c], 1558(ST1)[c], 1559(SM1)[c].

MARCH: 1560(ST2), 1561(ST2), 1562(ST2), 1563(ST2), 1564(ST2), 1565(ST2), 1566(ST2), 1567(ST2), 1568(WW2), 1569(WW2), 1570(WW2), 1571(WW2), 1572(WW2), 1573(WW2), 1574(PL1), 1575(PL1), 1576(ST2)[c], 1577(PL1), 1578(PL1)[c], 1579(WW2)[c].

APRIL: 1580(EM2)[c], 1581(EM2), 1582(HY2), 1583(HY2), 1584(HY2), 1585(HY2), 1586(HY2), 1587(HY2), 1588(HY2), 1589(HY2), 1590(HY2), 1591(GR2), 1592(SA2), 1593(SA2), 1594(SU1), 1595(SU1), 1596(EM2), 1597(PO2), 1598(PO2), 1599(PO2), 1600(PO2), 1601(PO2), 1602(PO2), 1603(HY2), 1604(EM2), 1605(SU1)[c], 1606(SA2), 1607(SA2), 1608(SA2), 1609(SA2), 1610(SA2), 1611(SA2), 1612(SA2), 1613(SA2), 1614(SA2), 1615(GR2)[c], 1616(HY2)[c], 1617(SU1), 1618(PO2)[c], 1619(EM2)[c], 1620(CP1).

MAY: 1621(HW2), 1622(HW2), 1623(HW2), 1624(HW2), 1625(HW2), 1626(HW2), 1627(HW2), 1628(HW2), 1629(ST3), 1630(ST3), 1631(ST3), 1632(ST3), 1633(ST3), 1634(ST3), 1635(ST3), 1636(ST3), 1637(ST3), 1638(ST3), 1639(WW3), 1640(WW3), 1641(WW3), 1642(WW3), 1643(WW3), 1644(WW3), 1645(SM2), 1646(SM2), 1647(SM2), 1648(SM2), 1649(SM2), 1650(SM2), 1651(SM2), 1652(SM2), 1653(WW3)[c], 1654(SM2), 1655(SM2), 1656(ST3)[c], 1657(SM2)[c].

JUNE: 1658(AT1), 1659(AT1), 1660(HY3), 1661(HY3), 1662(HY3), 1663(HY3), 1664(HY3), 1665(SA3), 1666(PL2), 1667(PL2), 1668(PL2), 1669(AT1), 1670(PO3), 1671(PO3), 1672(PO3), 1673(PL2), 1674(PL2), 1675(PO3), 1676(PO3), 1677(SA3), 1678(SA3), 1679(SA3), 1680(SA3), 1681(SA3), 1682(SA3), 1683(PO3), 1684(HY3), 1685(SA3), 1686(SA3), 1687(PO3), 1688(SU3)[c], 1689(SU3)[c], 1690(HY3)[c], 1691(PL2)[c].

JULY: 1692(EM3), 1693(EM3), 1694(ST4), 1695(ST4), 1696(ST4), 1697(SU2), 1698(SU2), 1699(SU2), 1700(SU2), 1701(SA4), 1702(SA4), 1703(SA4), 1704(SA4), 1705(SA4), 1706(EM3), 1707(ST4), 1708(ST4), 1709(ST4), 1710(ST4), 1711(ST4), 1712(ST4), 1713(ST4), 1714(SM3), 1715(SA4), 1716(SU2), 1717(SA4), 1718(EM3), 1719(EM3)[c], 1720(SA4), 1721(SA4), 1722(ST4), 1723(ST4), 1724(EM3)[c].

AUGUST: 1725(HY4), 1726(HY4), 1727(SM3), 1728(SM3), 1729(SM3), 1730(SM3), 1731(SM3), 1732(SM3), 1733(SM3), 1734(PO4), 1735(PO4), 1736(PO4), 1737(PO4), 1738(PO4), 1739(PO4), 1740(PO4), 1741(PO4), 1742(PO4), 1743(PO4), 1744(PO4), 1745(PO4), 1746(PO4), 1747(PO4), 1748(PO4), 1749(PO4).

SEPTEMBER: 1750(IR3), 1751(IR3), 1752(IR3), 1753(IR3), 1754(IR3), 1755(ST5), 1756(ST5), 1757(ST5), 1758(ST5), 1759(ST5), 1760(ST5), 1761(ST5), 1762(ST5), 1763(ST5), 1764(ST5), 1765(WW4), 1766(WW4), 1767(WW4), 1768(WW4), 1769(WW4), 1770(WW4), 1771(WW4), 1772(WW4), 1773(WW4), 1774(IR3), 1775(IR3), 1776(SA5), 1777(SA5), 1778(SA5), 1779(SA5), 1780(SA5), 1781(WW4), 1782(SA5), 1783(SA5), 1784(IR3)[c], 1785(WW4)[c], 1786(SA5)[c], 1787(ST5)[c], 1788(SA5), 1789(SA5).

OCTOBER: 1790(EM4), 1791(EM4), 1792(EM4), 1793(EM4), 1794(EM4), 1795(HW3), 1796(HW3), 1797(HW3), 1798(HW3), 1799(HW3), 1800(HW3), 1801(HW3), 1802(HW3), 1803(HW3), 1804(HW3), 1805(HW3), 1806(EM4), 1807(ST6), 1808(ST6), 1809(ST6), 1810(ST6), 1811(ST6), 1812(SM4), 1813(SM4), 1814(ST6), 1815(ST6), 1816(ST6), 1817(ST6), 1818(ST6), 1819(ST6), 1820(ST6), 1821(ST6), 1822(EM4), 1823(EM4), 1824(EM4), 1825(EM4), 1826(EM4), 1827(EM4)[c], 1828(HW3)[c], 1829(WW3)[c], 1830(PO5)[c], 1831(EM4)[c], 1832(HY5)[c].

NOVEMBER: 1833(HY6), 1834(SU3), 1835(SU3), 1836(ST7), 1837(ST7), 1838(ST7), 1839(ST7), 1840(ST7), 1841(ST7), 1842(SU3), 1843(SU3), 1844(SU3), 1845(SU3), 1846(SU3), 1847(SA6), 1848(SA6), 1849(SA6), 1850(SA6), 1851(SA6), 1852(SA6), 1853(SA6), 1854(SA6), 1855(SA6)[c], 1856(HY6)[c], 1857(ST7)[c], 1858(SU3)[c].

---

c. Discussion of numbered papers, arranged by divisions.

# AMERICAN SOCIETY OF CIVIL ENGINEERS

## OFFICERS FOR 1959

### PRESIDENT

FRANCIS S. FRIEL

### VICE-PRESIDENTS

*Term expires October, 1959:*

LOUIS R. HOWSON

*Term expires October, 1960:*

PAUL L. HOLLAND

LLOYD D. KNAPP

### DIRECTORS

*Term expires October, 1959:*

CLINTON [illegible] OVER, Jr.

LELAND [illegible] E

EDWARD [illegible] WORTH

[illegible] LAVERTY

[illegible] ET

[illegible] B. ALEXANDER

*Term expires October, 1960:*

PHILIP C. RUTLEDGE

WESTON S. EVANS

TILTON E. SHELBURNE

CRAIG P. HAZELET

DONALD H. MATTERN

JOHN E. SINNE

*Term expires October, 1961:*

THOMAS S. FRATAR

EARL F. O'BRIEN

DANIEL B. VENTRES

CHARLES W. BRITZIUS

EUGENE C. O'HARRA

FRED H. RHODES, JR.

N. T. VEATCH

### PAST PRESIDENTS

*Members of the Board*

[illegible] G. LOCH[illegible]

LOUIS R. HOWSON

[illegible] SECRETARY

H. WESLY

TREASURER

CHARLES E. TROUT

ASSISTANT SECRETARY

[illegible] CHANDLER

ASSISTANT TREASURER

ERNEST W. NEEB

## PROCEEDINGS OF THE SOCIETY

HAROLD T. LARSEN

*Director of Technical Publications*

PAUL [illegible] PARIS

*[illegible] of Technical Publications*

MARVIN SCHECHTER

*Assistant Editor of Technical Publications*

## COMMITTEE ON [illegible] PUBLICATIONS

[illegible] B. [illegible] TH, *Chairman*

PHILIP C. RUTLEDGE, *Vice-Chairman*

LELAND DURK[illegible]

CHARLES W. BRITZIUS

TILTON E. SHEL[illegible]

FRED H. RHODES, JR.